uOttawa

L'Université canadienne
Canada's university

FACULTÉ DES ÉTUDES SUPÉRIEURES ET POSTOCTORALES

uOttawa

L'Université canadienne
Canada's university

FACULTY OF GRADUATE AND POSDOCTORAL STUDIES

Stephanie Lynn Granville
AUTEUR DE LA THÈSE / AUTHOR OF THESIS

M.Sc. (Chemistry)
GRADE / DEGREE

Department of Chemistry
FACULTÉ, ÉCOLE, DÉPARTEMENT / FACULTY, SCHOOL, DEPARTMENT

Studies of Iron Polyfluorometallacycle Complexes Enroute to the "Green" Catalytic Synthesis of Hydrofluorocarbons

TITRE DE LA THÈSE / TITLE OF THESIS

T. Baker
DIRECTEUR (DIRECTRICE) DE LA THÈSE / THESIS SUPERVISOR

CO-DIRECTEUR (CO-DIRECTRICE) DE LA THÈSE / THESIS CO-SUPERVISOR

S. Gambarotta

D. Richeson

D. Richeson

Gary W. Slater
Le Doyen de la Faculté des études supérieures et postdoctorales / Dean of the Faculty of Graduate and Postdoctoral Studies

Studies of Iron Polyfluorometallacycle Complexes Enroute to the "Green" Catalytic Synthesis of Hydrofluorocarbons

By

Stephanie L. Granville

Thesis submitted to the

Faculty of Graduate and Postdoctoral Studies

University of Ottawa

in partial fulfillment of the requirements for the degree

Master of Science

Centre for Catalysis Research and Innovation

Department of Chemistry

Ottawa-Carleton Chemistry Institute

Faculty of Science

Your file Votre référence
ISBN: 978-0-494-79666-5
Our file Notre référence
ISBN: 978-0-494-79666-5

Table of Contents

Abstract

Chlorofluorocarbons were once commonly used as propellants and refrigerants due to their stability, low toxicity and excellent physical properties. They were phased out, however, after being identified as ozone-depleters, and have been replaced by hydrofluorocarbons (HFCs) and other fluorocarbon derivatives (FCDs). The high temperature-resistant characteristic of these materials is beneficial for many applications; however, the robust nature of the C-F bonds leads to their persistence in the environment. Frequently, the synthesis of HFCs and FCDs involves energy-intensive processes and toxic precursors, such as chlorocarbons and heavy metals. In accordance with the shift to greener, more sustainable chemistry, more energy efficient methods employing less hazardous and non-toxic materials for the generation of HFCs and FCDs need to be developed. Organometallic catalysis offers potential new routes to the synthesis of fluorinated compounds. We sought to study the reactivity of tetrafluoroethylene and 1,1-difluoroethylene with a variety of iron complexes to increase our understanding of the bonding and chemistry of coordinated fluoro-olefins. Crystal structures were obtained for the parent and dppe substituted metallaycles: $Fe(CF_2)_4(CO)_4$ and $Fe(CF_2)_4(\kappa^2\text{-dppe})(CO)_2$. Sterics were found to be responsible for the preferential formation of three- versus five-membered metallacycles through investigating the reactivity of TFE with iron phosphine- and phosphite-carbonyl complexes, as well as with the homoleptic complex pentakis(2,6-dimethylphenylisocyanide)iron and the anionic complex $K[FeCp(CO)_2]$. The five-membered metallacycle was selectively formed with the mono-substituted phosphine and phosphite complexes, whereas, the di-substituted complexes yield the olefin (three-membered metallacycle) complexes. With the goal of developing methods for iron-mediated fluoride abstraction, the reactivity of these iron fluoro-metallacycles with a variety of Lewis acids was probed. Extremely electrophillic fluoro-carbenes were generated. A more electron rich metal centre, as in the thermally synthesized $K[FeCp(CF_2)_4(CO)_2]$, is required to facilitate fluoride abstraction and stabilize the fluoro-carbene. The results that were obtained in this investigation set the stage well for further development of iron-based organofluorometallic chemistry and our desire to functionalize the α-carbon of the metallacycle enroute to the generation of novel FCs.

Table of Compounds

#	Compound	#	Compound
1	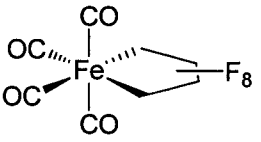	2	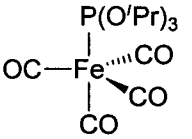
3	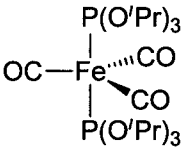	4	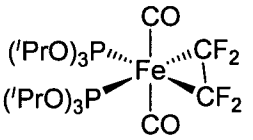
5	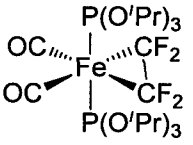	6	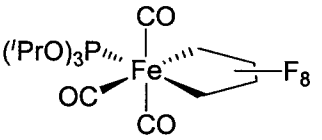
7	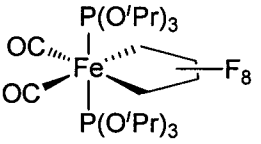	8	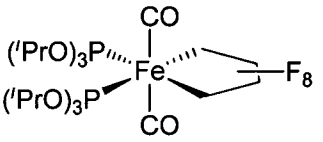
9	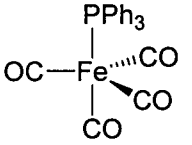	10	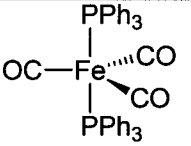
11	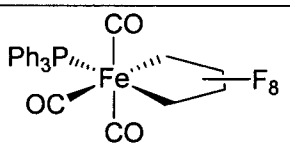	12	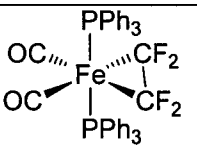
13	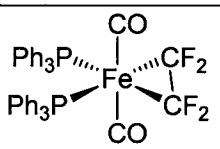	14	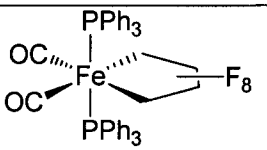
15	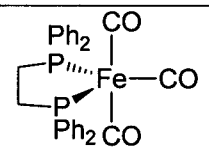	16	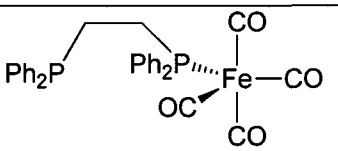
17	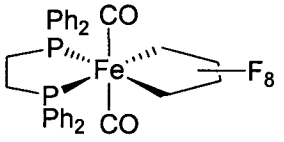	18	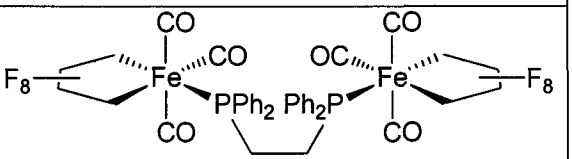

19	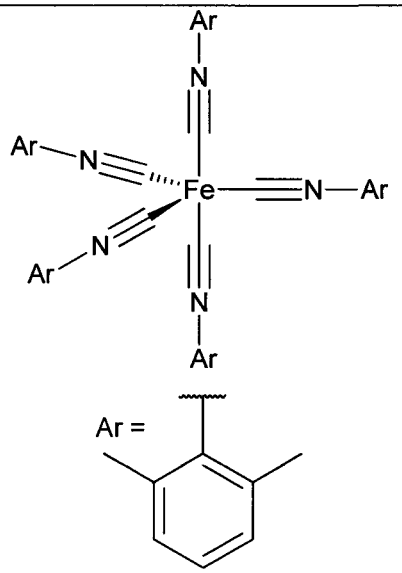	20	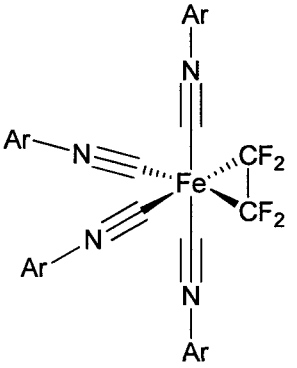
21	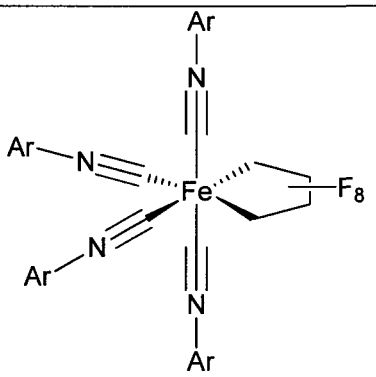	22	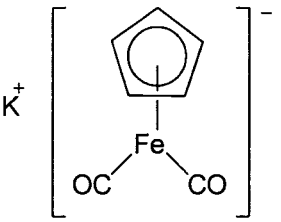
23	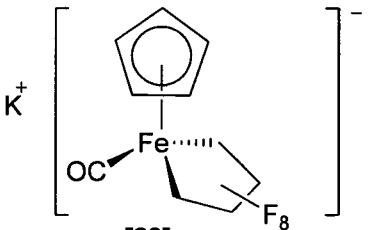 **[23]**	24	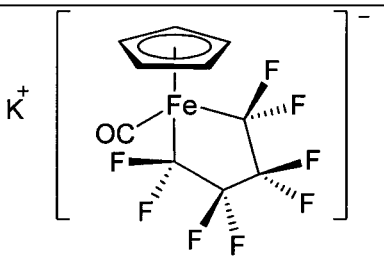 **[24]**
25	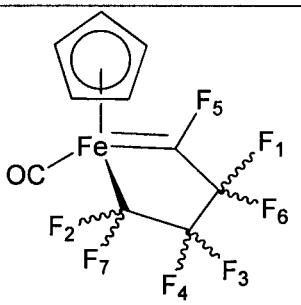	26	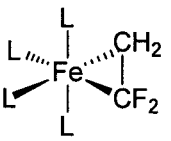 L = PPh_3 or CO [26]
		27	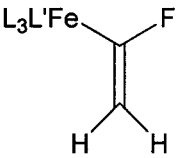 L = PPh_3 or CO L' = PPh_3 or F [27]

List of Figures

Chapter 1

Chapter 2

Chapter 3

Chapter 4

Chapter 5

Chapter 6

Appendix A

List of Tables

Chapter 1

Chapter 3

Chapter 4

Appendix B

List of Schemes

Chapter 1

Chapter 3

List of Symbols and Abbreviations

Å	angstroms
acac	acetylacetonate
app	apparent
atm	atmospheres
bipy	2,2'-bipyridine
br	broad
^{n}Bu	*n*-butyl
^{t}Bu	*tert*-butyl
°C	degrees centigrade
CFCs	chlorofluorocarbons
cod	cyclo-octa-1,5-diene
cm^{-1}	wavenumbers
Cp	cyclopentadienyl
d	doublet
dpm	2,2,6,6-Tetramethyl-3,5-heptanedionate
dppe	1,2-bis(diphenylphosphino)ethane
Et	ethyl
FC(s)	fluorocarbon(s)
FCDs	fluorocarbon derivatives
FT	fourier transform
HFCs	hydrofluorocarbons
HPLC	High performance liquid chromatography
HTFE	trifluoroethylene
Hz	Hertz
IR	infrared
K	kelvin

kPa	kilopascals
NMR	nuclear magnetic resonance
M	metal
Me	methyl
med	medium
mult	multiplet
^{i}Pr	isopropyl
R_F	perfluorinated group
RT	room temperature
Ph	phenyl
Py	pyridine
quart	quartet
quint	quintet
s	singlet
str	strong
TFE	tetrafluoroethylene
THF	tetrahydrofuran
tr	triplet
UV	ultraviolet
VDF	vinylidene fluoride
wk	weak
Δ	heating

Acknowledgements

I would like to thank my parents and Ian for your continual support and for always being there. Thank you to my supervisor, Prof. R. Tom Baker for your guidance and cooperation. Thank you to all of the members of the Baker group, especially Nicole Hunter, William Wright, Sib Mal, Daniel Harrison and Timo Ott for your friendship, advice and support throughout this process. Thank you Dr. Glenn Facey for teaching me so much, and getting me excited, about NMR, and for making sure that I always had a spectrometer to run ^{19}F NMR experiments on. Dr. Ilia Korobkov is thanked for X-ray crystallography. Thanks to NSERC funding in the form of a CGS M and for funding the research project through an NSERC Discovery Grant.

Chapter 1: Introduction

1.1 Introduction

Chlorofluorocarbons (CFCs) were once commonly used as propellants and refrigerants due to their stability, low toxicity and excellent physical properties. After being identified as ozone-depleters, CFCs were replaced by hydrofluorocarbons (HFCs) and other fluorocarbon derivatives (FCDs) in many of their applications. HFCs have become important compounds for refrigeration, air conditioning, metal and semiconductor degreasing, foaming and blowing agents, paint formulations, anaesthetics, and pharmaceuticals. As well, many FC-based polymers, such as Teflon®, Krytox® and Gore-Tex®, are highly valued.

The position of halogens, fluorine in this case, on the (hydro)carbon framework influences their properties; achieving the desired configuration and arrangement poses quite a challenge.[1] An effective and efficient catalytic process for this control is currently unavailable, but would be extremely useful.

The high temperature-resistant characteristic of HFCs and FCDs is beneficial for many applications; however, the robust nature of C-F bonds (they are far more resistant to high temperatures and oxidizing/corrosive conditions than their hydrocarbon analogues)[2] leads to their persistence in the environment.[3]

Frequently, the synthesis of HFCs and FCDs involves energy-intensive processes (high temperatures and/or pressures) and toxic precursors, such as chlorocarbons and heavy metals. Swarts-type processes, for example, utilize toxic metal complexes, such as antimony fluorides or chromium-based species, with HF as the source of fluorine, to generate FCs or FCDs from chlorocarbons. The conditions required for these processes include high temperatures and pressures, in excess of 100°C and 30 atm respectively.[2]

In accordance with the shift to greener, more sustainable chemistry, more energy efficient methods employing less hazardous and non-toxic materials for the generation of HFCs and FCDs need to be developed.

Organometallic catalysis, specifically with the abundant, inexpensive and relatively non-toxic metal iron, offers potential new routes to the synthesis of fluorinated compounds. Organofluorometallic chemistry and reactivity has been explored primarily with precious metals.[4] Development of effective FC-generating catalytic systems requires advancing our fundamental knowledge in this underdeveloped field, with a view of obtaining a fuller understanding of the bonding and chemistry of co-ordinated fluoro-olefins.

1.2 Transition Metal Complexes of Fluoro-olefins

The reactivity of low-valent transition metal complexes with unsaturated compounds bearing electron withdrawing substituents, and the subsequent formation of stable complexes, has received a considerable amount of attention. Reasons for interest in this area include: to study these model complexes in catalytic reactions, as well as to explore bonding in these complexes and how coordination of the olefin affects its reactivity.

The bonding between fluoro-olefins and transition metals is classified as retro-dative bonding. This synergetic effect involves σ-donation of electron density from the fluoro-olefin's filled π-orbital into a σ-symmetry orbital on the metal, accompanied by π-backbonding from the metal into the ligand's π-antibonding orbitals. The degree of backbonding will depend on the metal's oxidation state and the identity of the ancillary ligands.[5] Generally, the degree of backbonding is quite strong; the highly electronegative fluorine atoms lower the energy of the olefin's π-antibonding orbitals to achieve greater overlap with the metal's filled d orbitals.[6]

Depending on the metal and the ligand environment, several different types of reactivity with tetrafluoroethylene (TFE) have been reported. Typical reactions include: formation of a side-on bonded complex; insertion of TFE into a metal-metal bond; bridging of two

metal centers by two molecules of TFE; and coupling of two molecules of TFE at a metal center. Examples of each type of product from the oxidative addition of TFE to a transition metal are described here to demonstrate the possible reactivity that could be observed between TFE and a variety of iron complexes investigated for this thesis.

1.2.1 Formation of a side-on bonded complex

Side-on bound fluoro-olefin complexes have been interpreted spectroscopically in terms of structures having a rigid σ-bonded three-membered "metallo-cyclopropane" ring. Mono-fluoro-olefin complexes of the type $Pt(PPh_3)_2$(fluoro-olefin), where the fluoro-olefin is C_2F_4, C_2F_3Cl, $C_2F_3CF_3$, CF_2Cl_2, cyclo-C_4F_6, cyclo-C_6F_{10}, or CF_2:CFCF:CF_2, have been prepared from tetrakis(triphenylphosphine) platinum, as shown in Figure 1.[7,8] The robust Pt-C_F bond cannot be broken by treatment with triphenylphosphine or by heating. Reacting the complex with iodine solution, however, forms the complex $(Ph_3P)_2PtI_2$ by releasing the fluoro-olefin.

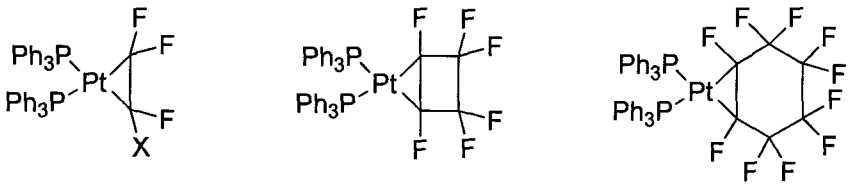

Figure 1: Platinum side-on bonded fluoro-olefin complexes.

Spectroscopic evidence points to the formal two electron oxidation of the metal upon side-on coordination of a fluoro-olefin, such as TFE, resulting in a change in hybridization of the olefinic carbon atoms from sp^2 to sp^3. The magnitude of F-F coupling constants of fluorines on sp^3 hybridized carbon atoms increases; geminal F-F coupling constants are on the order of 200 Hz.[7] Also, the NMR spectra do not change with temperature, indicating no free-rotation about the metal-olefin bond, which suggests that the metal-fluoro-olefin bonding is rigid in the form of a metallo-

cyclopropane ring. Further, the infrared spectrum does not show a band corresponding to a co-ordinated double bond.

Numerous other side-on bonded mono-fluoro-olefin complexes with platinum, and various other transition metals, have been reported. For example, TFE displaces one ethylene from both $[Rh(dpm)(C_2H_4)_2]$[9] and $[Rh(acac)(C_2H_4)_2]$.[10] The latter complex has been characterized crystallographically and provides important information about the bonding of fluoro-olefins. In this structure, the carbon atoms of the fluoro-olefin are held closer to the metal than those of ethylene, supporting the notion that metals are more strongly bound to fluoro-olefins than their hydrocarbon analogues.[10] Further, the Rh-C_H bond distances in this complex are longer than in the complex $[Rh(acac)(C_2H_4)_2]$. Thus the ethylene molecules are more weakly bound in the TFE complex than in the bis-ethylene complex.

Generally it has been found that, once formed, M-C_F bonds are quite robust. Treatment of $[Rh(acac)(C_2H_4)(C_2F_4)]$ with phosphines, amines, nitriles or cyanide ion displaces ethylene, but not TFE.[11] However, both are displaced upon reaction with 1,5-cyclooctadiene or carbon monoxide. An example with weaker fluoro-olefin coordination is $[(Ph_3P)_2Ir(C_2F_4)(CO)Cl]$. The M-$C_F$ bonds are weak enough that the complex readily evolves TFE in a benzene solution at 25°C or under vacuum at 100°C.[11]

1.2.2 Insertion of TFE into a metal-metal bond

It has been found that TFE inserts into the metal-metal bond of several homo- and heterobimetallic complexes. Dicobalt octacarbonyl reacts with TFE to yield $(OC)_4CoCF_2CF_2Co(CO)_4$, when pentane was employed as the solvent and the reaction mixture was allowed to stand in daylight for several days.[12] By irradiating with UV light, however, no such insertion product was observed. Conversely, the complex, $(CH_3)_3SnCF_2CF_2Co(CO)_4$, can be obtained by irradiating (trimethyltin)cobalt tetracarbonyl with TFE in pentane. This behavior is similar to that for the tin-manganese[13] and germanium-manganese[14] analogues, both of which react with TFE to give $(CH_3)_3SnCF_2CF_2Mn(CO)_5$ and $(CH_3)_3GeCF_2CF_2Mn(CO)_5$ respectively.

Trifluoroethylene, chlorotrifluoroethylene and fluoropropene also cleave the Sn-Mn and Ge-Mn bonds, however, no fluoro-olefin-bridged complexes were produced.

1.2.3 Bridging of two metal centers by two molecules of TFE

(IV) (V)

Figure 2: Chair-chair interconversion of a TFE bridged cyclo-octa-1,5-diene platinum dimer.

Another interesting type of reactivity exhibited by TFE with transition metal complexes is bridging of two metal centres by two molecules of TFE. Bis(cyclo-octa-1,5-diene)platinum exhibits quite different reactivity with TFE than tetrakis(triphenylphosphine) platinum (Section 1.2.1). Treatment of $Pt(cod)_2$ with TFE in diethyl ether generates the octafluoro-1,4-diplatinacyclohexane (IV) complex shown in Figure 2.[15] At room temperature, the complex undergoes rapid ring (chair-chair) interconversion as indicated by its ^{19}F NMR spectrum.

1.2.4 Coupling of two molecules of TFE at a metal center

Many factors influence the formation of a three-membered metallacycle, olefin-type complex, versus the formation of a five-membered ring, involving the coupling of two molecules of TFE at the metal centre. Metallacyclopentane complexes have been reported for nickel,[16] ruthenium,[17] rhodium,[18] iron,[19] and cobalt.[20]

The relative σ-donor and π-acceptor properties of the ligands delicately control the formation of three- versus five-membered metallacycles.[5] A stronger σ-donating ligand increases the nucleophilicity of the metal which favours five-membered metallacycle

formation by permitting the insertion of a second molecule of fluoro-olefin.[21,22] Steric control must be responsible if a stronger π-acid ligand preferentially forms a metallacyclopentane.[22] A critical factor at play for ring expansion with nickel complexes is access by the fluorocarbon to the metal center.[16]

A variety of nickelacyclopentane derivatives, (VII)-(XIV) in Figure 3, have been prepared from (cyclo-octa-1,5-diene)nickelacycle (VI) via ligand displacement.[16] Formation of the five-membered ring is considerably more favourable for zerovalent nickel complexes, whereas, platinum zero complexes exclusively form three-membered rings. Even with many variations in reaction conditions, attempts to prepare $(1,5\text{-}C_8H_{12})Ni(C_2F_4)$ were unsuccessful.

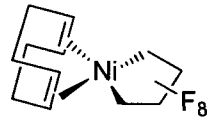

(VI)

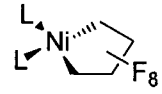

(VII) L = PEt_3
(VIII) L = $PMePh_2$
(IX) L = P^nBu_3
(X) L_2 = $Ph_2PCH_2CH_2PPh_2$
(XI) L = $P(OMe)_3$
(XII) L = 2,2'-bipy
(XIII) L = PPh_3
(XIV) L = γ-picoline

Figure 3: Nickelacyclopentane complexes of TFE.

A ruthenium metallacycle was prepared from $Ru(CO)_2(PPh_3)_3$ and TFE generated *in situ* from CF_2BrCF_2Br and zinc powder in ethanol.[17] The ruthenacyclopentane ring complex preferentially forms with two mutually *cis* CO's and two mutually *trans* PPh_3 ligands, as shown in Figure 4.

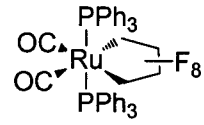

(XV)

Figure 4: A runthenacyclopentane complex of TFE.

Analogous rhodacyclopentane complexes have been generated by reacting TFE and chlorotrifluoroethylene with [Rh(acac)($PMePh_2$)$_2$], yielding complexes (XVI) and (XVII) respectively.[18] The rhodacycle resulting from chlorotrifluoroethylene was a five-membered ring with the head-to-tail linkage of two molecules of chlorotrifluoroethylene. Interestingly, the complex formed upon reaction of [Rh(acac)($PMePh_2$)$_2$] with bromotrifluoroethylene contains only one molecule of the olefin.

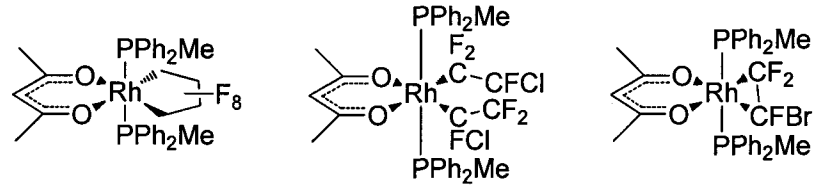

(XVI) (XVII) (XVIII)

Figure 5: Rhodacyclopentane complexes of TFE and chlorotrifluoroethylene, and a rhodium fluoro-olefin complex of bromotrifluoroethylene.

The isoelectronic complexes iron pentacarbonyl and cyclopentadienylcobalt dicarbonyl display similar behaviour in their reactivity with TFE. Both complexes form metallacycles via the coupling of two molecules of TFE at the metal centre.[19,20]

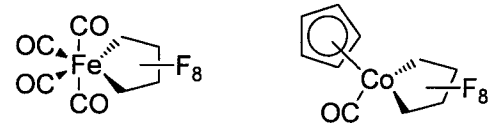

(XIX) (XX)

Figure 6: Isoelectronic iron and cobalt metallacycles of TFE.

The metallacycles described here were the first examples of metallocyclopentanes correctly described and reported in the literature. Metallacycles are now recognized as key intermediates in many syntheses involving transition metals.[23]

1.3 Reaction of TFE and its Derivatives with Iron Carbonyl Complexes

1.3.1 Preparation of mono-(fluoro-olefin) complexes of iron

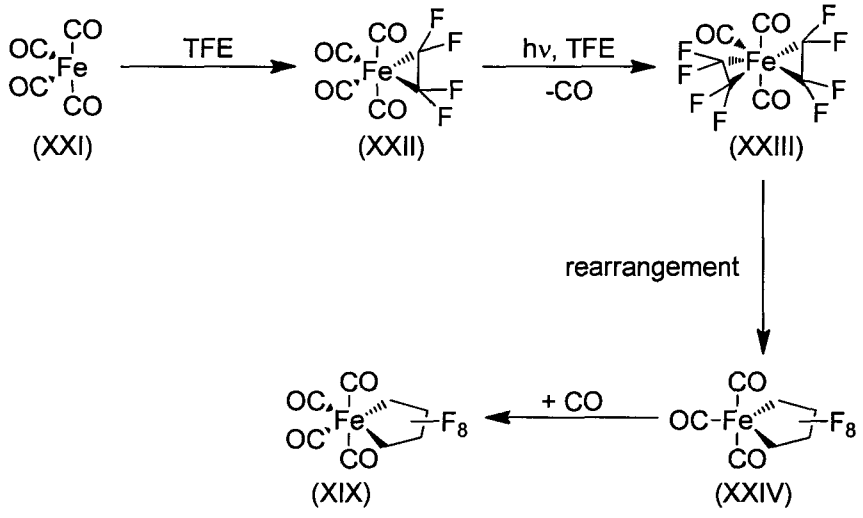

Scheme 1: Proposed reaction pathway for the production of the metallacycle $Fe(CF_2)_4(CO)_4$ from the mono-olefin complex.

The first mono-(fluoro-olefin) complex obtained from $Fe(CO)_5$ was $Fe(C_2F_4)(CO)_4$.[24] Spectroscopic evidence led to characterization of the complex containing the olefin coordinated equatorially with both carbon atoms in the x,y-plane. The coupling constants in the $CClFCF_2$ analogue are different enough from that in the uncoordinated olefin indicating that the carbon atoms must be near sp^3 hybridized. Further irradiation of the olefin complex (XXII) with TFE generates the metallacycle. This suggests that the mono-olefin complex is an intermediate in the preparation of the metallacycle. The proposed reaction pathway for this process is depicted in Scheme 1, whereby $Fe(CO)_5$ first loses one CO to open up a vacant site for coordination of TFE.[25]

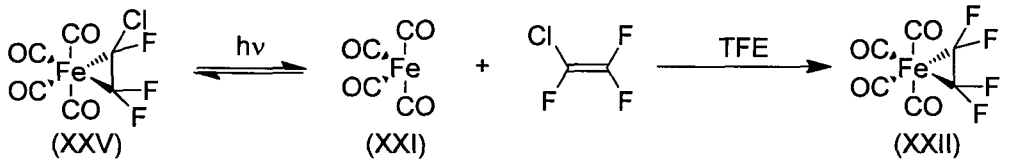

Scheme 2: Preparation of the iron tetracarbonyl TFE-olefin complex from chlorotrifluoroethylenetetracarbonyliron.

The olefin complex can also be prepared from chlorotrifluoroethylenetetracarbonyliron by irradiating with UV light in the presence of TFE, Scheme 2. This assessment was formulated based upon the ^{19}F NMR spectrum, however, no pure tetrafluoroethylene complex was isolated. Mono(fluoro-olefin) complexes of the type Fe(olefin)$(CO)_4$ were prepared by irradiating the corresponding olefin (where olefin = CF_2:CFCl, CF_2:CFBr, CF_2:CCl_2, CF_3CCF:CF_2, CF_3CH:CF_2, cyclo-C_4F_6, cyclo-C_5F_8, or cyclo-C_6F_{10}) with $Fe(CO)_5$.[25] For the complexes formed from cyclic olefins, such as cyclo-C_4F_6, the ^{19}F NMR signal for the vinylic fluorine atoms was significantly shifted upfield compared to the free olefin (57.5 ppm versus 98.8 ppm). Therefore, it is likely that they have become bridgehead fluorine atoms, as in Figure 7.

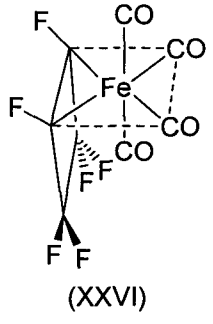

Figure 7: Olefin complex resulting from UV irradiation of $Fe(CO)_5$ with perfluorocyclobutene.

The iron phosphite carbonyl complexes *trans*-[$Fe(CO)_3L_2$] (where L = $P(OMe)_3$ or $P(OEt)_3$) react with fluoro-olefins to selectively produce the equatorially substituted mono-(fluoro-olefin) complexes with the geometry of (XXVII) in Scheme 3.[26] Even upon prolonged irradiation there was no evidence of metallacycle formation. However, when the complex *trans*-[$Fe(CO)_3(P(OEt)_3)_2$] was reacted with trifluorothylene, the

metallacycle formed, with the phosphites in the axial, *trans* configuration. The ^{19}F NMR spectrum showed two broad multiplets at -69.5 ppm and -213.0 ppm indicating a symmetrical arrangement. Nonetheless, there is not sufficient information to claim, with certainty, whether the heterocyclic ring contains the two HTFE groups in head-to-head or tail-to-tail orientation, complexes (XXVIII) and (XXIX).

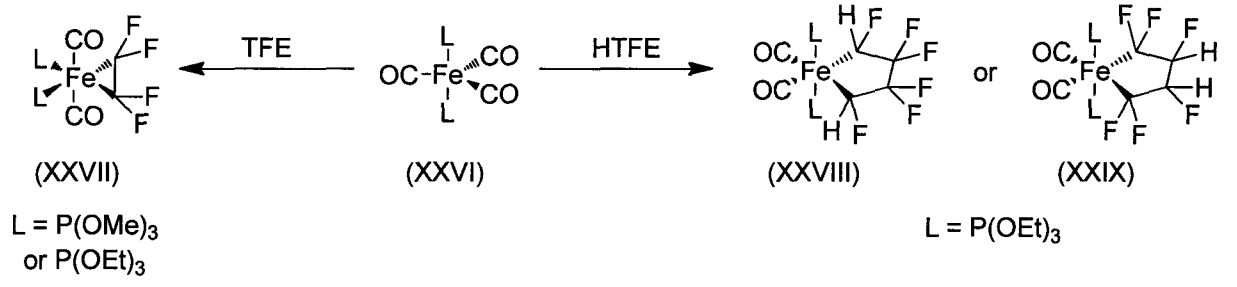

Scheme 3: Selective formation of an iron metallacycle from HTFE.

The difference in reactivity of TFE and HTFE depicts the delicate balance of factors leading to the formation of five- versus three-membered rings. There have been two possible reaction pathways suggested to form the five-membered ring; one involves the capture of an ionic-intermediate (Scheme 4).[27] Formation of a five-membered ring from $Pt[(CF_3)_2CNH](PPh_3)_2]$ takes place via ring expansion on reaction with hexafluoroacetone.[28] This ring expansion is a second possible reaction pathway that could generate a metallacycle from fluoro-olefins.

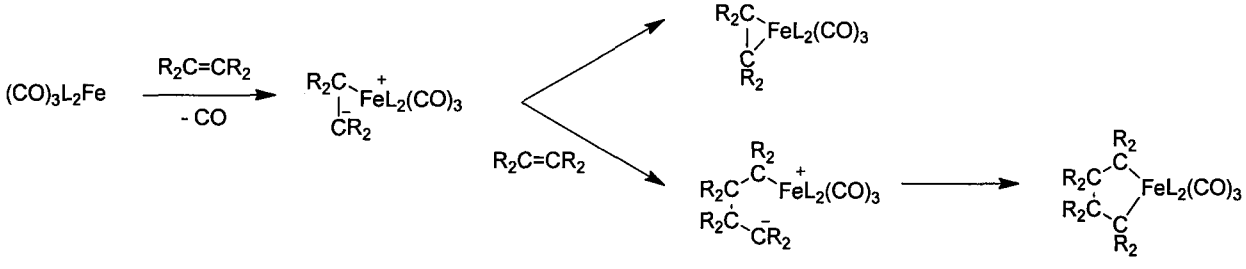

Scheme 4: Formation of a five-membered metallacycle via capture of an ionic-intermediate.

Hexafluorobuta-1,3-diene reacts with $Fe(CO)_5$ to give $Fe(CO)_4(C_4F_6)$, which could not easily be formed by the initial coordination of a single olefin, but could form via the capture of an ionic intermediate prior to normal ring closure.[29,30] However, this mechanism is no longer widely accepted. The coordination of two molecules of olefin, followed by subsequent metallacycle formation as shown in Scheme 1 is more plausible.

Fe and Ru phosphite complexes react with fluoro-olefins in the same manner, stereochemically; they both give the bis-substituted phosphite olefin complex with the phosphites in the equatorial plane with the olefin. The reactivity of Ru phosphine complexes differs, however, selectively generating the olefin complexes with the more electron-donating phosphines in the axial configuration. No comparison can be made to Fe phosphine complexes; the complexes investigated were unreactive towards fluoro-olefins.[26] Attempts to isomerize were unsuccessful, indicating that these reactions are governed by thermodynamic rather than kinetic control, thus again underscoring the delicate balance between various factors which govern the formation of five- versus three-membered rings.

1.3.2 Iron polyfluorometallacyclopentane complexes

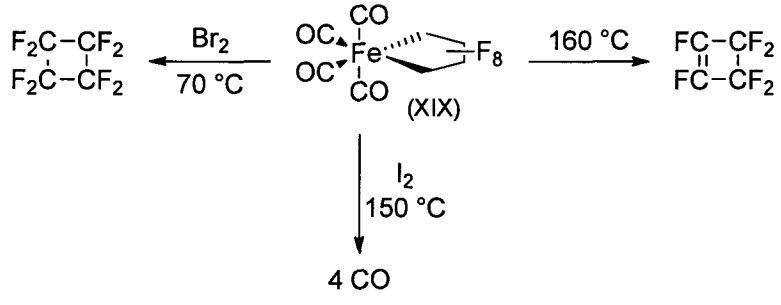

Scheme 5: Reactivity of $Fe(CF_2)_4(CO)_4$.

As mentioned previously, the pioneering example of an iron-containing organofluorometallic complex was a perfluorometallacyclopentane, complex (XIX),

prepared from $Fe(CO)_5$ and tetrafluoroethylene (TFE), shown in Scheme 5.[19] The liberation of four equivalents of carbon monoxide from complex (XIX) by reacting with I_2 at 150°C, demonstrates that it does indeed contain an $Fe(CO)_4$ group. When what was later proven to be the same compound as complex (XIX)[31] was first synthesized by Watterson and Wilkinson, it was believed to contain an $Fe(CO)_3$ group.[32] The compound had been formulated as the olefin complex $Fe(C_2F_4)_2(CO)_3$ and could only be explained by invoking a strange type of π-bonding.

The lack of reactivity of the metallacycle portion of complex (XIX)[34] speaks to the strength of the Fe-C_F sigma-bonds. These bonds owe their high stability to the very electronegative (i.e. electron-withdrawing) fluorine substituents on the carbon atoms, which remove electron density from the metal much more efficiently than alkyl groups. Extreme conditions are necessary to liberate the metallacycle from the metal centre (Scheme 5).

Over the past 50 years, the only reactivity that was explored with complex (XIX) involved ancillary ligand substitution or oxidative demetallation. The CO groups on complex (XIX) can be replaced by combining with the desired ligand in light petroleum and irradiating with U.V. light or heating in a sealed tube at 80°C.[34] In this reaction, the metallacycle remains unchanged. Triphenylphosphine, triphenylarsine, triphenylstibine and triphenyl phosphite each displace one CO to generate the monosubstituted complex $[Fe(CF_2)_4(CO)_3L]$ (Table 1, entries 1-4). Triethyl phosphite yields a mixture of the mono- and disubstituted products, whereas, pyridine gives only the disubstituted complex $[Fe(CF_2)_4(CO)_2L_2]$. 2,2'-Bipyridyl and *o*-phenanthroline produced the expected chelated dicarbonyl complexes (entries 7 and 8). 1,2-Bis(diphenylphosphino)ethane gave the analogous chelated dicarbonyl complex, as well as the bridged dimer $[\{Fe(CF_2)_4(CO)_3\}_2(\mu\text{-dppe})]$.

Table 1: Synthesis of mono- and bis-substituted iron carbonyl fluorometallacycle complexes.

Entry	Ligand	Complex
1	PPh_3	$[Fe(CF_2)_4(CO)_3PPh_3]$
2	$AsPh_3$	$[Fe(CF_2)_4(CO)_3AsPh_3]$
3	$SbPh_3$	$[Fe(CF_2)_4(CO)_3SbPh_3]$
4	$P(OPh)_3$	$[Fe(CF_2)_4(CO)_3P(OPh)_3]$
5	$P(OEt)_3$	$[Fe(CF_2)_4(CO)_3P(OEt)_3]$
		$[Fe(CF_2)_4(CO)_3(P(OEt)_3)_2]$
6	Pyridine	$[Fe(CF_2)_4(CO)_3Py_2]$
7	2,2'-Bipyridyl	$[Fe(CF_2)_4(CO)_3bipy]$
8	*o*-Phenanthroline	$[Fe(CF_2)_4(CO)_3(o\text{-phen})]$
9	$Ph_2P\text{-}CH_2CH_2\text{-}PPh_2$ (dppe)	$[Fe(CF_2)_4(CO)_2(dppe)]$ $[\{Fe(CF_2)_4(CO)_3\}_2)(\mu\text{-dppe})$

The mono-substituted, non-chelating ligand containing complexes could have one of two possible configurations: complex (XXX) or complex (XXXI), in which there is replacement of a CO in either an axial or an equatorial position, respectively. The configuration generated could be determined based upon the ^{19}F NMR spectrum. For complex (XXX), the fluorine atoms on each of the CF_2 groups would be inequivalent. There would be four peaks expected in the spectrum, each a doublet with a large geminal coupling constant (ca. 220 Hz).[33] What was observed, however, were two signals assigned to the two α–CF_2 groups, and a single signal for the two β–CF_2 groups.

The two signals for the α–CF_2 groups had different doublet coupling constants if the ligand contained a phosphorus donor atom.

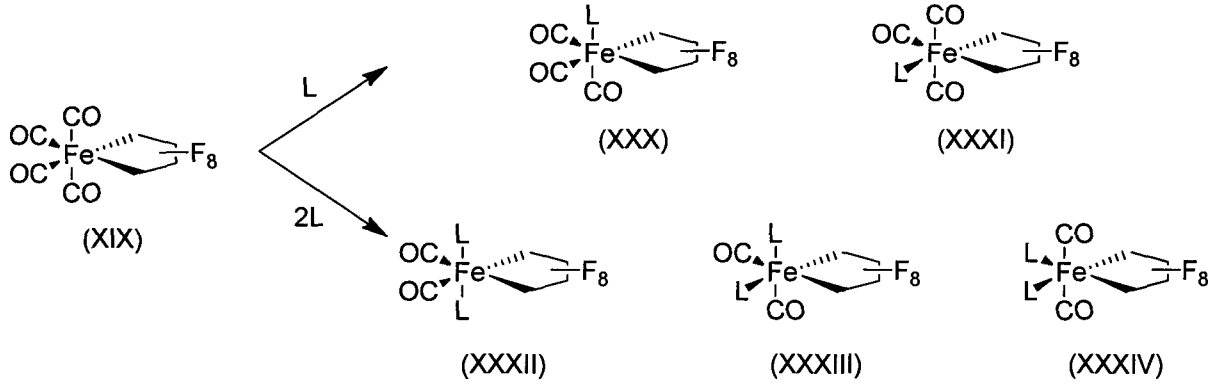

Scheme 6: Ligand substitution of $Fe(CF_2)_4(CO)_4$.[34]

For the disubstituted complex $[Fe(CF_2)_4(CO)_3(P(OEt)_3)_2]$, three configurations are possible, as shown in Scheme 6 for complexes (XXXII), (XXXIII), and (XXXIV). Because there were two CO bands in the IR spectrum, and the ^{19}F NMR spectrum displayed a triplet and a singlet of equal intensity, the configuration must be that of complex (XXXII). For the chelating ligands, entries 7, 8, and 9 in Table 1, the configuration of complex (XXXII) would not be possible; spectroscopic analysis favours that of complex (XXXIV).

1.4 Hydrogenolysis of Perfluorometallacycle Complexes

1.4.1 Nickel complex-catalyzed hydrodimerization of hydrofluoroalkenes

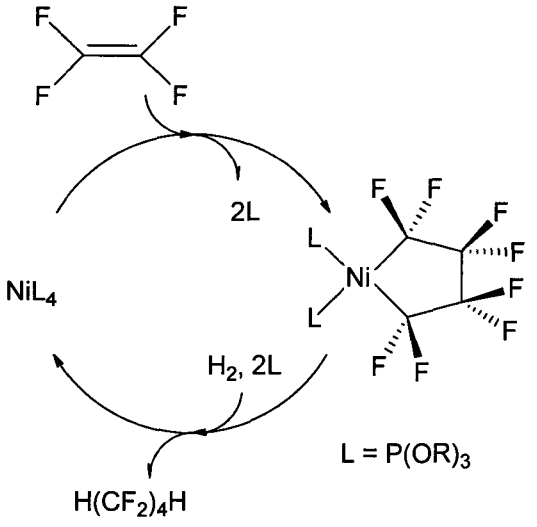

Scheme 7: Nickel complex-catalyzed hydrodimerization of TFE.

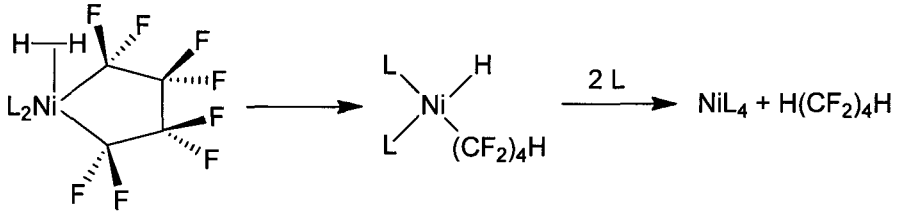

Scheme 8: Hydrogenolysis of a nickel perfluorometallacycle complex.

In a series of patents, Baker *et al.* have shown that HFCs can be obtained in high yields from the Ni complex-catalyzed hydrodimerization of hydrofluoroalkenes (Scheme 7). Evidence suggests that the process relies on the presence of π-acid ligands that presumably enhance the acidity of Ni-bound dihydrogen ligands in the hydrogenolysis step (Scheme 8). In an alternative approach to the hydrodimerization of hydrofluoroalkenes, Ni complexes with chelating nitrogen ligands may be activated by oxidation to the d^6 tetravalent state.[35] [1] In an investigation by another group, a ruthenacycle, $[Ru(C_4F_8)(PPh_3)_4]$, and a series of nickelacycles, $[Ni(C_4F_8)L_2]$ where L = PPh_3, or L_2 = $Ph_2P(CH_2)_2PPh_2$, $Ph_2P(CH_2)_3PPh_2$, 2,2'-bipy, derived from TFE were

studied for hydrogenolysis of the metallacycle. Hydrogenolysis attempts were unsuccessful with hydrogen at 20 bar, even in the presence of 2% palladium on Al_2O_3.[36]

1.4.2 Hydrogenolysis of $Fe(CF_2)_4(CO)_4$

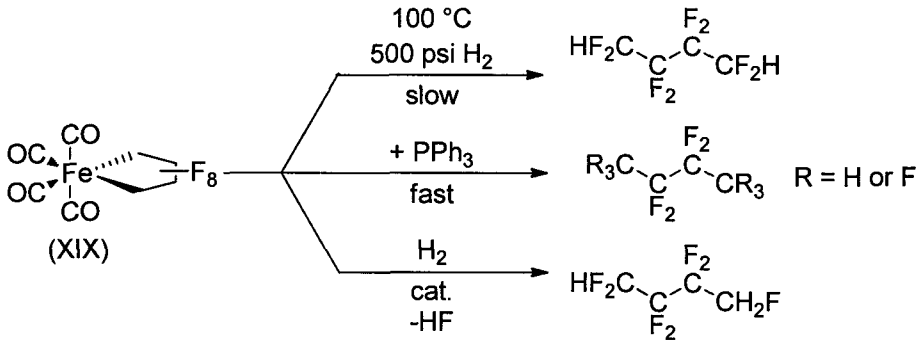

Scheme 9: Hydrogenolysis of $Fe(CF_2)_4(CO)_4$.

Baker *et al.* have shown that the Fe-based perfluorometalacycle, complex (XIX), undergoes the slow hydrogenolysis of the Fe-C_F bonds to give multiple organic products (Scheme 9).[1] There is less selectivity for the hydrogenolysis of $Fe(CF_2)_4(CO)_4$ than its unsaturated d^8 analogues. Hydrogenolysis is accompanied by defluorination at the metal bound carbon. Upon the addition of PPh_3 to the system, the reaction occurred at a much faster rate, however, there was decreased selectivity; organic products were obtained with one through three hydrogens on the terminal carbons. Catalysts such as $RuHCl(PPh_3)_3$ increased the rate and gave good selectivity. The results of the hydrogenolysis of $Fe(CF_2)_4(CO)_4$ are reported in Table 2. All reactions were carried out at 500 psig (3550 kPa) H_2 for 20 hours at 100°C unless otherwise noted. 100 % conversion was achieved with both $RhCl(PPh_3)_3$ and $RuHCl(PPh_3)_3$ as the catalyst (runs no. 4 and 9 respectively). Decreasing the hydrogenolysis time from 20 to 10 hours decreased the percent conversion for the rhodium catalyst (run no. 4 versus 5), but slightly increased it for the ruthenium catalyst (run no. 8 versus 9). Changing the pressure to 500 psig (3550 kPa) $H_2(1)/CO(1)$ significantly decreased the percent conversion (run no. 7). In most cases, the major product was $H(CF_2)_3CFH_2$.

Table 2: Vapour and liquid phase analysis for the hydrogenolysis of $Fe(CF_2)_4(CO)_4$ with a variety of catalysts. ([a] hydrogenolysis time 10 hours, [b] pressure 500 psig (3550 kPa) $H_2(1)/CO(1)$, [c] dppb = 1,4-bis(diphenylphosphino)butane)

Run			Vapour Phase Analysis			Liquid Phase Analysis		
No.	Additives	% Conv.	$H(CF_2)_4H$/ $H(CF_2)_3CFH_2$	$C_4H_4F_6$ Isomers	Perfluoro-cyclobutene	$H(CF_2)_4H$	$H(CF_2)_3CFH_2$	$CH_2F(CF_2)_2CH_2F$
1	None	49	97.5	-	1.5	59.5	38	-
2	Rh/ Carbon	25	42.5	-	47.5	18	16	6
3	Pd/Carbon	16	88.5	9	2.5	4.5	80.5	15
4	$RhCl(PPh_3)_3$	100	72	6	15.5	4.5	78	17.5
5[a]	$RhCl(PPh_3)_3$	93	90.5	6.5	3	8.5	77	14.5
6	$RhCl(PPh_3)_3$	98	89	9.5	1	1	73.5	25.5
7[b]	$RhCl(PPh_3)_3$	5	93.5	1.5	1.5	12.5	83.5	4
8	$RuHCl(PPh_3)_3$	97.5	46.5	28.5	2	7	62	31
9[a]	$RuHCl(PPh_3)_3$	100	92	3.5	2.5	3.5	90.5	6
10	PPh_3	84.5	90	6.5	3.5	13.5	71.5	15
11[c]	$[Rh(cod)(dppb)]BF_4$	88	86.5	-	12.5	37	63	-
12	$P(O\text{-}p\text{-}tol)_3$	15	96	0.5	0.5	64	26	-

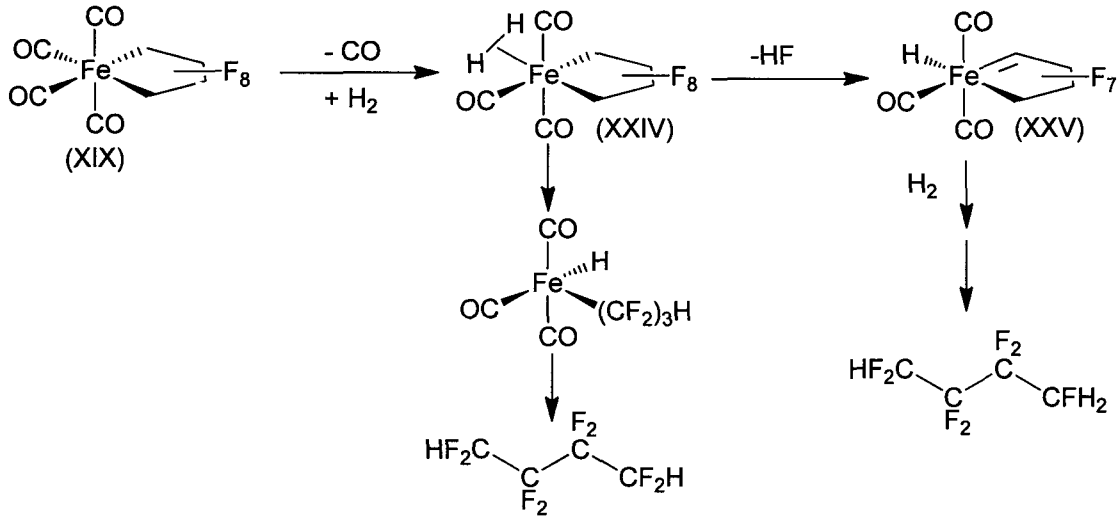

Scheme 10: Proposed mechanism for the hydrogenolysis of $Fe(CF_2)_4(CO)_4$.

Unlike the coordinatively unsaturated Ni complexes, d^6 six coordinate metallacycles need to lose a ligand to activate H_2. The proposed mechanism for this reaction first involves the loss of a CO to generate a vacant coordination site for dihydrogen (Scheme 10). The protic hydrogen of this dihydrogen intermediate (XXIV) can either protonate one of the alpha fluorines to give HF and the carbene (XXV), or one of the alpha carbons to give the alkyl hydride which can subsequently undergo reductive elimination. Elimination of HF was not observed in the hydrogenolysis of the Ni metallacycles. Activation of the C-F bond to generate the proposed fluoroalkyl-carbene complex (XXV) is quite intriguing. Further studies of the reactivity of these complexes would be valuable as it could form the basis for new catalysis involving the carbene intermediate.

1.5 Iron Difluorocarbene Complexes

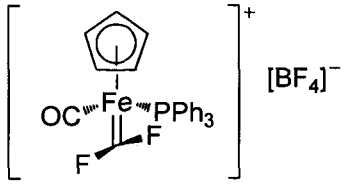

(XXXVI)

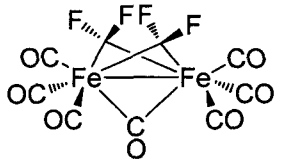

(XXXVII)

Figure 8: Terminal and bridging iron difluorocarbene complexes.

There is precedent for the formation of fluoro-carbene complex (XXV) based upon the synthesis and isolation of several iron difluorocarbene complexes. Difluorocarbene complexes of iron have been prepared with both the terminal,[37,38] $[CpFeL(CO)(CF_2)][BF_4]$ where L = CO or PPh_3, and bridging coordination modes, μ-carbonyl(di-μ-difluoromethylene)bis(tricarbonyliron), as shown in Figure 8.[39] Terminal difluorocarbene complexes have been synthesized using BF_3 as the Lewis acid. Fluoride abstraction by BF_3 from $[CpFe(CO)_2CF_3]$ generated the complex $[CpFe(CO)_2(CF_2)][BF_4]$ as determined by a tensimetric titration, IR spectroscopy and elemental analysis.[37] This extremely moisture sensitive complex easily undergoes hydrolysis to yield $[CpFe(CO)_3][BF_4]$. Partial hydrolysis also occurs when dissolved in polar solvents such as CH_3CN or CH_3NO_2, thus making characterization by NMR impossible.

Phosphine substitution for one of the CO ligands leads to the more stable complex (XXXVI) by reacting BF_3 with $[CpFe(CF_3)(CO)(PPh_3)]$.[38] PPh_3 is a better electron donor than CO; since the dihalocarbene behaves as a π-acid, the PPh_3-substituted complex would be expected to provide more stabilization for carbene formation. $[CpFe(CF_2)(CO)(PPh_3)][BF_4]$ has been crystallographically characterized. Variable temperature ^{19}F NMR of the carbene complex indicates that there is a low barrier to rotation about the $Fe{=}CF_2$ bond as there is only a single peak due to the difluorocarbene from room temperature to -80°C.

When attempts were made to extend this reactivity to perfluorometallacycles, specifically with the nickelacycle $Ni(PEt_3)_2(CF_2)_4$, fluoride abstraction with BF_3 was achieved; however, the electrophilic carbene was only transiently stable.[40] Phosphine migration from the metal center led to the ylide complex (XXXVIII). Fluoride abstraction from the metallacycle $Fe(CF_2)_4(CO)_4$ was attempted, but the complex was found to be unreactive with BF_3.[40] No further attempts toward carbene formation from fluorometallacycles have been reported.

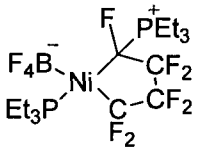

(XXXVIII)

Figure 9: Ylide-like structure resulting from phosphine migration following fluoride abstraction from nickelacycle $Ni(CF_2)_4(PEt_3)_2$.

In this thesis, efforts to explore the effect of ancillary ligands on the formation of three- versus five-membered metallacycles on iron from TFE are described. As well, attempts to generate and characterize carbene complexes from the metallacycles are examined. Finally, results in the investigation of the reactivity of vinylidene fluoride with a variety of iron complexes are presented.

1.6 References

[1] Baker, R.T.; Beatty, R.P.; Farnham, W.B.; Wallace, R.L. Jr. *US Patent* 5,760,282, **1998**.

[2] Chambers, R.D. *Fluorine in Organic Chemistry, 2nd Ed.*; Blackwell: Oxford, **2004**.

[3] Scott, B.F.; Spencer, C.; Mabury, S.A.; Muir, D.C.G. *Environ. Sci. Technol.* **2006**, *40*, 7167.

[4] Hughes, R.P. *Adv. Organomet. Chem.* **1990**, *31*, 183.

[5] Stone, F.G.A. *Pure Appl. Chem.* **1972**, *30*, 551.

[6] Cramer, R.; Kline, J.B.; Roberts, J.D. *J. Am. Chem. Soc.* **1969**, *91*, 2519.

[7] Green, M.; Osborn, R.B.L; Rest, A.J.; Stone, F.G.A. *Chem. Commun.* **1966**, 502.

[8] Green, M.; Osborn, R.B.L; Rest, A.J.; Stone, F.G.A. *J. Chem. Soc. (A)* **1968**, 2525.

[9] Jarvia, A.C.; Kemmitt, R.D.W. *J. Organomet. Chem.* **1974**, *81*, 415.

[10] Evans, J.A.; Russell, D.R. *Chem. Commun.* **1971**, 197.

[11] Cramer, R.; Parshall, G.W. *J. Am. Chem. Soc.* **1965**, *87*, 1392.

[12] Beveridge, A.D.; Clark, H.C. *J. Organomet. Chem.* **1968**, *11*, 601.

[13] Clark, H.C.; Tsai, J.H. *Inorg. Chem.* **1966**, *5*, 1407.

[14] Clark, H.C.; Cotton, J.D.; Tsai, J.H. *Inorg. Chem.* **1966**, *5*, 1582.

[15] Green, M.; Howard, J.A.K.; Laguna, A.; Murray, M.; Spencer, J.L.; Stone, F.G.A. *J.C.S. Chem. Comm.* **1975**, 451.

[16] Cundy, C.S.; Green, M.; Stone, F.G.A. *J. Chem. Soc. (A)*, **1970**, 1647.

[17] Kuwae, R.; Kawakami, K.; Tanaka, T. *Inorg. Chim. Acta.*, **1977**, *22*, 39.

[18] Mukhadkar, A.J.; Mukhedkar, V.A.; Green, M.; Stone, F.G.A. *J. Chem. Soc. (A)*, **1970**, 3166.

[19] Manuel, T.A.; Stafford, S.L.; Stone, F.G.A. *J. Am. Chem. Soc.* **1961**, *83*, 249.

[20] Coyle, T.D.; Kings, R.B.; Pitcher, E.; Stafford, S.L.; Treichel, P.; Stone, F.G.A. *J. Nucl. Inorg. Chem.* **1961**, *20*, 172.

[21] Green, M. Shakshooki, S.K.; Stone, F.G.A *J. Chem. Soc. (A)* **1971**, 2828.

[22] Empsall, H.D.; Green, M.; Stone, F.G.A. *J. Chem. Soc. (A)* **1972**, 96.

[23] Wilke, G. *Pure Appl. Chem.* **1978**, *50*, 677.

[24] Fields, R.; Germain, M.M.; Haszeldine, R.N.; Wiggans, P.W. *Chem. Comm.* **1967**, 243.

[25] Fields, R.; Germain, M.M.; Haszeldine, R.N.; Wiggans, P.W. *J. Chem. Soc. (A).* **1970**, 1969.

[26] Burt, R.; Cooke, M.; Green, M. *J. Chem. Soc. (A)* **1970**, 2975.

[27] Ashley-Smith, J.; Green, M.; Wood, D.C. *J. Chem. Soc. (A)* **1970**, 1847.

[28] Ashely-Smith, J.; Green, M.; Stone, F.G.A. *J. Chem. Soc. (A)* **1970**, 3161.

[29] Hitchcock, P.B.; Mason, R. *Chem. Comm.* **1967**, 242.

[30] Hunt, R.L.; Roundhill, D.M.; Wilkinson, G. *J. Chem. Soc. (A)* **1967**, 982.

[31] Watterson, K.F.; Wilkinson, G. *Chem. and Ind.* **1960**, 1358.

[32] Watterson, K.F.; Wilkinson, G. *Chem. and Ind* **1959**, 991.

[33] Coyle, T.D.; King, R.B.; Pitcher, E.; Stafford, S.L.; Treichel, P.; Stone, F.G.A. *J. Inorg. Nuclear Chem.* **1961**, *20*, 172.

[34] Fields, R.; Germain, M.M.; Haszeldine, R.N.; Wiggans, P.W. *J. Chem. Soc. (A) Inorg. Phys. Theor.* **1970**, 1964.

[35] Harmjanz, M. *et al.,* submitted for publication, **2010**.

[36] Gasafi-Martin, W.; Oberendfellner, G.; von Werner, K. *Can. J. Chem.* **1996**, *74*, 1922.

[37] Richmond, T.G.; Crespi, A.M.; Shriver, D.F. *Organometallics* **1984**, *3*, 314.

[38] Crespi, A.M.; Shriver, D.F. *Organometallics* **1985**, *4*, 1830.

[39] (a) Seel, F.; Röschenthaler, G.V. *Z. Anorg. Allg. Chem.* **1971**, *386*, 297. (b) Seel, F.; Röschenthaler, G.V. *Angew. Chem. Int. Ed.* **1970**, *9*, 166.

[40] Burch, R.R.; Calabrese, J.C.; Ittel, S.D. *Organometallics, **1988,** 7,* 1642.

Chapter 2: Experimental Methods

2.1 General Procedures

2.1.1 Reaction Conditions

Synthetic experiments were carried out at room temperature, unless otherwise stated, using standard glove box and Schlenk line techniques under an inert atmosphere of N_2. All stirred reactions employed a Teflon-coated magnetic stir bar in glassware dried at 115°C in an oven and cooled under vacuum. All reactions performed in NMR tubes (NORELL™ J Young valve NMR tubes with Teflon valve screw caps) were carried out without stirring, but inverted several times periodically throughout the course of the reaction.

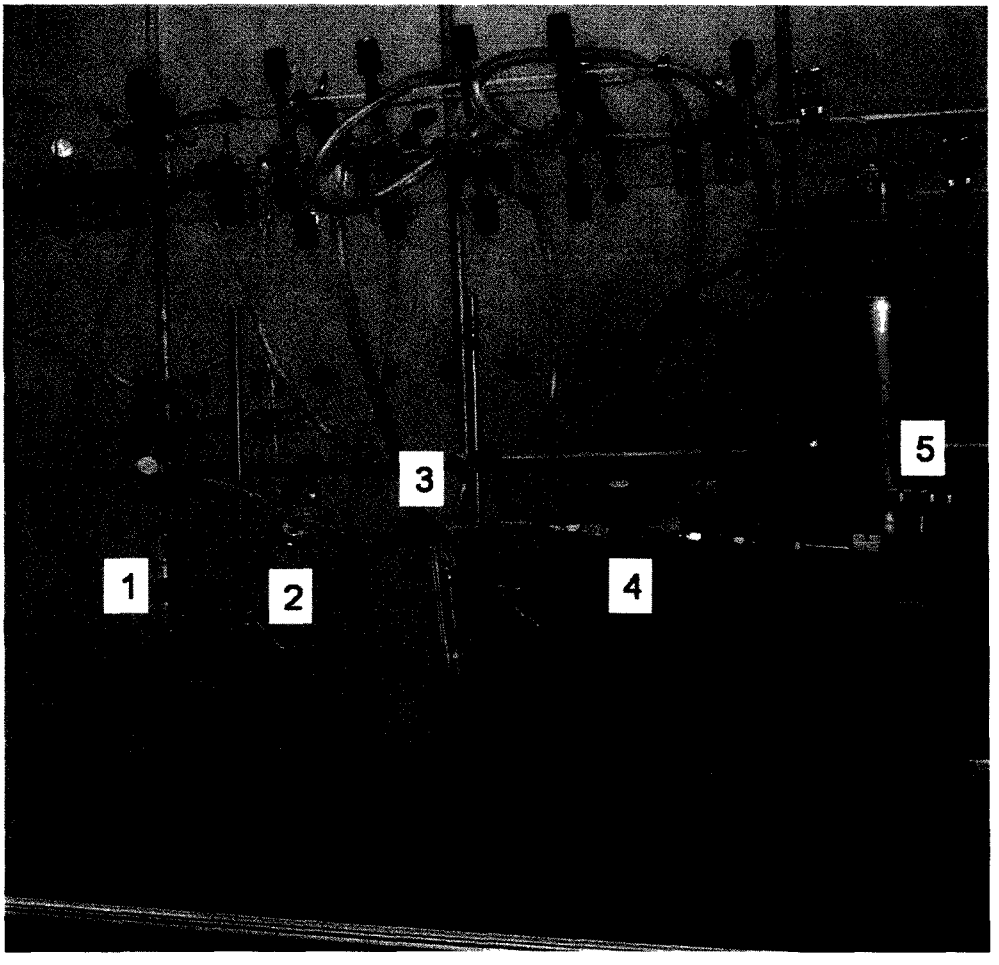

Figure 1: Gas apparatus with valves labeled.

All reactions involving gases were performed in either a NORELL™ J Young valve NMR tube or an Airfree® storage vessel with a Teflon valve screw cap equipped with a Teflon coated stir bar. The gas administering apparatus included: a three-way valve (**2**) between the reaction vessel, Schlenk line and gas cylinder. A bubbler with a pressure release valve (**3**) was connected between the lecture bottle of gas equipped with a valve (**4**) and the aforementioned three-way valve (**2**). The general procedure for gas reactions is as follows: prepare the reaction mixture, other than the gas, inside the glove box and seal the reaction vessel by completely closing the Teflon screw cap (**1**); attach the reaction vessel to the side of the three-way valve (**2**) not connected to the Schlenk line or gas cylinder via the bubbler. With the cap on the reaction vessel (**1**), gas cylinder (**4**) and (**5**), and check valve on the bubbler (**3**) all closed, the entire apparatus is evacuated through the Schlenk line via vacuum. After evacuating the apparatus, with the check valve on the bubbler (**3**) opened, it is refilled with N_2; the evacuation and refilling procedure is repeated twice, for a total of three times. The reaction mixture is then degassed by two or three freeze-pump-thaw cycles. The gas is added by first opening the valve (**5**) directly on the lecture bottle, while keeping the additional valve (**4**) closed. The three-way valve (**2**) is adjusted so that the apparatus is isolated from the Schlenk line. Next the valve on the bubbler (**3**) is opened, the valve on the reaction vessel (**1**) opened slowly to prevent the solvent from bumping up into the apparatus, and finally the valve on the gas lecture bottle (**4**) is opened slowly until bubbles start to form in the oil of the bubbler. This valve is then quickly closed (**4**), and the valve on the reaction vessel (**1**) closed (at the same time if possible). The valve on the bubbler (**3**) is closed, as well as the main valve on the lecture bottle (**5**), and the entire apparatus evacuated via the Schlenk line to ensure that the valve on the reaction vessel (**1**) is completely closed and no gas can escape. Lastly, the entire apparatus is purged with N_2 with the valve on the bubbler (**3**) opened for several minutes to remove any excess gas. To prevent wasting gas, the pieces of tubing for all of the connections are as short as possible.

UV lamp used in photolysis reactions was a high UVB mercury vapour 160 watt flood lamp with a UVB output of 150 $\mu W/cm^2$. The UV lamp was placed approximately 8-10"

away from the reaction mixture, and heats the air in proximity of the reaction vessel to 45 °C.

2.1.2 Solvents

Dry, oxygen-free toluene and hexanes (HPLC grade) were obtained using an MBraun solvent purification system and stored over Linde 4 Å activated molecular sieves. Acetonitrile, anhydrous 99.8%, was opened in the glove box and stored over Linde 4 Å activated molecular sieves and used as is. Other solvents were purified and degassed by distillation. THF and diethyl ether were distilled from Na and benzophenone. Methanol was distilled from CaH_2. Chlorobenzene was vacuum transferred from P_2O_5. Deuterated solvents were purchased from Cambridge Isotope Laboratories. C_6D_6 was distilled from sodium and benzophenone. CD_3CN was distilled from CaH_2.

2.1.3 Reagents

Most commercial reagents were purchased from Aldrich and used without further purification. $[FeCp(CO)_2]_2$, anhydrous $FeCl_2$, 1,2-bis(diphenylphosphino)ethane, and $B(C_6F_5)_3$ were purchased from Strem. $B(C_6F_5)_3$ was purified by sublimation at 86°C under reduced pressure. Magnesium turnings, $BF_3{\cdot}Et_2O$ and PPh_3 were purchased from Alfa Aesar. Trimethylsilyltrifluoromethanesulfonate was purchased from Fluka. Tetrafluoroethylene and 1,1-difluoroethylene were purchased from SynQuest Labs. Triisopropyl phosphite was dried by distilling from sodium under reduced pressure.

2.1.4 NMR Spectroscopy

^1H (300, 400, or 500 MHz), ^{19}F (282, 376 or 471 MHz)), $^{19}F\{^1H\}$ (282 or 376 MHz), $^{31}P\{^1H\}$ (121 MHz), ^{11}B and $^{11}B\{^1H\}$ (96 or 160 MHz), $^{13}C\{1H\}$ (75 or 126 MHz), and 2D-correlation spectra (^{19}F-^{19}F COSY, ^{19}F-^{13}C HMQC) were recorded on an Bruker Avance-300 ($^1H/^{13}C/^{31}P/^{19}F/^2H$ QNP probe with Z gradient), Avance-400 (broadband probe with

Z gradient) and Avance-500 (inverse broadband probe with Z gradient) spectrometers at 25°C. All samples were prepared in the glove box using Teflon screw valve J Young NMR tubes. The spectral widths used for the acquisition of NMR spectra, unless otherwise noted, were δ (ppm): ^{1}H, + 15 to – 5; ^{19}F, 0 to – 200, $^{31}P\{^{1}H\}$, + 200 to – 50, ^{11}B, + 150 to - 150, $^{13}C\{^{1}H\}$, + 350 to – 100. Coupling constants are given as absolute values in Hz. ^{1}H and ^{13}C NMR spectra were referenced to residual solvent peaks. ^{31}P NMR spectra were externally referenced to 85% H_3PO_4 at δ 0.0 ppm. ^{19}F NMR spectra were externally referenced to trifluoroacetic acid in D_2O at δ -76.55 ppm or trifluorotoluene at -63.72 ppm. ^{11}B NMR spectra were externally referenced to $BF_3 \cdot Et_2O$ at 0.0 ppm.

2.1.5 IR Spectroscopy

FT-IR spectra were obtained on a Varian 640-IR FT-IR spectrometer over a range of 4000-700 cm-1; a Nujol mull of the solid was prepared and placed between two NaCl disks. The IR spectrum for complex [17] was obtained in a solution of toluene, in a solution cell containing two NaCl plates.

2.1.6 X-ray Diffraction

X-ray diffraction (XRD) analysis of single crystals was performed by Dr. Ilia Korobkov. Data for the structures of [1] and [17] were collected at 200 K on a Bruker Kappa X8 APEX CCD single-crystal diffractometer equipped with a sealed Mo tube and graphite monochromator (λ = 0.71073 Å). The crystals were mounted in Hampton cryoloop using light oil to prevent exposure to air and water. The SHELX software package (Bruker) was used to solve and refine the structure.[1] An empirical absorption correction was applied using the SADABS program.[2] The structure was solved by direct methods and refined by the full-matrix least-squares method minimization of $(\Sigma w(Fo - Fc)^2)$.

2.2 Synthesis of Iron Fluoro-metallacycle Complexes

2.2.1 Synthesis of perfluorotetramethyleneiron tetracarbonyl [1] ($Fe(CF_2)_4(CO)_4$), Method 1

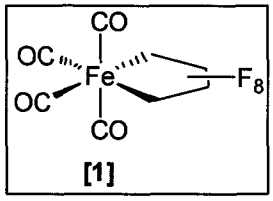

[1]

A two-necked round bottom flask with a ground-glass stopcock was equipped with a magnetic stir bar and 20 mL of hexanes. A balloon was attached to one neck of the flask, a solid addition arm containing $Fe_2(CO)_9$ (1.060 g, 2.91 mmol) was attached to the second neck and the stopcock was connected to tubing to the gas cylinder of TFE. The balloon was inflated with TFE. The solution was magnetically stirred for 30 minutes. The $Fe_2(CO)_9$ was added to the mixture from the solid addition arm. The solution was swirled back into the solid addition arm to get all residual solid. After 12 hours of stirring, the balloon was not completely deflated; a red/brown precipitate had formed in a green solution. After stirring for 4 days, the resulting red/brown residue was rinsed with hexanes and filtered through a frit to give 0.439 g of orange powder, and an opaque solution. The solvent was removed from the filtrate via vacuum to give a black/green waxy residue.

2.2.2 Improved synthesis of perfluorotetramethyleneiron tetracarbonyl [1] ($Fe(CF_2)_4(CO)_4$), Method 2

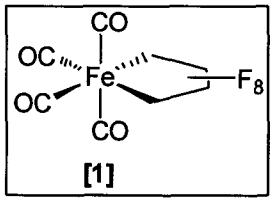

[1]

Following a variation to a literature preparation,[3] $Fe_2(CO)_9$ (0.980 g, 2.69 mmol) was transferred to a 100 mL Schlenk tube with a Teflon stopcock. 20 mL of hexanes was added; stirring gave an orange slurry in a green solution. TFE was added via the method described in section 2.1.1 using the gas apparatus, and the resulting mixture was stirred and irradiated with the UV lamp for 24 hours to give an opaque black solution with an orange precipitate. The mixture was cannula-transferred and filtered through Celite and a frit on the Schlenk line. The residue on the Celite/frit was rinsed with 2-3 mL of hexanes three times until it ran colorless. The clear yellow/brown solution was stored in the glove box fridge. Pale beige needles precipitated (187 mg, 18.7 % yield) from solution overnight and were collected on a chilled frit. ^{19}F NMR (282 MHz, C_6D_6, 298 K,

δ): -72.29 (s, 4F, α-CF_2); -137.18 (s, 4F, β-CF_2). $^{13}C\{^1H\}$ NMR (75 MHz, C_6D_6, 298 K, δ): 114.39 (trtr, $^1J_{CF}$ = ca. 275 Hz, $^2J_{CF}$ = 25 Hz, 2C, β-CF_2); 140.59 (tr, $^1J_{CF}$ = ca, 310 Hz, 2C, α-CF_2); 196.44 (app quint, $^3J_{CF}$ = ca. 7 Hz, 2C, CO); 196.91 (app quint, $^3J_{CF}$ = ca. 8 Hz, 2C, CO). IR (Nujol mull, NaCl plates, cm^{-1}): 2163 (wk, C≡O); 2095 (med, C≡O); 2075 (med, C≡O); C-F in region 1300-1000: 1263 (wk); 1168 (wk); 1103 (wk); 1065(wk, br); 972(wk); 908 (wk, br); 723 (wk). The orange precipitate was analyzed; IR (Nujol mull, NaCl plates, cm^{-1}): 1459 (str, C=O); 1377 (str, C=O). Colorless needle-shaped crystals were obtained from the solution and analyzed by single crystal X-ray diffraction (XRD). See Appendix B for further XRD details.

2.2.3 Synthesis of (triisopropylphosphite)iron tetracarbonyl [2] ($Fe[P(O^iPr)_3](CO)_4$) and bis(triisopropylphosphite)iron tricarbonyl [3] ($Fe[P(O^iPr)_3]_2(CO)_3$)

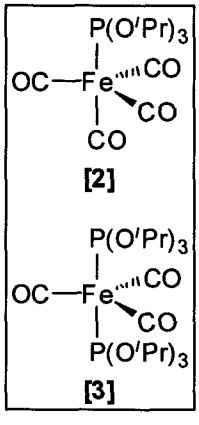

$Fe_2(CO)_9$ (1.001 g, 2.75 mmol) and $P(O^iPr)_3$ (5.730 g, 27.5 mmol) were combined in a 100 mL Schlenk tube and dissolved in 20 mL of toluene. The resulting mixture was stirred under static vacuum on the Schlenk line and irradiated with the UV lamp for 1 hour. The reaction mixture's appearance changed from an opaque, dark green solution to a dark black/green solution with green residue/precipitate on the sides of the flask. The reaction mixture was stirred overnight with no further irradiation. The mixture was then cannula-filtered into an evacuated flask on the Schlenk line. The filtrate was a clear pale olive solution and the residue was a dark green black oily solid. Approximately half of the solvent was evaporated from the filtrate via vacuum on the Schlenk line resulting in a color change to cloudy, dark green. The remaining solvent was removed yielding a brown, waxy solid. The residue was digested with hexanes to give an opaque brown solution, which was filtered to give a clear yellow/brown solution. Removing the solvent *in vacuo* yielded a yellow, gel-like solid. $^{31}P\{^1H\}$ NMR (121 MHz, C_6D_6, 298 K, δ): 170.65 (s, 1P,[2]); 183.37 (s, 2P, [3]). Relative integrals of [2]:[3] = 1:2.2. $^{13}C\{^1H\}$ NMR (75 MHz, C_6D_6, 298 K, δ): 23.97 (s, 2C, $P(OCH(\mathbf{C}H_3)_2)_3$, [2]); 24.30 (s, 4C, $P(OCH(\mathbf{C}H_3)_2)_3$, [3]); 70.43 (s, 2C, $P(O\mathbf{C}H(CH_3)_2)_3$, [3]); 71.89 (s, 1C, $P(O\mathbf{C}H(CH_3)_2)_3$, [2]); 213.77 (d, $^3J_{CF}$ = 24 Hz, 4C, CO, [2]); 213.82 (t, $^3J_{CF}$ = 39 Hz, 3C, CO, [3]).

2.2.4 Synthesis of *cis*-bis(triisopropylphosphite) perfluorodimethyleneiron dicarbonyl [4], *trans*-bis(triisopropylphosphite) perfluorodimethyleneiron dicarbonyl [5] ($Fe(CF_2)_2[P(O^iPr)_3]_2(CO)_2$) and triisopropylphosphite perfluorotetramethyleneiron dicarbonyl [6] ($Fe(CF_2)_4[P(O^iPr)_3](CO)_3$)

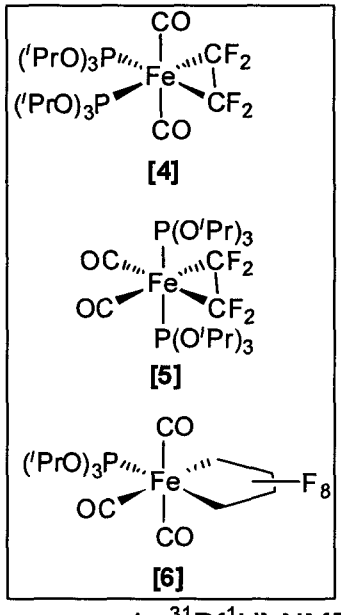

The mixture of [2] and [3] (0.300 g) was dissolved in 2 mL of toluene to give a clear, pale yellow solution. TFE was added using the gas apparatus; the resulting mixture was stirred and irradiated with the UV lamp (without irradiation, the starting material is unreactive towards TFE). After 1 hour of irradiation, the color changed to a clear, pale green solution. Following 6 hours of irradiation, the color had deepened to a bright green. Stirring the reaction mixture overnight without irradiating resulted in a color change to a clear, yellow/brown solution. Irradiating the solution for 2 hours changed the color back to a bright green. The solvent was removed via vacuum to give a green gel. $^{31}P\{^1H\}$ NMR (121 MHz, C_6D_6, 298 K, δ): 140.74 (s, $P(O^iPr)_3$); 155.91 (s, 2P, [4] and [5]); 165.67 (s, [6]); 170.49 (s, 1P, [2]); 183.47 (s, 2P, [3]). ^{19}F NMR (282 MHz, C_6D_6, 298 K, δ): -75.60 (s, 2F, α-CF_2, [6]); -79.26 (s, 2F, α-CF_2, [6]); -111.56 (s, 4F, [4]); -112.27 (s, 4F, [5]) -137.21 (s, 2F, β-CF_2, [6]); -137.98 (s, 2F, β-CF_2, [6]). $^{13}C\{^1H\}$ NMR (75 MHz, C_6D_6, 298 K, δ): 24.16 (s, 2C, $P(OCH(\mathbf{C}H_3)_2)_3$, [2]); 24.30 (s, 4C, $P(OCH(\mathbf{C}H_3)_2)_3$, [3]); 70.48 (s, 2C, $P(O\mathbf{C}H(CH_3)_2)_3$, [3]); 71.64 (d, J = 5 Hz, 1C, $P(O\mathbf{C}H(CH_3)_2)_3$, [2]); 204.06 (mult, CO); 207.31 (mult, CO); 213.81 (d, $^3J_{CF}$ = ca. 35 Hz, 4C, CO, [2]); 213.91 (tr, $^3J_{CF}$ = 39 Hz, 3C, CO, [3]).

2.2.5 Synthesis of *trans*-bis(triisopropylphosphite) perfluorotetramethyleneiron dicarbonyl [7] and *cis*-bis(triisopropylphosphite) perfluorotetramethyleneiron dicarbonyl [8] ($Fe(CF_2)_4[P(O^iPr)_3]_2(CO)_2$)

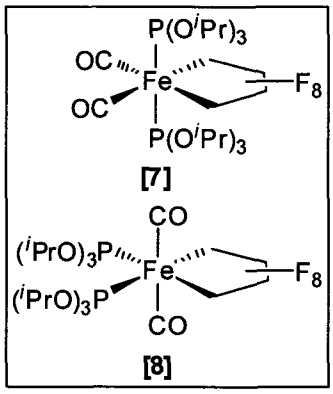

Complex [1] (0.010 g, 0.027 mmol), was dissolved in 10 drops of C_6D_6 in a vial to give a clear, pale beige solution. A clear, colorless solution of $P(O^iPr)_3$ (0.022 g, 0.106 mmol) in 10 drops of C_6D_6 was added drop-wise to give a clear, pale beige solution. No change in appearance was observed after stirring the reaction mixture for 24 hours. An aliquot was analyzed by NMR spectroscopy after approximately 30 hours of stirring. $^{31}P\{^1H\}$ NMR (121 MHz, C_6D_6, 298 K, δ): 140.40 (s, $P(O^iPr)_3$); 183.94 (s, [2]). The solution was heated in a sand bath at 80°C in a vial in the glove box for 30 hours to give a clear, colorless solution. $^{31}P\{^1H\}$ NMR (121 MHz, C_6D_6, 298 K, δ): 140.40 (s, $P(O^iPr)_3$); 183.94 (s, [2]). The reaction mixture was stirred in a capped vial under N_2, and irradiated with the UV lamp. After 21 hours of irradiation, there was a slight color change to a very pale yellow. $^{31}P\{^1H\}$ NMR (121 MHz, C_6D_6, 298 K, δ): 6.06 (s); 140.70 (s, $P(O^iPr)_3$); 153.58 (app quint, J_{PF} = 19.7 Hz, 2P [8]); 157.05 (mult, J_{PF} = ca. 20, 7 Hz, 2P [7]). ^{19}F NMR (282 MHz, C_6D_6, 298 K, δ): -72.78 (s, 4F, α-CF_2 [1]); -81.16 (app tr, J_{PF} = 19.7 Hz, 4F, α-CF_2 [8]); -91.05 (d, J_{PF} = 27 Hz, 4F, α-CF_2 [7]); -125.48 (s, 4F, β-CF_2 [7]); -137.18 (s, 4F, β-CF_2 [1]); -138.42 (s, 4F, β-CF_2 [8]).

2.2.6 Synthesis of triphenylphosphineiron tetracarbonyl [9] ($Fe(PPh_3)(CO)_4$) and bis(triphenylphosphine)iron tricarbonyl [10] ($Fe(PPh_3)_2(CO)_3$)

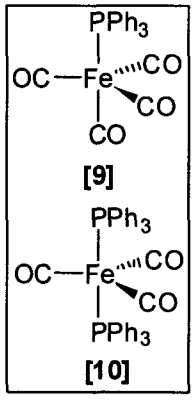

The known compounds [9] and [10] were prepared according to a variation on the literature method.[4] $Fe_2(CO)_9$ (0.098 g, 0.269 mmol) and PPh_3 (0.076 g, 0.290 mmol) were combined in a Schlenk tube and dissolved in 5 mL of diethyl ether to give a dark green solution with an orange suspension. Stirring the reaction mixture overnight gave a mint green precipitate in a dark green solution. The mixture was filtered through a frit to give a clear dark green solution, and 20 mg of a

beige/mint green powder [10]. Solvent was removed via vacuum from the solution fraction, to give 45 mg of a green crystalline solid. $^{31}P\{^1H\}$ NMR (121 MHz, C_6D_6, 298 K, δ): 82.59 (s, [10]). $^{31}P\{^1H\}$ NMR (121 MHz, C_6D_6, 298 K, δ): 71.94 (s, [9]); 82.60 (s, [10]). Relative integration [9]:[10] 1:0.1.

2.2.7 Synthesis of triphenylphosphine perfluorotetramethyleneiron tricarbonyl [11] ($Fe(CF_2)_4(PPh_3)(CO)_3$), *trans*-bis(triphenylphosphine) perfluorodimethyleneiron dicarbonyl [12] and *cis*-bis(triphenylphosphine) perfluorodimethyleneiron dicarbonyl [13] ($Fe(CF_2)_2(PPh_3)_2(CO)_2$)

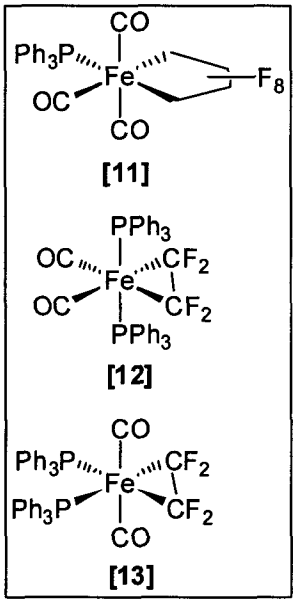

The mixture of [9] and [10] (1:0.1, 0.010 g), was dissolved in 1 mL C_6D_6 to give a clear dark green solution. In a J Young NMR tube, TFE was added to the solution and the mixture was irradiated with U.V. light for 19 hours to give a pale yellow solution with a brown precipitate. ^{19}F NMR (282 MHz, C_6D_6, 298 K, δ): -74.51 (s, 2F, α-CF_2,, [11]); -82.12 (s, 2F, α-CF_2, [11],); -113.38 (s, 4F, [12]); -116.90 (s, 4F, [13]); -139.57 (s, 2F, β-CF_2, [11]); -139.98 (s, 2F, β-CF_2, [11]). $^{31}P\{^1H\}$ NMR (121 MHz, C_6D_6, 298 K, δ): -5.69 (s, PPh_3); 24.39 (s, 1P, [11]); 49.09 (s, 2P, [12]); 56.63 (s, 2P, [13]); 71.96 (s, [9]); 82.61 (s, [10]). Relative integration [11]:[12]:[13] 1.0:6.1:2.3; relative % yield 19:59:22.

2.2.8 Synthesis of triphenylphosphine perfluorotetramethyleneiron tricarbonyl [11] ($Fe(CF_2)_4(PPh_3)(CO)_3$) and iron carbonyl tetrafluoroethylene clusters.

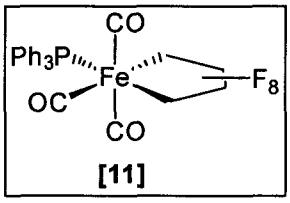

Complex [10] (0.010 g, 0.015 mmol), was dissolved in 1 mL C_6D_6 to give a clear pale green solution. In a J Young NMR tube, TFE was added to the solution and the mixture was irradiated with UV light for 19 hours to give an orange/red solution with a brown precipitate. $^{31}P\{^1H\}$ NMR (121 MHz, C_6D_6, 298 K, δ): -5.68 (s, PPh_3); 22.24 (s, [11]); 82.61 (s, [10]). ^{19}F NMR (282 MHz, C_6D_6, 298 K, δ): many peaks; suggests production of Fe CO TFE clusters.

2.2.9 Synthesis of triphenylphosphine perfluorotetramethyleneiron tricarbonyl [11] ($Fe(CF_2)_4(PPh_3)(CO)_3$), *trans*-bis(triphenylphosphine) perfluorotetramethyleneiron dicarbonyl [14] ($Fe(CF_2)_4(PPh_3)_2(CO)_2$)

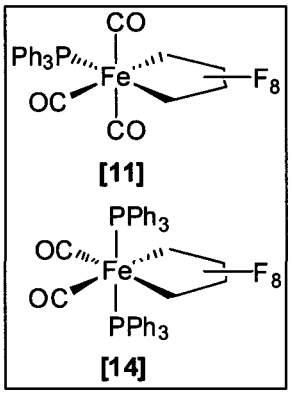

Similar to the method reported for the synthesis of [11],[5] [1] (0.054 g, 0.146 mmol) was dissolved in 1 mL of toluene to give a clear, green solution. A clear, colorless solution of PPh_3 (0.038 g, 0.145 mol) in 3 mL of toluene was added drop-wise to give a clear, green solution. On the Schlenk line, the round bottom reaction flask was equipped with a reflux condenser. The reaction mixture was stirred and heated at 89.1 °C under N_2 for 3 hours. The color of the solution changed to clear, pale yellow. The reaction mixture was allowed to cool to room temperature while stirring under N_2 overnight. The clear, pale yellow, solution was concentrated under vacuum. The solution was stored in a vial in the glove box freezer. Colorless needles formed in the solution (presumed to be unreacted starting material) but redissolved upon warming to room temperature. $^{31}P\{^1H\}$ NMR (121 MHz, toluene, 298 K, δ): -5.65 (s, PPh_3); 24.83 (s, 1P, [11]); 40.80 (unresolved trtr, 2P, [14]); 82.60 (s, [10]). ^{19}F NMR (282 MHz, toluene, 298 K, δ): -72.29 (s, 4F, α-CF_2 [1]); -79.80 (s, 4F, α-CF_2 [14]); -137.45 (s, 4F, β-CF_2 [1]); -137.88 (s, 4F, β-CF_2 [14]).

2.2.10 Synthesis of κ^2-[1,2-bis(diphenylphosphino)ethane]iron tricarbonyl [15] $Fe(\kappa^2\text{-dppe})(CO)_3$) and κ^1-(1,2-bis(diphenylphosphino)ethane)iron tetracarbonyl [16] ($Fe(\kappa^1\text{-dppe})(CO)_4$)

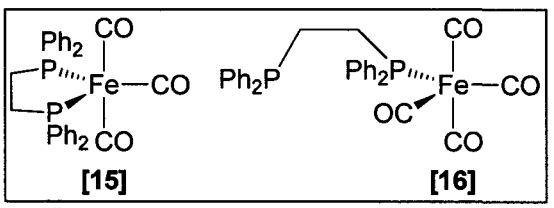

$Fe_2(CO)_9$ (0.506 g, 1.39 mmol) and dppe (1.025 g, 2.57 mmol) were combined in a Schlenk tube and dissolved in 10 mL of diethyl ether to give an orange/brown slurry in an orange/brown solution upon stirring. Stirring the reaction mixture for four days in the glove box yielded a milky, yellow solution with brown residue on the sides of the flask. The reaction mixture was filtered through a frit to give 285 mg of a beige powder, and a clear, bright

yellow solution. The beige powder was unreacted dppe. The solvent was removed from the filtrate via vacuum to give a waxy yellow solid. The solid was dissolved in 10 mL of toluene to give a clear, bright yellow solution and a small amount of insoluble yellow residue. The mixture was filtered through glass wool to give a clear, bright yellow solution. The solvent was removed via vacuum to give a waxy yellow solid (0.757 g, 54 % crude yield of [15]). $^{31}P\{^1H\}$ NMR (121 MHz, CD_3CN, 298 K, δ): -15.74 (s, [16]); 66.46 (s, [15]); 92.93 (s, [16]).

2.2.11 Attempted Synthesis of κ²-[1,2-bis(diphenylphosphino)ethane] perfluorotetramethyleneiron iron dicarbonyl [17] ($Fe(CF_2)_4(dppe)(CO)_2$)

The waxy, yellow solid mixture of [15] and [16] (0.070 g) was dissolved in 1.5 mL of C_6D_6 to give a clear, bright yellow solution. TFE was added; after sitting at room temperature for 2 days, no color change was observed. The reaction mixture, in the NMR tube, was heated in an oil bath at 83 °C overnight. After 18 hours of heating, there was no change in appearance and the reaction mixture was allowed to cool to room temperature. The reaction mixture was irradiated with the UV lamp for 15 hours resulting in no observable color change. $^{31}P\{^1H\}$ NMR (121 MHz, CD_3CN, 298 K, δ): 93.06 (s, [16]). ^{19}F NMR (471 MHz, C_6D_6, 298 K, δ): -132.78 (s, TFE); -137.75 (d, J_{FF} = 56 Hz, octafluorocyclobutane, C_4F_8).

2.2.12 Synthesis of κ²-[1,2-bis(diphenylphosphino)ethane] perfluorotetramethyleneiron dicarbonyl [17] ($Fe(dppe)(CO)_2(CF_2)_4$)

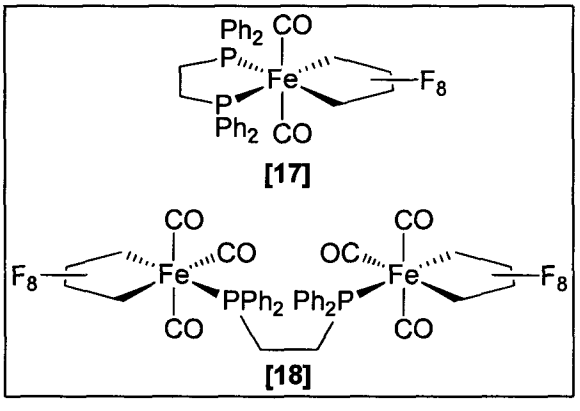

[17]

[18]

Complex [1] (0.093 g, 0.25 mmol) was dissolved in 5 mL of toluene to give a clear, pale green solution. A clear, colorless solution of dppe (0.098 g, 0.25 mmol) in 5 mL of toluene was added drop-wise to give a clear, pale green solution. On the Schlenk line, the round bottom reaction flask was equipped with a reflux condenser. The reaction mixture was stirred and heated at 126.6 °C under N_2 for 3 hours. The colour of

the solution changed to clear, pale yellow. The reaction mixture was allowed to cool to room temperature while stirring under N_2 for 2 days to give a cloudy, pale yellow solution. The reaction mixture was filtered through glass wool to give a clear, pale yellow solution. The solution was concentrated to approximately ¾ of the volume via vacuum and stored in a vial in the glove box freezer; yellow crystals formed, 50 mg were isolated (28 % isolated yield). ^{1}H NMR (300 MHz, CD_3CN, 298 K, δ): 2.811 (s, 2H, CH_2); 2.867 (s, 2H, CH_2); 7.490 (m, 12H, ArH); 7.688 (m, 8H, ArH). ^{19}F NMR (282 MHz, CD_3CN, 298 K, δ): -64.07 (d quart, $^2J_{FF}$ = 253 Hz, $^3J_{FF}$ = 26 Hz, [18]); -72.17 (dd, $^2J_{FF}$ = 272 Hz, $^3J_{FF}$ = 17 Hz, [18]) -75.63 (apparent tr (unresolved dd), $^3J_{FP}$ = ca. 12 Hz, 4F, α-CF_2 [17]); -77.61 (dtr, $^2J_{FF}$ = 252 Hz, $^3J_{FF}$ = 14 Hz, [18]); -91.21 (d quint, $^2J_{FF}$ = 272 Hz, $^3J_{FF}$ = 16 Hz, [18]); -129.07 (dd, $^2J_{FF}$ = 249 Hz, $^3J_{FF}$ = 100 Hz, [18]); -138.27 (s, 4F, β-CF_2 [17]); -142.28 (d mult, $^2J_{FF}$ = 249 Hz, $^3J_{FF}$ = 11, 6 Hz, [18]); -145.59 (d mult, $^2J_{FF}$ = 249 Hz, $^3J_{FF}$ = 11, 6 Hz, [18]). ^{31}P{^{1}H} NMR (121 MHz, CD_3CN, 298 K, δ): 57.53 (app quint, $^3J_{PF}$ = ca. 25 Hz, 2P, [18]); 61.36 (app quint, 3J = ca. 13.5 Hz, 2P, [17]). ^{13}C{^{1}H} NMR (75 MHz, CD_3CN, 298 K, δ): 29.05 (d, J = 9.7 Hz, 1C, CH_2); 29.47 (d, J = 9.4 Hz, 1C, CH_2); 130.31 (tr, J = ca. 5 Hz, 8C, ArC); 132.34 (s, 4C, ArC); 133.43 (d, J = 9.7 Hz, 8C, ArC); 157.95 (s, 4C, ArC); 212.34 (mult, 2C, CO). ^{19}F-^{13}C HMQC (471 MHz,, 250 Hz coupling, CD_3CN, 298 K, δ): -75.61, 144.06 (α-CF_2); -75.61, 146.66 (α-CF_2); -138.14, 113.62 (β-CF_2); -138.14, 115.73 (β-CF_2). IR (toluene solution, NaCl plates, cm^{-1}): 2037 (med); 1994 (str); 1942 (med); 1859 (wk, br); 1801 (wk, br); 1618 (str); 1586 (str); 1468 (med); 1413 (med); 1389 (str); 1387 (str); 1155 (med); 1102 (med); 1065 (str); 1044 (str); 1022 (str); 952 (med); 895 (str). Yellow crystals were obtained from the solution and analyzed by single crystal X-ray diffraction (XRD). See Appendix B for further XRD details.

2.2.13 Synthesis of pentakis(2,6-dimethylphenylisocyanide)iron [19] (Fe(2,6-$(CH_3)_2C_6H_4NC)_5$)

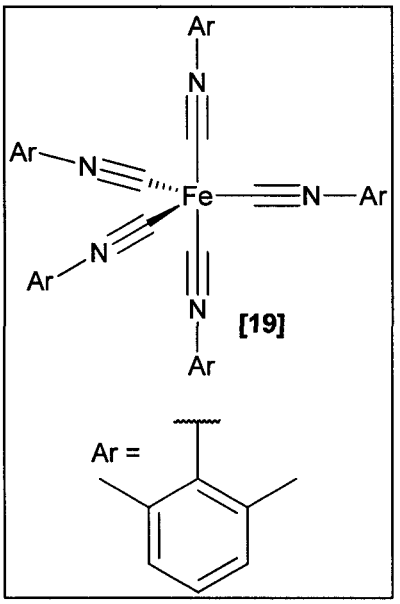

$[Fe(ArNC)_4Cl][FeCl_4]$ was prepared by a published method,[6] and reduced with Mg to give [19]. Anhydrous $FeCl_2$ (0.697 g, 5.50 mmol), a beige powder, was transferred to a Schlenk tube in the glove box. In air, 2,6-dimethylphenyl isocyanide (2.905 g, 22.1 mmol) was transferred to another Schlenk tube. On the Schlenk line, the isocyanide was dissolved in 20 mL of dry MeOH to give a clear, pale peach/yellow solution. The $FeCl_2$ was dissolved in 25 mL of MeOH to give a clear, orange solution, which was then cooled in an ice bath (~3 °C). Using a syringe, the isocyanide solution was added drop-wise to the cooled $FeCl_2$ solution. A precipitate formed in a cloudy yellow/brown solution. The mixture was allowed to warm to room temperature under dynamic N_2 giving a cloudy brown solution with a milky brown precipitate. After stirring for two days, the solution changed to an opaque bright orange colour with a fine beige precipitate. The precipitate, 0.014 g of a beige orange solid, was collected on a frit in the glove box. The filtrate was a clear, bright orange solution. The solvent was removed from the filtrate under vacuum to give an orange oil. The solid was dissolved in a minimum amount of MeOH, giving an opaque, bright orange solution. Cannula filtering into an evacuated 100 mL Schlenk tube yielded a clear bright orange solution. After no crystals formed in the solution over the course of two weeks while stored in the freezer, the solvent was removed under vacuum to give an orange oil. The oil was washed with 10 mL of diethyl ether to yield a yellow/orange flaky precipitate and a clear, bright orange solution. The orange powder (2.113 g, 59 % yield) was collected on a frit.

The orange powder (2.113 g, 3.24 mmol) was dissolved in 20 mL of THF; stirring gave an orange suspension. Under N_2, Mg turnings (0.38 g, 15.6 mmol) were added to the suspension. Upon stirring, the solution turned dark orange, then red, brown, and finally black, to give an opaque black solution. The reaction mixture was stirred under N_2 for

24 hours. The solvent was evaporated under vacuum to give a greasy black solid. The product was extracted into 10 mL of diethyl ether to give a cloudy orange solution, which was then filtered through a frit. Solvent was removed from the filtrate to give the orange powder (0.120 g, 5.2% yield). ^{1}H NMR (500 MHz, C_6D_6, 298 K, δ): 2.43 (s, 30H, CH_3); 6.78 (s, 15H, ArH). $^{13}C\{^{1}H\}$ NMR (75 MHz, C_6D_6, 298 K, δ): 19.68 (s, 10C, CH_3); 125.55 (s, 10C, ArC); 131.16 (s, 5C, ArC); 132.54 (s, 5C, ArC); 133.71 (s, 10C, ArC); 197.08 (s, 5C, CN). IR (Nujol mull, NaCl plates, cm^{-1}): 2033 (med, br, C≡N); 1976 (med, br, C≡N). Comparison of spectroscopic data with literature confirmed production of [19].

2.2.14 Synthesis of tetrakis(2,6-dimethylphenylisocyanide) perfluorodimethyleneiron [20] ($Fe(2,6\text{-}(CH_3)_2C_6H_4NC)_4(CF_2)_2$) and tetrakis(2,6-dimethylphenylisocyanide) perfluorotetramethyleneiron [21] ($Fe(2,6\text{-}(CH_3)_2C_6H_4NC)_4(CF_2)_4$)

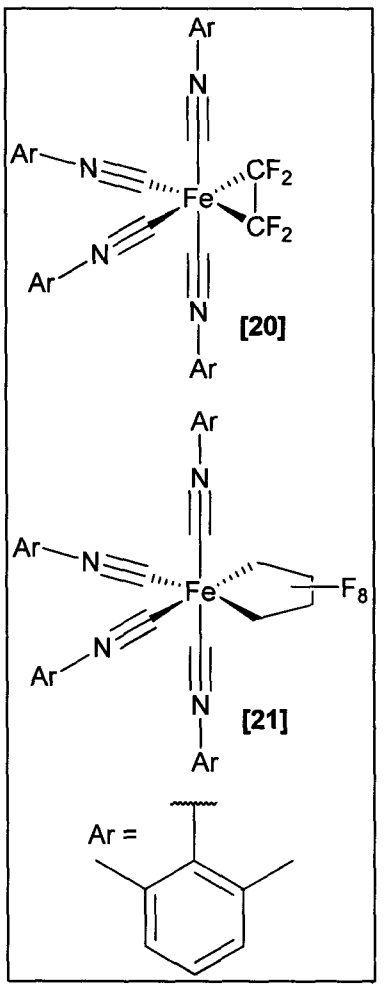

Complex [19] (0.045 g, 0.063 mmol) was dissolved in 8 mL of toluene to give a clear, bright red/orange solution in a 25 mL storage vessel. TFE was added using the gas apparatus and the reaction mixture stirred at room temperature. No color change was initially observed. The resulting solution was stirred for 48 hours to give an opaque, yellow/brown solution. The excess gas and solvent were removed via vacuum to give an oily green/brown residue. The residue was dissolved in 1 mL of THF and filtered through glass wool. The solvent was removed from the filtrate to give a green/brown residue (0.048 g). ^{1}H NMR (500 MHz, C_6D_6, 298 K, δ): 2.33 (s, 12H, CH_3 [20]); 2.34 (s, 12H, CH_3 [21]); 2.35 (s, 12H, CH_3 [20]); 2.36 (s, 12H, CH_3 [21]); 6.58 (d, J_{HH} = 7.7 Hz, 8H, ArH [21]); 6.61 (d, J_{HH} = 7.5 Hz, 8H, ArH [20]); 6.70 (tr, J_{HH} = 7.4 Hz, 4H, ArH [20]); 6.78 (tr, J_{HH} = 7.6 Hz, 4H, ArH [21]). $^{13}C\{^{1}H\}$ NMR (126 MHz, C_6D_6, 298 K, δ): 18.88 (s, 4C, CH_3 [21]); 18.97 (s, 4C, CH_3 [20]); 19.16 (s, 4C, CH_3 [21]);

19.35 (s, 4C, CH_3 [20]); 127.30 (s, 4C, *meta*ArC); 127.76 (s, 4C, *meta*ArC); 128.24 (s, 2C, *para*ArC); 128.30 (s, 2C, *para*ArC); 129.50 (s, 2C, *ipso*ArC); 130.69 (s, 2C, *ipso*ArC); 134.98 (s, 4C, *ortho*ArC); 135.39 (s, 4C, *ortho*ArC); 135.55 (s, 1C, olefin C_F); 135.87 (s, 1C, olefin C_F); 178.20 (s, 2C, CN); 183.29 (s, 2C, CN). ^{13}C peak assignments were made based upon dept-135, see Appendix A. ^{19}F NMR (471 MHz, C_6D_6, 298 K, δ): -83.89 (s, 4F, α-CF_2, [21]); -115.66 (s, 4F, [20]); -136.35 (s, 4F, β-CF_2, [21]). ^{19}F-^{13}C HMQC NMR (471 MHz/126 MHz, C_6D_6, 289 K, δ):-115.63 (^{19}F), 135.45 (^{13}C) ([20]). IR (Nujol mull, NaCl plates, cm^{-1}): 2104 (str, br, C≡N); 2051 (str, br, C≡N); 1727 (med,C=N); 1591 (w, C=N); alkyl fluorides 1300-1000: 1263 (med, br); 1135 (med); 1070 (med); 1004 (med); 945 (med); 894 (med); 784 (med); 666 (med).

2.2.15 Synthesis of potassium cyclopentadienyliron dicarbonyl [22] ($K[FeCp(CO)_2]$)

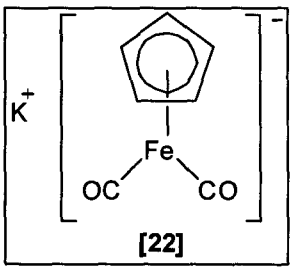

[22]

$[FeCp(CO)_2]_2$ (3.040 g, 8.59 mmol) was dissolved in 60 mL of THF to give an opaque, red/purple solution. Adding potassium (1.33 g, 34.0 mmol) and stirring yielded a very dark opaque solution. On the Schlenk line, the round bottom flask was equipped with a reflux condenser. The reaction mixture was heated at 65°C in an oil bath and stirred under dynamic nitrogen for 3 days. The resulting opaque, dark black solution, with a small amount of black precipitate was cooled to room temperature and cannula-filtered to an evacuated Schlenk tube to give a waxy black residue and an opaque black/brown solution for the filtrate. The solvent was removed from the filtrate *in vacuo* to give an orange residue. The residue was dissolved in 20 mL of CH_3CN and filtered through a frit to give a black residue and dark red solution. Solvent was removed from the filtrate via vacuum to give an orange powder (1.697 g, 46 % crude yield). ^1H NMR (500 MHz, CD_3CN, 298 K, δ): 4.24 (s, 5H, Cp [22]); 5.62 (s, 5H, KCp). Relative integrals: 0.89:1.00. $^{13}C\{^1H\}$ NMR (126 MHz, CD_3CN, 298 K, δ): 77.24 (s, KCp); 105.54 (s, 5C, Cp [22]); 229.60 (s, 2C, CO [22]). IR (Nujol mull, NaCl plates, cm^{-1}): 1866 (wk, br, C=O); 1766 (wk, br, C=O); 1159 (wk, br); 975 (wk, br).

2.2.16 Synthesis of two potassium cyclopentadienyl perfluorotetramethyleneiron carbonyl complexes [23] and [24] K[FeCp$(CF_2)_4$(CO)]

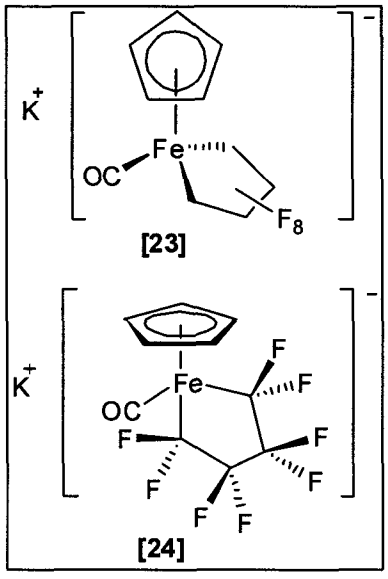

[22] (0.300 g, 1.39 mmol) was dissolved in 5 mL of CH_3CN to give a clear, red/orange solution in a 25 mL storage vessel. Adding TFE resulted in an almost instant color change to a darker blood red. The reaction mixture was stirred at room temperature for 40 hours to give an opaque, very dark red solution. Residual gas and solvent were removed under vacuum a waxy purple solid. The solid was washed with 2-3 mL of diethyl ether and the solvent decanted off to give an opaque, dark red solution. The remaining residue was dried under vacuum to give a red brown powder (0.121 g, 22 %). ^1H NMR (500 MHz, CD_3CN, 298 K, δ): 4.88 (s, 10H, [FeCp$(CO)_2]_2$); 4.92 (s, Cp); 5.01 (s, Cp); 5.11 (s, Cp, [24]) Relative integration: 1.00:0.11:0.11:0.14. $^{13}C\{^1H\}$ NMR (126 MHz, CD_3CN, 298 K, δ): 86.69 (s, 5C, Cp, [FeCp$(CO)_2$] derivative); 87.13 (s, 5C, Cp [24]); 87.29 (s, 5C, Cp, [FeCpCO$)_2$] derivative); 89.86 (s, 5C, [FeCp$(CO)_2]_2$); 129.32 (mult, 4C, C_F, [24]); 214.95 (s, CO, [FeCp$(CO)_2$] derivative); 215.18 (s, CO [24]); 216.67 (s, CO [FeCp$(CO)_2]_2$). ^{19}F NMR (282 MHz, CD_3CN, 298 K, δ): -56.56 (dd, $^2J_{FF}$ = 59 Hz, [23]); -61.34 (tr, $^3J_{FF}$ = 4.7 Hz, 2F, α-CF_2 [24]); -61.36 (tr, $^3J_{FF}$ = 4.7 Hz, 2F, α-CF_2 [24]); -84.01 (d, $^2J_{FF}$ = 58 Hz, [23]); -105.50 (d, $^2J_{FF}$ = 55 Hz); -113.37 (d, $^2J_{FF}$ = 56 Hz); -120.84 (dd, $^2J_{FF}$ = 57, $^3J_{FF}$ = 2.5 Hz); -123.65 (d, $^2J_{FF}$ = 58 Hz); -126.76 (tr, $^3J_{FF}$ = 4.6 Hz, 2F, β-CF_2, [24]); -126.96 (tr, $^3J_{FF}$ = 4.6 Hz, 2F, β-CF_2 [24]); ca. -134.54 (mult, $^2J_{FF}$ = ca. 86, [23]); ca. -134.56 (mult, $^2J_{FF}$ = ca. 86 Hz, [23]). IR (Nujol mull, NaCl plates, cm^{-1}): 2164 (str, br, C≡O); 2045 (str, C≡O); 1997 (str, C≡O); 1959 (med, C≡O); 1791 (med, C=O); alkyl fluorides: 1300-1000: 1168 (wk, br); 1098 (wk, br); 1013 (w); 937 (wk, br); 845 (wk, br).

2.3 Synthesis of Iron Fluoro-carbene Complexes

General Procedure:

Unless otherwise stated, the iron complex and corresponding Lewis acid were each dissolved in a small amount of a deuterated solvent. The solution of the Lewis acid was added drop-wise to the solution of the iron complex. The resulting reaction mixture was stirred in a vial in the glove box at room temperature. The solution was analyzed by NMR directly, without work-up.

Sublimed $B(C_6F_5)_3$

^1H NMR (500 MHz, C_6D_6, 298 K, δ): 4.62 (s); 6.24 (t, J_{HF} = ca. 1.6 Hz, C_6F_5H). $^{13}C\{^1H\}$ NMR (500 MHz, C_6D_6, 298 K, δ): 138.04 (d mult, $^2J_{CF}$ = 252 Hz, ArC_{meta}); 144.92 (d mult, $^2J_{CF}$ = 271 Hz , ArC_{para}); 148.72 (d, $^2J_{CF}$ = 252 Hz, ArC_{ortho}). ^{19}F NMR (471 MHz, C_6D_6, 298 K, δ): -130. 87 (s, 6F, ArF_{ortho}); -136.15 (d, J_{FF} = 19 Hz, 6F, $ArF_{ortho\ water\ adduct}$); -143.50 (s, 3F, ArF_{para}); -156.67 (tr, J_{FF} = 21 Hz, $ArF_{para\ water\ adduct}$); -161.88 (s, 6F, ArF_{meta}); -164.59 (br dd, J_{FF} = ca. 18 Hz, 6F, $ArF_{meta\ water\ adduct}$). ^{11}B NMR (160 MHz, C_6D_6, 298 K, δ): -10.66 (s); 61.69 (br s).

2.3.1 Attempted carbene formation from $Fe(CF_2)_4(CO)_4$ [1] with $B(C_6F_5)_3$

Complex [1] (0.029 g, 0.078 mol) and $B(C_6F_5)_3$ (0.043 g, 0.084 mmol) were dissolved in 1 mL of C_6D_6 to give a clear, pale beige solution. The reaction mixture was stirred for 20 hours to give a pale beige/yellow solution. An additional 50 mg (0.098 mmol) of $B(C_6F_5)_3$ was added and the mixture was stirred at room temperature for 10 days. No change in appearance was observed. The reaction mixture was heated in a sand bath at 50 °C in a capped vial in the glove box for 4 days to give a cloudy, pale beige/pink solution. ^{19}F NMR (376 MHz, C_6D_6, 298 K, δ): -72.20 (s, 4F, α-CF_2 [1]); -129.69 (s, 6F, borane ArF_{ortho}); -133.46 (dd, J_{FF} = ca. 20.5, 7 Hz, 1F, *A*); -134.43 (s, borane); -135.21 (d, J_{FF} = ca. 20.5 Hz, 1F, borane); -137.14 (s, 4F, β-CF_2 [1]); -139.86 (ddddd, J_{FF} = ca.

24, 10, 10, 2.3, 1 Hz, 1F, *B*); -143.02 (s, 3F, ArF_{para} borane); -144.72 (ddddd, J_{FF} = ca. 20.5, 20.5, 4, 4, 0.5 Hz, 2F, *C*); -154.89 (ddddd, J_{FF} = ca. 24, 20.5, 2.8, 1, 1 Hz, 2F, *D*); -155.93 (app tr, J_{FF} = ca. 21 Hz, borane); -160.71 (dddd, J_{FF} = 20.5, 11, 11, 3.5 Hz, 2F, *E*); -160.99 (s, 6F, ArF_{meta} borane); -163.14 (dddd, J_{FF} = 24, 20.5, 8, 7 Hz, 2F, *F*);-163.79 (app tr, J_{FF} = ca. 18H, borane); -165.16 (s, borane). ^{11}B NMR (160 MHz, C_6D_6, 298 K, δ): -17.58 (s); -10.60 (s); -0.03 (s); 38.57 (s); 58.58 (s).

2.3.2 Attempted carbene formation from tetrakis(2,6-dimethylphenylisocyanide) perfluorodimethyleneiron [20] ($Fe(CF_2)_2(2,6\text{-}(CH_3)_2C_6H_4NC)_4$) and tetrakis(2,6-dimethylphenylisocyanide) perfluorotetramethyleneiron [21] ($Fe(CF_2)_4(2,6\text{-}(CH_3)_2C_6H_4NC)_4$) with $B(C_6F_5)_3$

Dissolution of a mixture of complexes [20] and [21] (0.010 g) and $B(C_6F_5)_3$ (0.010 g, 0.020 mmol) in 1 mL of C_6D_6 gave a clear, pink solution. The reaction mixture was stirred at room temperature for 16 hours to give a clear, golden yellow solution. ^{19}F NMR (471 MHz, C_6D_6, 298 K, δ): -130.51 (app quint, J_{FF} = 6 Hz); -132.91 (dd, J_{FF} = 23, 7 Hz, ArF_{ortho}); -133.54 (dd, J_{FF} = 24, 7 Hz, *A*); -135.21 (d, J_{FF} = ca. 21 Hz); -139.86 (ddd, J_{FF} = ca. 24, 10, 10 Hz, *B*); -149.55 (tr, J_{FF} = 19 Hz, *C*) -154.81 (app tr, J_{FF} = 21 Hz, *D*); -155.52 (app tr, J_{FF} = 21 Hz, ArF_{para}); -155.71 (app tr, J_{FF} = 20 Hz, borane); -157.30 (s, borane); -161.01 (ddd, J_{FF} = ca. 24, 21, 8 Hz, *E*); -163.17 (trd, J_{FF} = 22, 9 Hz, ArF_{meta}); -163.64 (app tr, J_{FF} = ca. 20 Hz, *F*); -166.24 (s, borane).^{11}B NMR (160 MHz, C_6D_6, 298 K, δ): -21.00 (s); -9.70 (s); 2.83 (br s).

2.3.3 Attempted carbene formation from *trans*-bis(triisopropylphosphite) perfluorotetramethyleneiron dicarbonyl [7] and *cis*-bis(triisopropylphosphite) perfluorotetramethyleneiron dicarbonyl [8] ($Fe(CF_2)_4[P(O^iPr)_3]_2(CO)_2$) with $B(C_6F_5)_3$

Dissolution of the entire sample from reaction 2.2.5 containing [7] and [8], and $B(C_6F_5)_3$ (0.006 g, 0.012 mmol) in 0.5 mL C_6D_6 gave a clear, colorless solution. The reaction mixture was stirred for 20 hours to give a very pale yellow/beige solution. $^{31}P\{^1H\}$ NMR (121 MHz, C_6D_6, 298 K, δ): 139.35 (s, $P(O^iPr)_3$); 152.11 (app quint, $^3J_{PF}$ = 19.7 Hz, [8]). ^{11}B NMR (96 MHz, C_6D_6, 298 K, δ): approximately 16.29 (d, $^1J_{BF}$ = ca. 135 Hz); -1.95 (br s). ^{19}F NMR (282 MHz, C_6D_6, 298 K, δ): -72.74 (s, 4F, α-CF_2); -81.16 (app tr, J_{PF} = 19.7

Hz, 4F, α-$CF_{2\ axial}$); -130.62 (dd, J_{FF} = 24, 7 Hz, 6F, ArF_{ortho}); -134.68 (s, borane B-F) -135.19 (dd, J_{FF} = 22, 6 Hz, *A*); -135.44 (app dtr, 23, 6 Hz, *R*); ; -137.18 (s, 4F, β-CF_2); -138.32 (s, 4F, β-$CF_{2\ axial}$); -157.99 (mult, 3F, ArF_{para}); -162.86 (tr, J_{FF} = 20 Hz, *S*); -164.84 (trd, J_{FF} = 22, 9 Hz, *E*); -164.84 (ddd, J_{FF} = 24, 20, 6 Hz, *T*); -165.48 (dtr, J_{FF} = 24, 7 Hz, ArF_{meta}); -166.13 (dddd, J_{FF} = 24, 20, 8, 7 Hz, *F*); -167.14 (trd, J_{FF} = 21, 7 Hz, *U*).

2.3.4 Attempted carbene formation from potassium cyclopentadienyl perfluorotetramethyleneiron carbonyl isomers [23] and [24] K[FeCp$(CF_2)_4$(CO)] with $B(C_6F_5)_3$

Treatment of a mixture of complexes [23] and [24] (0.010 g, 0.024 mmol) with a solution of $B(C_6F_5)_3$ (0.013 g, 0.025 mmol) in 1 mL of CD_3CN gave an opaque, dark red solution. The reaction mixture was stirred in a vial in the glove box for 3 hours; no color change was observed. ^{19}F NMR (471 MHz, CD_3CN, 298 K, δ): -61.35 (tr, J_{FF} = 4.7 Hz, 2F, α-CF_2); -61.36 (tr, J_{FF} = 4.7 Hz, 2F, α-CF_2); -126.77 (tr, J_{FF} = 4.3 Hz, 2F, β-CF_2); -126.89 (tr, J_{FF} = 4.3 Hz, 2F, β-CF_2); -135.15 (s, *H* borane 1); -135.54 (d, J_{FF} = 21 Hz); -135.86 (d, J_{FF} = 21 Hz, *I*); -136.88 (d, J_{FF} = 22 Hz, borane 2); -138.49 (s, borane 3); -140.9 (app quint, J_{FF} = ca. 10 Hz); -141.14 (dd, J_{FF} = 21, 8 Hz); -148.25 (app quint, J_{FF} = ca. 12 Hz, *J*); -156.43 (d, J_{FF} = 19 Hz); -156.52 (tr, J_{FF} = 19 Hz, *D*); -160.65 (tr, J_{FF} = ca. 14 Hz); -160.81 (tr, J_{FF} = 19 Hz, *K*); -161.43 (tr, J_{FF} = 20 Hz); -162.07 (s, *L* borane 1); -162.40 (s); -162.97 (tr, J_{FF} = 21 Hz) -163.82 (tr, J_{FF} = 20 Hz, borane 2); -164.24 (tr, J_{FF} = 20 Hz); -164.38 (trd, J_{FF} = 21, 8 Hz); -166.77 (trd, J_{FF} = 20, 8 Hz, *N*); -166.91 (s); -167.15 (tr, J_{FF} = 19.5 Hz, borane 3); -167.23 (s, *O* borane 1); -167.68 (trd, J_{FF} = 21, 8 Hz, borane 2); -168.07 (tr, J_{FF} = 19 Hz); -173.32 (tr, J_{FF} = 22 Hz, borane 3). ^{11}B NMR (160 MHz, CD_3CN, 298 K, δ): -41.16 (s); -13.12 (s); -11.74 (d, J_{BF} = 30 Hz); -10.51 (s); -4.15 (s). ^{1}H NMR (500 MHz, CD_3CN, 298 K, δ): 1.12 (tr); 2.59 (s); 3.29 (s); 3.96 (s); 4.88 (s); 5.11 (s); 6.46 (s); 6.55 (s); 7.66 (s); 8.45 (s). $^{13}C\{^1H\}$ NMR (126 MHz, C_6D_6, 298 K, δ): 87.20 (s); 89.92 (s); 138.25 (mult, J_{CF} = 252 Hz, ArC_{meta}); 142.77 (m, ArC_{para}); 149.21 (m, ArC_{ortho}); 157.96 (s).

2.3.5 Attempted carbene formation from $Fe(CF_2)_4(CO)_4$ [1] with TMSOTf

Complex [1] (0.010 g, 0.027 mmol) and TMSOTf (0.014 g, 0.063 mmol) in 1 mL of C_6D_6 gave a clear, pale beige solution. The reaction mixture was stirred for 3 days, yielding a clear, pale pink/beige solution with a fine brown precipitate. ^{19}F NMR (282 MHz, C_6D_6, 298 K, δ): -72.37 (s, 4F, α-CF_2); -78.69 (s, 3F, TMSOTf); -137.28 (s, 4F, β-CF_2). An additional 14 mg of TMSOTf was added. The reaction mixture was heated in a sand bath at 50 °C in a capped vial in the glove box for 3 days to give a clear, pale pink/beige solution. ^{19}F NMR (471 MHz, C_6D_6, 298 K, δ): -72.37 (s, 4F, α-CF_2 [1]); -78.26 (s, 3F, TMSOTf); -137.17 (s, 4F, β-CF_2 [1]).

2.3.6 Attempted carbene formation from $Fe(CF_2)_4(CO)_4$ [1] with BF_3•Et_2O

Complex [1] (0.020 g, 0.054 mmol) and BF_3•Et_2O (0.011 g, 0.078 mmol) in 3 mL of toluene gave a clear, colorless solution. The reaction mixture was stirred at room temperature in the capped vial for 2 days, after which there was no change in appearance. ^{19}F NMR (471 MHz, C_6D_6, 298 K, δ): -72.20 (s, 4F, α-CF_2); -137.25 (s, 4F, β-CF_2); -152.62 (s, BF_3Et_2O). ^{11}B NMR (160 MHz, C_6D_6, 298 K, δ): 0.00 (s, BF_3Et_2O). The mixture was stirred for a further 17 days with no change.

2.3.7 Attempted carbene formation from potassium cyclopentadienyl perfluorotetramethyleneiron carbonyl complexes [23] and [24] $K[FeCp(CF_2)_4(CO)]$ with BF_3Et_2O in CD_3CN

A mixture of complexes [23] and [24] (0.030 g, 0.072 mmol) and 2 drops of BF_3Et_2O (0.020 g, 0.141 mmol) were combined in a vial in the glove box. Upon addition of 0.5 mL of CD_3CN while stirring, a very dark red solution resulted and a white gas was evolved. The reaction mixture was stirred in a capped vial for 21 hours with no observable color change. ^1H NMR (300 MHz, CD_3CN, 298 K, δ): 1.12; 1.94; 2.95; 3.42; 4.15; 4.88; 6.46; 6.56. ^{19}F NMR (282 MHz, CD_3CN, 298 K, δ): -61.28 (s, 4F, α-CF_2); -126.70 (s, 2F, β-CF_2); -126.90 (s, 2F, β-CF_2); -146.50 (s); -148.12 (s); -149.09 (s); -152.18 (s); -152.40 (dd, J_{FF} = 32, 15 Hz). ^{11}B NMR (96 MHz, CD_3CN, 298 K, δ): -0.56 (s); 0.30 (app quart, J_{BF} = 16 Hz). An additional 2 drops of BF_3Et_2O was added,

producing more white gas. The reaction mixture was stirred for 18 hours. ^{1}H NMR (300 MHz, CD_3CN, 298 K, δ):1.13 (tr, J_{HF} = 7 Hz); 3.65 (app quart, J_{HF} = 7 Hz); 4.07 (s); 4.80 (s); 5.28 (s); 5.66 (s). ^{19}F NMR (282 MHz, CD_3CN, 298 K, δ): -147.70 (d mult, J_{FF} = ca. 67 Hz); -148.39 (dd, J_{BF} = 16 Hz)); -150.71 (s); -152.40 (app quart, J_{FF} = 16 Hz). ^{11}B NMR (96 MHz, CD_3CN, 298 K, δ): 0.70 (s); 1.42 (s).

2.3.8 Attempted carbene formation from potassium cyclopentadienyl perfluorotetramethyleneiron carbonyl complexes [23] and [24] K[FeCp(CF$_2$)$_4$(CO)] with BF$_3$Et$_2$O in chlorobenzene

A mixture of complexes [23] and [24] (0.029 g, 0.070 mmol), was dissolved in 1 mL of chlorobenzene by stirring for 15 minutes. Not everything was soluble, resulting in an opaque, very dark black solution with a small amount of black powder. Two drops of BF_3Et_2O (0.020 g, 0.141 mmol) were added and the mixture was stirred overnight. ^{11}B NMR (96 MHz, chlorobenzene, C_6D_6 internal standard, 298 K, δ): 0.50 (s).^{19}F NMR (282 MHz, chlorobenzene, C_6D_6 internal standard, 298 K, δ): -117.90 (d, J_{FF} = 60 Hz); -152.52 (s); -153.39 (s).

2.3.9 Synthesis of a fluoro-carbene complex of K[FeCp(CF$_2$)$_4$(CO)]

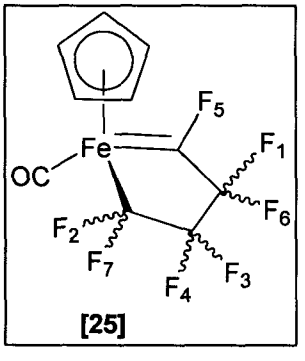

[25]

A mixture of complexes [23] and [24] (0.023 g, 0.055 mmol), was dissolved in 0.5 mL of CD_3CN. A solution of TMSOTf (0.014 g, 0.063 mmol) in 0.5 mL of CD_3CN was added drop-wise to give an opaque, dark red solution. The reaction mixture was stirred for 2 days at room temperature to yield an opaque, dark purple solution. ^{19}F NMR (471 MHz, CD_3CN, 298 K, δ): -61.34 (tr, $^{2}J_{FF}$ = 5 Hz, 4F, α-CF_2 [24]); -61.36 (tr, $^{2}J_{FF}$ = 5 Hz, 4F, α-CF_2 [24]); -78.49 (s, 3F, OTf); -86.48 (dd, $^{3}J_{FF}$ = 104 Hz, $^{2}J_{FF}$ = 39 Hz, *1*); -103.31 (dd, $^{2}J_{FF}$ = 59 Hz, $^{3}J_{FF}$ = 3 Hz, *2*); -122.88 (d, $^{2}J_{FF}$ = 83 Hz, *3*); -124.87 (d, $^{2}J_{FF}$ = 83 Hz, *4*); -126.75 (tr, $^{2}J_{FF}$ = 5 Hz, 2F, β-CF_2 [24]); -126.87 (tr, $^{2}J_{FF}$ = 5 Hz, 2F, β-CF_2 [24]); -132.12 (dd, $^{3}J_{FF}$ = 113, 104 Hz, *5*); -139.04 (dd, $^{3}J_{FF}$ = 114 Hz, $^{2}J_{FF}$ = 39 Hz, *6*); -148.19 (ddd, $^{2}J_{FF}$ = 78 Hz, $^{3}J_{FF}$ = 6, 5 Hz, *7*); -157.67 (decet, $^{3}J_{HF}$ = 7Hz, TMSF). ^{1}H NMR (500 MHz, CD_3CN, 298 K, δ): -0.07 (s); 0.04 (s); 0.15 (s); 0.19 (d, $^{3}J_{HF}$ = 7 Hz, TMSF); 0.35 (s, TMSOTf); 0.37 (s);

0.38 (s); 0.47 (s); 4.13 (s, [22]); 4.85 (s, [$FeCp(CO)_2$] derivative); 4.86 (s, [$FeCp(CO)_2$] derivative); 5.35 (s); 5.73 (s).

2.3.10 Fluoride abstraction from κ^2-[1,2-bis(diphenylphosphino)ethane] perfluorotetramethyleneiron iron dicarbonyl [18] ($Fe(CF_2)_4(dppe)(CO)_2$) with TMSOTf

Complex [18] (0.020 g, 0.028 mmol) was dissolved in 0.5 mL of CD_3CN to give a clear, yellow solution. Three drops of TMSOTf (approximately 0.014 g, 0.063 mmol) were added to the solution, giving off a small amount of white gas. The resulting mixture became a darker yellow/orange almost instantly. The reaction mixture was stirred overnight. ^{19}F NMR (282 MHz, CD_3CN, 298 K, δ): -64.07 (d quart, $^2J_{FF}$ = 253 Hz, $^3J_{FF}$ = 26 Hz, [18]); -72.17 (dd, $^2J_{FF}$ = 272 Hz, $^3J_{FF}$ = 17 Hz, [18]) -75.63 (app tr (unresolved dd), 4F, α-CF_2 [17]); -77.61 (dtr, $^2J_{FF}$ = 252 Hz, $^3J_{FF}$ = 14 Hz, [18]); -78.53 (s, OTf); -91.21 (d quint, $^2J_{FF}$ = 272 Hz, $^3J_{FF}$ = 16 Hz, [18]); -129.07 (dd, $^2J_{FF}$ = 249 Hz, $^3J_{FF}$ = 100 Hz, [18]); -138.27 (s, 4F, β-CF_2 [17]); -142.28 (d mult, $^2J_{FF}$ = 249 Hz, $^3J_{FF}$ = 11, 6 Hz, [18]); -145.59 (d mult, $^2J_{FF}$ = 249 Hz, $^3J_{FF}$ = 11, 6 Hz, [18]); -157.69 (decet, $^3J_{HF}$ = 7 Hz, TMSF).

2.4 Synthesis of Iron Complexes of 1,1-difluoroethylene (vinylidene fluoride)

2.4.1 Synthesis of iron carbonyl vinylidene fluoride complexes

$Fe_2(CO)_9$ (0.653 g, 1.80 mmol) was dissolved in toluene to give a dark green solution. The Schlenk tube was equipped with a balloon, which was then filled with 1,1-difluoroethylene. After stirring for 3 days, the reaction mixture was a dark opaque green/brown solution with a dark green precipitate. The mixture was filtered through Celite on a frit, giving a black brown residue on the Celite and a dark green filtrate. The solvent was removed from the filtrate *in vacuo* to give a brown/green residue. The residue was extracted into 15 mL of diethyl ether, yielding a dark green/brown solution. Adding acetonitrile (approximately 8 mL) turns the solution to dark purple. No precipitate formed. The solvent was removed *in vacuo* to give a dark black/purple residue. ^{19}F

NMR (376 MHz, C_6D_6, 298 K, δ): -40.52 (d, J_{HF} = 11.4 Hz); -47.75 (d, J_{HF} = 9 Hz); -48.02 (d, J_{HF} = 9 Hz); -48.63 (dd, J_{HF} = 8.5, 2.5 Hz); -49.09 (dd, J_{HF} = 8.5, 3 Hz); -49.50 (d, J_{HF} = 9 Hz). $^{19}F\{^1H\}$ NMR (376 MHz, C_6D_6, 298 K, δ): -40.52 (s); -47.75 (s); -48.02 (s); -48.63 (s); -49.09 (s); -49.50 (s). Relative integrals: 1.00:0.28:0.13:4.41:0.28:0.16.

2.4.2 Attempted Synthesis of iron carbonyl complexes of vinylidene fluoride at increased pressure

$Fe_2(CO)_9$ (0.850 g, 2.34 mmol) was transferred to a glass liner, equipped with a flea-sized stir bar, and loaded into the autoclave in the glove box. Hexane (15 mL) was carefully added on top of the iron. A slight green color formed in the solvent. The autoclave was assembled in the glove box and attached to the gas cylinder with minimal agitation of the reaction mixture. The autoclave was then pressurized with 1,1-difluoroethylene to 150 psi. There was an initial drop in pressure to ~90 psi. Upon stirring, the pressure dropped slightly more. The reaction mixture was stirred and heated in an oil bath at 63 °C. After 1 hour, the pressure was constant at 90 psi. After stirring overnight, the temperature was 61 °C and the pressure 90 psi. The autoclave was removed from the oil bath and allowed to cool for 2 hours. In the fume hood, the hose and autoclave were vented. The autoclave was brought into the glove box and disassembled. The reaction mixture was a clear, dark green solution with a green precipitate. The mixture was filtered through a frit to collect 0.085 g of a green/grey powder and some dark green/black crystals. The filtrate was a clear green solution; the solvent was removed under vacuum to give a dark green/black waxy residue. ^{19}F NMR indicates that there is no fluorine in the either "product". The dark green/black waxy solid was analyzed: IR (Nujol mull, NaCl plates, cm^{-1}): 2052 (wk); 2027 (wk). The green/grey powder was analyzed: IR (Nujol mull, NaCl plates, cm^{-1}): 2045 (wk br). IR spectra are consistent with $Fe_2(CO)_9$; traces of $Fe_3(CO)_{12}$ give them the green color.

2.4.3 Attempted photochemical synthesis of iron carbonyl complexes of vinylidene fluoride

$Fe_2(CO)_9$ (0.500 g, 1.37 mmol) was dissolved in hexanes to give an orange slurry in a green solution. Addition of 1,1-difluoroethylene using the gas apparatus resulted in an instant slight color change from dark green to darker green/black. Stirring and irradiating the reaction mixture for 3 hours gives a dark brown opaque solution. After 20 hours of irradiation, a dark brown precipitate formed in a dark green/brown solution. The reaction mixture was cannula-filtered through Celite on a frit to give a dark green opaque solution and green/brown residue on Celite. The residue was washed 3 times with 2-3 mL of hexanes. The solution was stored in the glove box freezer. The brown residue in the reaction flask was extracted into diethyl ether to give an opaque dark green solution. Filtering through a frit gives a small amount of brown residue and an opaque dark green solution. The solvent was removed from the filtrate *in vacuo* to give a dark green residue. Both solid samples were analyzed by NMR in C_6D_6; ^{19}F NMR indicated no fluorine.

2.4.4 Attempted Synthesis of Iron phosphite carbonyl complexes of vinylidene fluoride

$Fe_2(CO)_9$ (0.989 g, 2.72 mmol) was dissolved in 12 mL of toluene. $P(OiPr)_3$ (2.32 g, 11.1 mol) was added and stirring yielded a clear, dark green solution. $^{31}P\{^1H\}$ NMR (121 MHz, toluene, 298 K, δ): 140.80 ($P(O^iPr)_3$); 171.08 ($Fe[P(O^iPr)_3](CO)_4$); 183.76 ($Fe[P(O^iPr)_3]_2(CO)_3$); integral 1:1.5. The reaction mixture was transferred to the autoclave. The autoclave was assembled in the glove box, including the attachment of the gas cylinder. The autoclave was pressurized with 100 psi of 1,1-difluoroethylene. After stirring for 2 minutes, there was an initial drop in pressure to 70 psi. The reaction mixture was stirred and heated in an oil bath at 65 °C for 24 hours. The reaction mixture was allowed to cool to room temperature. The apparatus was brought into the fume hood and residual gas in the line connecting the autoclave to the gas cylinder was vented. The autoclave was brought into the glove box and disassembled. The reaction mixture, a cloudy yellow solution, was transferred to a round bottom flask. The solution was filtered through Celite and a frit to give a clear, bright yellow solution. The solvent

was removed *in vacuo* to give an orange solid. Pentane was added and the mixture was filtered through a frit. An orange oil was obtained. $^{31}P\{^1H\}$ NMR (161 MHz, toluene, 298 K, δ): 140.71 ($P(O^iPr)_3$); 171.58 ($Fe[P(O^iPr)_3](CO)_4$); 183.03 ($Fe[P(O^iPr)_3]_2(CO)_3$) integral 1:1.65. ^{19}F NMR indicated no fluorine.

2.4.5 Attempted complexation of vinylidene fluoride by triphenylphosphineiron tetracarbonyl ($Fe(PPh_3)(CO)_4$)

A 1:0.1 mixture of complexes [10] and [9] (0.012 g) was dissolved in 1 mL of C_6D_6. In a J Young NMR tube, 1,1-difluoroethylene was added to the solution. After irradiating the reaction mixture for 2 hours, the color changed from clear, dark green solution to a clear, pale yellow solution. After irradiating for 18 hours, the color changed to yellow and an orange precipitate formed. $^{31}P\{^1H\}$ NMR (121 MHz, C_6D_6, 298 K, δ): 71.94 (s, $Fe(CO)_4(PPh_3)$); 82.60 (s, $Fe(CO)_3(PPh_3)_2$). Relative integration - mono: bis 1:0.9. The reaction mixture was irradiated for a further 18 hours for a total of 36 hours. There was no further observable color change or precipitate formation. $^{31}P\{^1H\}$ NMR (121 MHz, C_6D_6, 298 K, δ): 56.86 (broad singlet); 71.94 (s, $Fe(CO)_4(PPh_3)$); 82.59 (s, $Fe(CO)_3(PPh_3)_2$). Relative integration mono: bis 1:1.57, new peak integration 0.83. ^{19}F NMR (282 MHz, C_6D_6, 298 K, δ): -79.31 (br s); -82.64 (mult, CH_2CF_2).

2.4.6 Synthesis of a vinylidene fluoride complex from bis(triphenylphosphine)iron tricarbonyl [10] ($Fe(PPh_3)_2(CO)_3$)

Complex [10] (0.006 g, 0.009 mmol) was dissolved in 1 mL of C_6D_6. In a J Young NMR tube, 1,1-difluoroethylene was added to the solution. After 2 hours of irradiation, the reaction mixture changed color from a cloudy, pale olive green solution to a clear, pale yellow solution. After irradiating for 18 hours, the color changed to yellow and an orange precipitate formed. $^{31}P\{^1H\}$ NMR (121 MHz, C_6D_6, 298 K, δ): -5.66 (s, PPh_3); 24.42 (s); 82.59 (s, $Fe(CO)_3(PPh_3)_2$). Relative integrals: 2.64:0.16:1.00. ^{19}F NMR (282 MHz, C_6D_6, 298 K, δ): -82.58 (mult, CH_2CF_2); -116.32 (ddd, J = 86, 55, 22 Hz); -142.85 (tr, J = 50 Hz). Relative integrals: -116.32:-142.85, 1.00: 0.22.

2.4.7 Attempted thermal complexation of vinylidene fluoride by pentakis(2,6-dimethylphenylisocyanide)iron [19] ($Fe(2,6\text{-}(CH_3)_2C_6H_4NC)_5$)

Complex [19] (0.010 g, 0.014 mmol) was dissolved in 1 mL of C_6D_6 to give a clear, bright red solution. In a J Young NMR tube, VDF was added using the gas apparatus and the reaction mixture was allowed to sit overnight at room temperature. There was no observable change in appearance. ^{19}F NMR (471 MHz, C_6D_6, 298 K, δ): -82.58 (mult, CH_2CF_2). The reaction mixture was heated in an oil bath at 83 °C for 21 hours after which the color changed to a clear, darker red. ^{19}F NMR (282 MHz, C_6D_6, 298 K, δ): no fluorine-containing products observed.

2.4.8 Attempted photochemical complexation of vinylidene fluoride by pentakis(2,6-dimethylphenylisocyanide)iron [19] ($Fe(2,6\text{-}(CH_3)_2C_6H_4NC)_5$)

Complex [19] (0.010 g, 0.014 mmol) was dissolved in 1 mL of C_6D_6 to give a clear, bright red solution. In a J Young NMR tube, VDF was added using the gas apparatus and the reaction mixture was irradiated with the UV lamp for 3 hours, which caused a color change to a darker red. The reaction mixture was irradiated for a further 17 hours to give an opaque, dark red solution. ^{19}F NMR (282 MHz, C_6D_6, 298 K, δ): no fluorine-containing products observed.

2.4.9 Attempted complexation of vinylidene fluoride by potassium cyclopentadienyliron dicarbonyl [22] ($K[FeCp(CO)_2]$)

Complex [22] (0.085 g, 0.393 mmol) was dissolved in 5 mL of CH_3CN and filtered through glass wool to give a dark red solution in a 25 mL storage vessel. VDF was added using the gas apparatus and the reaction mixture was stirred at room temperature for 4 days to give a clear, darker red solution. Any residual gas and the solvent were removed under vacuum. 53 mg of red waxy residue was obtained, which was dissolved in 1 mL of CD_3CN to give a dark, red opaque solution. ^{19}F NMR (282 MHz, C_6D_6, 298 K, δ): no fluorine-containing products observed.

2.4.10 Attempted complexation of vinylidene fluoride by potassium cyclopentadienyliron dicarbonyl [22] (K[FeCp(CO)$_2$])

Complex [22] (0.030 g, 0.139 mmol) was dissolved in 1 mL of CD_3CN to give a clear, bright orange solution. In a J Young NMR tube, VDF was added using the gas apparatus and the reaction mixture was irradiated with the UV lamp for 3 hours; no color change was observed. ^{19}F NMR (471 MHz, C_6D_6, 298 K, δ): no fluorine-containing products observed. Further irradiation (17 horus) gave an opaque dark red solution but the ^{19}F NMR spectrum still showed no fluorine-containing products.

2.4 References

[1] Sheldrick, G. M. *SHELXS-97*; University of Göttingen: Göttingen, Germany, **1997**.

[2] Sheldrick, G. M. *SADABS*; University of Göttingen: Göttingen, Germany, **1996**.

[3] Fields, R.; Germain, M.M.; Haszeldine, R.N.; Wiggans, P.M. *Chem. Comm.* **1967**, 243.

[4] Farrer, N.J.; McDonald, R.; McIndoe, J.S. *Dalton Trans.* **2006**, 4570.

[5] Fields, R.; Germain, M.M.; Haszeldine, R.N.; Wiggans, P.W. *J. Chem. Soc. (A)* **1970**, 1969.

[6] Drew, M.G.B.; Dodd, G.H.; Williamson, J.M.; Willey, G.R. *J. Organomet. Chem.* **1986**, *314*, 163.

Chapter 3: Synthesis and Characterization of Iron Metallacycle and Olefin Complexes of Tetrafluoroethylene

3.1 Introduction

As discussed in Chapter 1, since the synthesis and accurate characterization of perfluorotetramethyleneiron tetracarbonyl,[1] complex [1], little work has been done to explore its reactivity. With the goal of developing iron catalysts for the efficient production of novel hydrofluorocarbons, furthering the knowledge and understanding of iron-based organofluorometallic chemistry is a necessity. This chapter discusses the synthesis and characterization of iron complexes of TFE, and the effects that various ancillary ligands have on metallacycle formation.

3.2 Preparation of $Fe(CF_2)_4(CO)_4$

Three slightly different methods for the synthesis of $Fe(CF_2)_4(CO)_4$, [1], have been reported. The earliest method involved the irradiation of iron pentacarbonyl with tetrafluoroethylene,[1] which was later shown to go through the intermediate mono-olefin complex.[2] A more involved method necessitated cracking polytetrafluoroethylene at ca. 500 °C, condensing the gas and finally taking it off from a trap at -80 °C through soda lime before use.[3] The gas was then condensed onto $Fe_3(CO)_{12}$ in a thick-walled glass tube. The sealed tube was heated at 110-120 °C for 10-15 hours, cooled in liquid oxygen and lastly the excess olefin and other volatile materials were removed. The third reported preparation of complex [1] used either both $Fe(CO)_5$ and $Fe_3(CO)_{12}$, or $Fe_2(CO)_9$, as the iron precursor.[4] When a combination of both $Fe(CO)_5$ and $Fe_3(CO)_{12}$, in various proportions, was irradiated with TFE in light petroleum, low to moderate yields of [1] were obtained. Reacting $Fe_2(CO)_9$ with TFE in hexane at 80 °C generated [1] in 7% yield. The extent of characterization of this complex has been limited to: ^{19}F NMR spectroscopy, IR spectroscopy, and mass

spectrometry, and to its oxidative demetallation, which confirmed the presence of 4 CO ligands coordinated to iron.

$Fe_2(CO)_9$ is a safer, and therefore, more appealing starting material than the extremely toxic, highly flammable liquid $Fe(CO)_5$. In solution, $Fe_2(CO)_9$ breaks up into $Fe(CO)_5$ and the coordinatively unsaturated $Fe(CO)_4$, thus providing a vacant site for binding TFE.

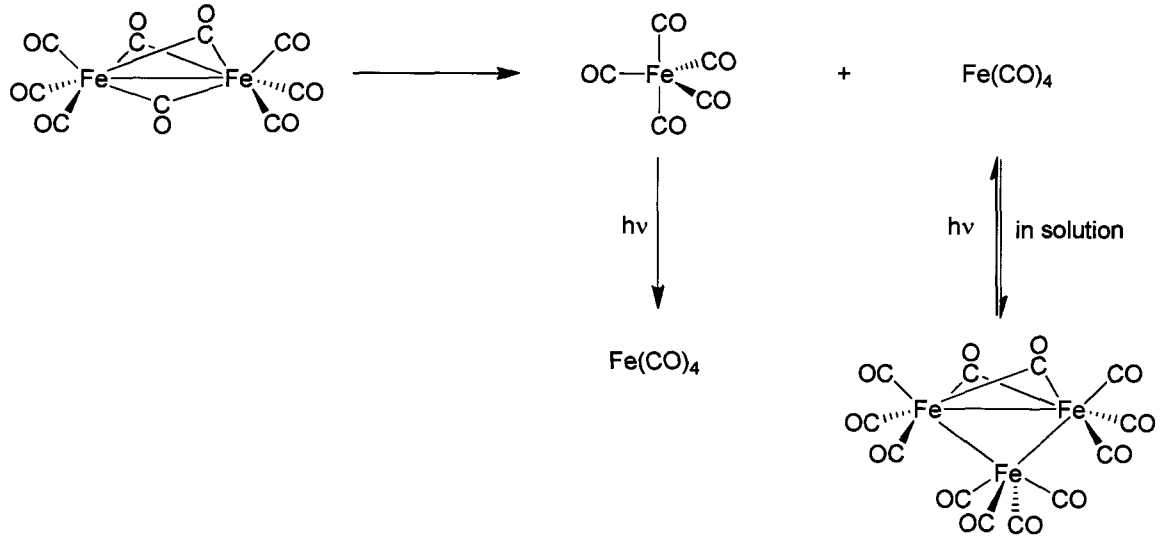

Scheme 1: Behavior of $Fe_2(CO)_9$ in solution and upon interaction with UV light.

There is danger associated with condensing gases; if this approach can be avoided to employ TFE as a reagent, it would be desirable. Exploring the reactivity of $Fe_2(CO)_9$ with TFE at atmospheric pressure and temperature has led to the successful synthesis of [1]. A reaction flask containing hexane and $Fe_2(CO)_9$ in a solid addition arm was equipped with a balloon filled with TFE; when the reagents were stirred at room temperature without irradiation for four days, trace amounts of complex [1] were produced, as confirmed by ^{19}F NMR spectroscopy. It is necessary to dissolve some of the TFE in hexane before adding the iron. If there is no ligand in solution for $Fe(CO)_4$ to react with, it will

form $Fe_3(CO)_{12}$ (Scheme 1), which is unreactive towards TFE under these conditions. Therefore, after stirring TFE and hexane for 30 minutes, $Fe_2(CO)_9$ was added through the solid addition arm. The reaction was stirred for four days as that was how long it took for the balloon to deflate; either all of the TFE had dissolved in the solvent and subsequently reacted with the $Fe_2(CO)_9$, or the balloon was porous enough for the gas to eventually leak through.

An alternative approach was required because of the extremely low yield (not enough of the complex was produced to be isolated) and the lack of reproducibility of these reaction conditions, such as: the amount of gas filled into the balloon, the porosity of the balloon, etc. A new apparatus was configured for the addition of gases to reaction mixtures that eliminates the need to condense the gas and prevents wasting copious amounts of expensive, toxic fluorinated gas. The apparatus is depicted in Figure 1 Chapter 2, and the procedure for the addition of the gas is described in Section 2.2.1.

To make all of the iron in the reaction mixture "available" to react with TFE, the reaction mixture needs to be irradiated with UV light. The UV light serves to break metal-CO bonds, thus liberating at least one equivalent of CO from $Fe(CO)_5$, as well as severing the interactions between iron and the bridging CO's in $Fe_3(CO)_{12}$. Irradiating and magnetically stirring a hexane solution of $Fe_2(CO)_9$ and TFE for 24 hours generated colorless needles of complex [1] in 18.7 % (isolated) yield; the structure is shown in Figure 2. Not all of the $Fe_2(CO)_9$ reacted; an orange solid collected on the sides of the reaction vessel.

Complex [1] has been characterized by ^{19}F and $^{13}C\{^1H\}$ NMR spectroscopy, X-ray crystallography, and IR spectroscopy. The ^{19}F NMR spectrum contains two singlets at -72.29 and -137.18 ppm, each due to four fluorine atoms on the metallacycle. The CF_2 group adjacent to the metal gives rise to the resonance at lower field,[5] while the β–CF_2 group generates the peak at -137.18 ppm. At this temperature, the coupling between the α and β fluorine atoms is not resolved. It was postulated by Stone that the apparent chemical equivalence of both fluorine atoms in a given CF_2 group is a result of either the metallacyclopentane ring

being planar or adopting an envelope structure which undergoes rapid conformational change, and that the uncertainty would be resolved with solid state structural characterization.[6]

X-ray crystallographic analysis of complex [1] shows that it adopts a puckered "envelope" structure whereby the α-carbons of the metallacycle are in the same plane as iron and the equatorial CO's, while one β-carbon is angled above the plane and the other is angled below the plane, as shown in Figure 1. No other examples of structurally characterized iron fluorometallacyclopentane complexes have been reported in the literature. The solid-state structure of an example of the hydrocarbon analogue where one of the equatorial carbonyls is substituted by a PPh_3 has been published. $Fe(CH_2)_4(CO)_3(PPh_3)$ is geometrically similar to $Fe(CF_2)_4(CO)_4$.[7]

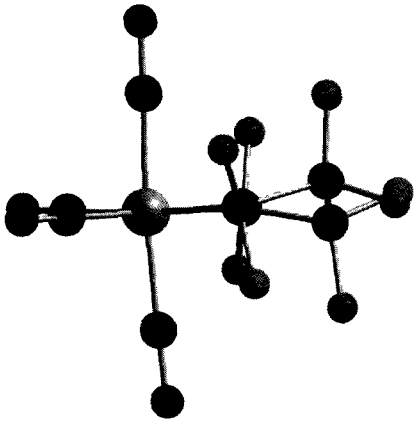

Figure 1: Configuration of the iron metallocyclopentane complex [1].

As anticipated based upon spectroscopic evidence, complex [1] crystallizes with pseudo-octahedral geometry, in the monoclinic space group C2/c. The atom labeling scheme is shown in Figure 2. Two carbonyl ligands (1 and 4) assume the axial positions of the octahedron, with a C(1)-Fe-C(4) bond angle of 175.26(12)°. The perfluorometallaycle and two carbonyl groups reside in the

equatorial plane; the total bond angle for the four ligands in this plane is approximately 360° (actual 360.02°). The largest angle in this plane, opened from its ideal value, is formed by the two CO's (C(2)-Fe-C(3) 97.96(11)°). The metallacycle forces the C(5)-Fe-C(8) bond angle to be acute at 85.50(11)°.

The equatorial carbonyl ligands show slightly longer Fe-C bond lengths than the axial ones; Fe-C(1) and Fe-C(4) are equivalent at 1.846(3) Å, while Fe-C(2) and Fe-C(3) are 1.853(3) and 1.865(3) Å, respectively. All four C-O bond distances are equivalent within the experimental error. The differences between the axial versus equatorial Fe-C bond lengths indicate that iron is not π-backbonding with the equatorial CO's as strongly as the axial ones; therefore, more electron density is being withdrawn by the fluorocarbon ring than if the CO's were *trans* to another CO. The perfluorometallacycle, formally two σ–bonded C_F ligands are better π-acids than CO; the lengthening of the Fe-C bonds in $Fe(CF_2)_4(CO)_4$ versus $Fe(CO)_5$ confirms this. The reported Fe-C bond lengths in $Fe(CO)_5$ are 1.811(2) and 1.804(2) Å for the axial and equatorial CO's, respectively.[8] Lending further evidence to the excellent electron-withdrawing ability of the fluorometallacycle are the significantly longer Fe-C_H bonds in $[Fe(CH_2)_4(CO)_3(PPh_3)]$ (2.107(4) Å *trans* to PPh_3 and 2.141(4) Å *trans* to CO).[7]

The shortest bond in the metallacycle is the C(6)-C(7) bond, forming the side opposite the metal centre. The C-F bond lengths range from 1.346(4) to 1.384(3) Å; the C-F bonds on the α-carbons are slightly longer than those on the β-carbons. The geometry of each of the carbons on the metallacycle is pseudo-tetrahedral, consistent with being sp^3 hybridized.

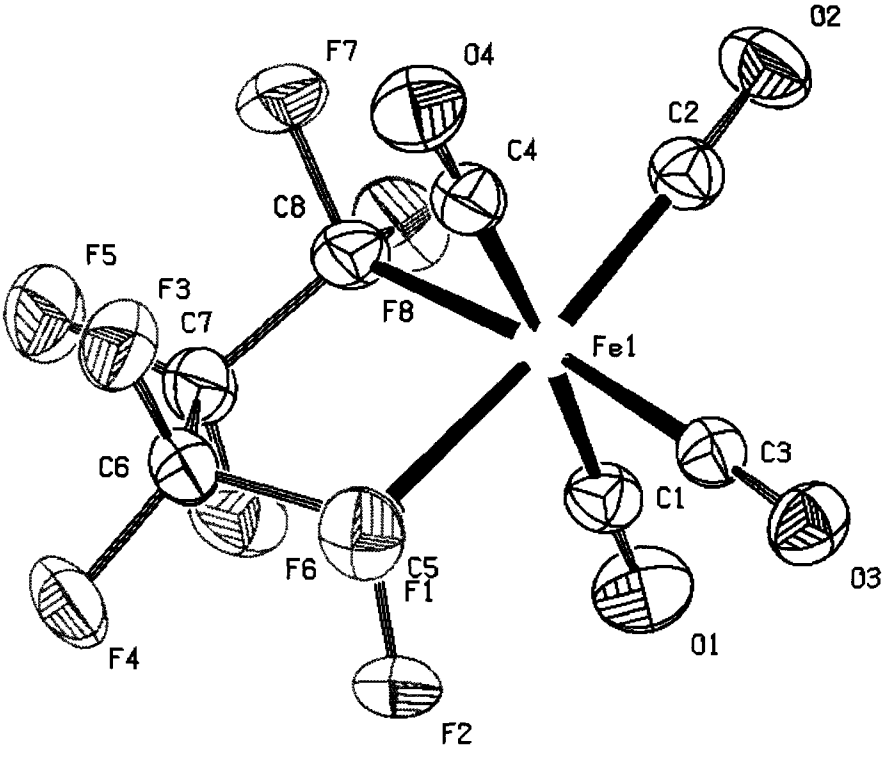

Figure 2: ORTEP diagram of complex [1], $Fe(CF_2)_4(CO)_4$, showing the atom labeling scheme. Representative bond lengths and angles: Fe-C(1) 1.846(3) Å, Fe-C(2) 1.853(3) Å, Fe-C(3) 1.865(3) Å, Fe-C(4) 1.846(3) Å, C(1)-O(1) 1.118(3) Å, C(2)-O(2) 1.124(4) Å, C(3)-O(3) 1.120(3) Å, C(4)-O(4) 1.123(3) Å, Fe-C(8) 2.024(3) Å, Fe-C(5) 2.010(3) Å, C(8)-C(7) 1.532(4) Å, C(7)-C(6) 1.525(4) Å, C(6)-C(5) 1.535(4) Å, C(8)-F(8) 1.372(3) Å, C(8)-F(7) 1.372(3) Å, C(7)-F(6) 1.347(4) Å, C(7)-F(5) 1.354(3) Å, C(6)-F(4) 1.356(3) Å, C(6)-F(3) 1.346(4) Å, C(5)-F(2) 1.368(3) Å, C(5)-F(1) 1.384(3) Å, C(1)-Fe-C(4) 175.26(12)°, C(8)-Fe-C(2) 87.69(11)°, C(2)-Fe-C(3) 97.96(11)°, C(3)-Fe-C(5) 88.87(10)°, C(5)-Fe-C(8) 85.50(11)°, Fe-C(8)-C(7) 109.64(17)°, C(8)-C(7)-C(6) 108.1(2)°, C(7)-C(6)-C(5) 108.3(2)°, C(6)-C(5)-Fe 110.12(17)°, F(7)-C(8)-F(8) 104.3(2)°, F(5)-C(7)-F(6) 107.7(2)°, F(3)-C(6)-F(4) 107.2(2)°, F(1)-C(5)-F(2) 103.91(19)°, O(1)-C(1)-Fe 178.4(3)°, O(2)-C(2)-Fe 176.3(3)°, O(3)-C(3)-Fe 176.9(2)°, O(4)-C(4)-Fe 178.4(3)°.

The peaks corresponding to the metallacycle carbon atoms are observable in the $^{13}C\{^{1}H\}$ NMR spectrum despite their decrease in intensity from C-F coupling. Consistent with the relative chemical shift of the α- versus β-CF_2 groups in the ^{19}F NMR spectrum, the ^{13}C NMR resonance for the α-CF_2 is shifted further downfield due to deshielding by the iron. The β-CF_2 gives rise to a triplet of triplets at 114.39 ppm with C-F coupling constants $^{1}J_{CF}$ = 275 Hz and $^{3}J_{CF}$ = 7 Hz. The ^{13}C NMR of the α-CF_2 resonates at 140.59 ppm. The coupling constant for fluorine directly bonded to carbon is slightly greater for α-CF_2, $^{1}J_{CF}$ = 310 Hz, while the coupling constant for the α-carbon and β-fluorine atoms is not easily distinguished due to the low S/N. There are two signals from the two types of inequivalent CO groups coordinated to the iron. Both are coupled to four apparently chemically equivalent fluorines as both are apparent quintets with single resolvable carbon-fluorine coupling constants of ca. 7 and 8 Hz.

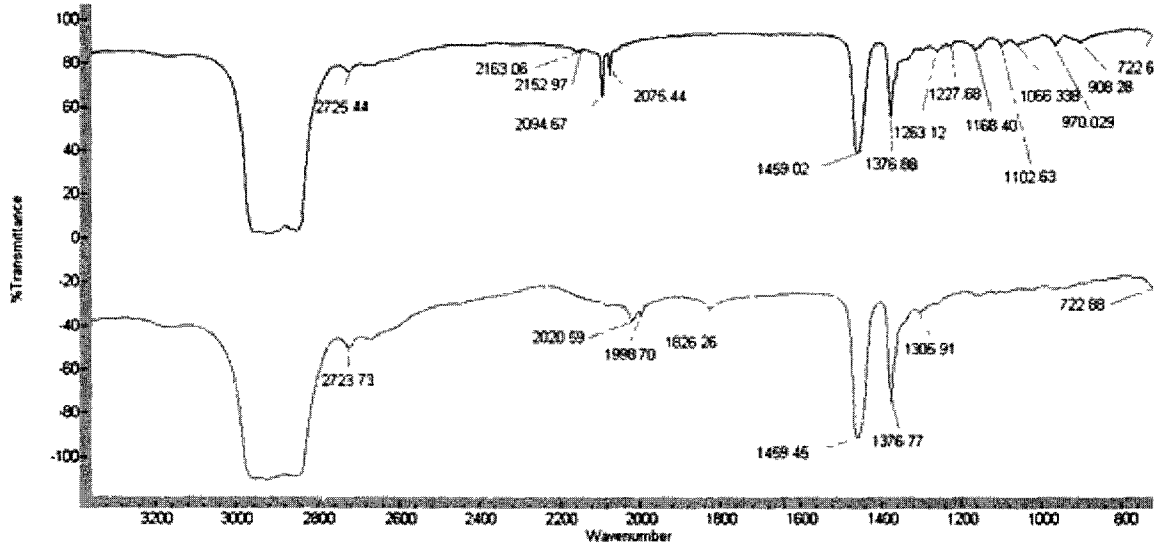

Figure 3: IR spectra of $Fe_2(CO)_9$ (bottom) and complex [1] (top), in a Nujol mull.

IR spectra were recorded for $Fe(CF_2)_4(CO)_4$ and the orange precipitate from the same reaction, noted above. The IR spectrum of the orange precipitate

confirmed it to be unreacted $Fe_2(CO)_9$; the bands at 2021 and 1999 cm^{-1} are for the terminal carbonyls and the band at 1826 cm^{-1} for the bridging carbonyls. In the IR spectrum for complex [1], there are two weak bands at 2163 and 2153 and two stronger bands at 2095 and 2075 cm^{-1} These CO stretches are at higher frequency than those in $Fe_2(CO)_9$ in keeping with the reduced back-bonding from divalent iron. The bands corresponding to the C-F bonds fall in the region of 1400-1000 cm^{-1}.

3.3 Selective Three- *versus* Five-membered Ring Formation from Iron Phosphite- and Phosphine-Carbonyl Complexes

3.3.1 Olefin and metallacycle iron phosphite carbonyl complexes of TFE

Introduction of phosphite ligands to the iron-fluorometallacycle complex should not greatly perturb the electronic properties; however, it provides a new reporter nucleus for NMR analysis. Previous studies involving the di-substituted iron carbonyl complexes *trans*-$[Fe(CO)_3L_2]$ where L = $P(OMe)_3$ and $P(OEt)_3$ generated only the bis-equatorial substituted olefin complexes from TFE, with no evidence of metallacycle formation by ^{19}F NMR spectroscopy.[9]

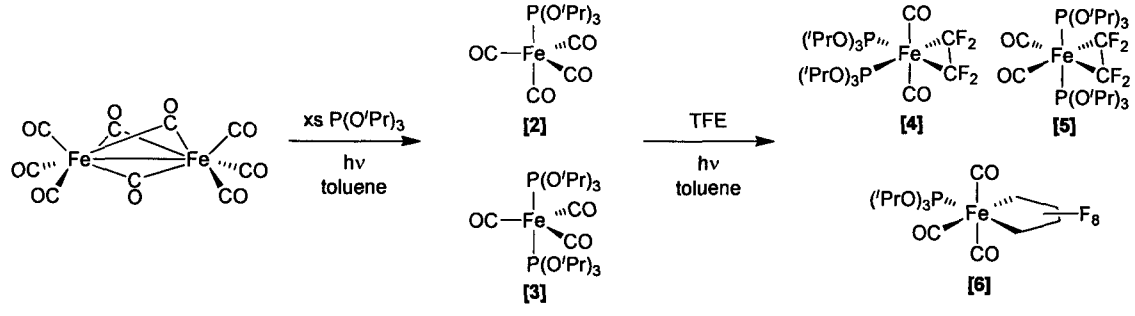

Scheme 2: Synthesis of mono-phosphite substituted metallacycle and bis-phosphite substituted olefin complexes of TFE.

Mono- and disubstituted phosphite iron carbonyl complexes, [2] and [3], can be generated photochemically from $Fe_2(CO)_9$ in an approximately 1:1 ratio (relative

proportion determined from integrals of the peaks in the $^{31}P\{^1H\}$ NMR spectrum). The photochemical reaction of TFE with the mixture of these complexes selectively yields the metallacycle for the mono-substituted complex [6], whereas the disubstituted complex favors the formation of isomeric olefin complexes with both phosphites in either equatorial [4] or axial [5] positions (Scheme 2).

Neither the two α-CF_2 nor two β-CF_2 groups on the metallacycle synthesized in this reaction are chemically equivalent as in the symmetrical complex [1]; in the ^{19}F NMR spectrum, there are two signals for the α-CF_2 fluorine atoms, at -75.60 and -79.26 ppm, and two for the β-CF_2 fluorine atoms, -137.21 and -137.98 ppm. Because the two sets of α-CF_2 and β-CF_2 fluorine atoms are chemically inequivalent, the complex must not be symmetrical; therefore, there must be only one phosphite coordinated to iron. If the phosphite was in the axial position, the ^{19}F spectrum would be expected to contain two signals for the α-CF_2's and two signals for the β-CF_2's, however, they would each be a doublet with a large geminal F-F coupling constant on the order of 200 Hz. However, they are singlets, and the phosphite must thus be in an equatorial position.

The major products for this reaction are isomeric bis-phosphite olefin complexes, giving a large singlet at -111.56 ppm for the major isomer and a smaller, slightly overlapping singlet at -112.27 ppm in the ^{19}F NMR spectrum, consistent with the chemical shift previously reported for $Fe(CF_2)_2(CO)_2[P(OMe)_3]_2$ at -112 ppm.[9] The two phosphites in this complex are *cis* to each other, with the CO's mutually *trans* in the axial positions, as determined by IR. In this case with triisopropyl phosphite, because the product contains more than one complex, IR spectroscopic analysis would not provide conclusive evidence towards determining the configuration of the major isomer.

Both olefin complexes must be symmetrical because all four fluorine atoms in the metallacyclopropane ring are chemically equivalent; both phosphites are either in the axial or equatorial positions. The major isomer is likely the bis-equatorially substituted complex in which the triisopropyl phosphites are *cis* to each other as

in the complexes with $P(OMe)_3$ and $P(OEt)_3$, despite the $P(O^iPr)_3$'s being more sterically demanding (cone angle = 130 vs. 107, 109).[10]

The peaks in the $^{31}P\{^1H\}$ NMR for the disubstituted isomers are coincidentally overlapped at 155.9 ppm and a singlet was observed at 165.7 ppm for complex [6]. The relative integration of these two peaks is 1:4.6 for [6]:[4]/[5]. Therefore, the approximate yield is 30 % of the mono-substituted metallacycle and 70 % of the bis-substituted olefin complexes. The lack of a unique $^{31}P\{^1H\}$ NMR signal for both olefin complexes indicates that perhaps one of the olefin complexes contains no phosphites coordinated to the iron. This complex $Fe(CF_2)_2(CO)_4$, has been reported, but not isolated in 1967.[2] The approximate ^{19}F NMR chemical shift for this complex is -90.35 ppm, inconsistent with what is observed in this study. Hence, both complexes [4] and [5] must contain phosphite ligands.

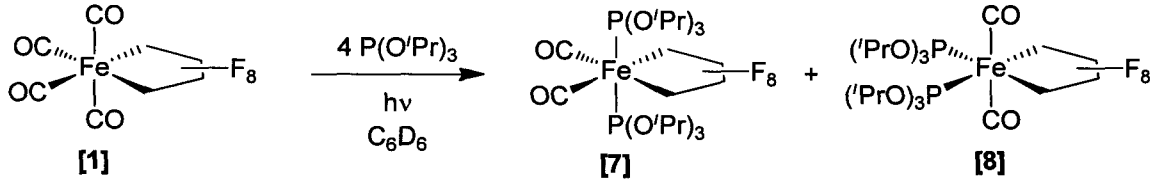

Scheme 3: Synthesis of bis-phosphite substituted iron metallacycle complexes of TFE.

The perfluorometallacyclopentane analogues of the disubstituted phosphite complexes can be prepared by reacting complex [1] with excess phosphite and irradiating with UV light for 24 hours. Similar reactions have been reported where the phosphite is $P(OPh)_3$ or $P(OEt)_3$ (the products for these reactions are given in Table 1, Chapter 1).[11] These complexes were synthesized by heating $Fe(CF_2)_4(CO)_4$ with the phosphite in light petroleum at 80 °C.

Ligand substitution with triisopropyl phosphite was attempted with complex [1] in C_6D_6 by heating the reaction mixture to 80 °C for 30 hours; no conversion was observed. The reaction mixture was irradiated with UV light for 21 hours to achieve partial conversion of [1] to the bis-substituted complexes [7] and [8] (Scheme 3). The equatorial, *cis* configuration of the phosphite is preferred, i.e. complex [8]. The $^{31}P\{^1H\}$ NMR contains an apparent quintet at 153.58 ppm

corresponding to complex [8] with a phosphorus-fluorine coupling constant of 19.7 Hz (Figure 4). The disubstituted metallacycle [7] gives a triplet of triplets in the $^{31}P\{^{1}H\}$ NMR at 157.05 ppm. These differences in coupling can be explained as follows: with the phosphites in the equatorial plane with the metallacycle, a given phosphite ^{31}P sees both fluorine atoms on an α-CF_2 as being chemically equivalent. Alternatively, with both phosphites configured as in complex [7], a given phosphite ^{31}P is effectively *cis* to the α-fluorine on the same plane of the ring as it and *trans* to the α-fluorine below the plane, thus generating a triplet of triplets with $^{3}J_{PF}$ = ca. 20 and 7 Hz. The α-CF_2's and β-CF_2's of complex [8] have chemical shifts of -81.16 and -138.42 ppm, respectively, in the ^{19}F NMR spectrum; the signal for the α-CF_2 is an apparent triplet with $^{3}J_{PF}$ = 19.7 Hz, consistent with the $^{31}P\{^{1}H\}$ NMR spectrum, and the β-CF_2 signal is a singlet. There is a considerably greater effect on the ^{19}F chemical shift for both the α- and β-CF_2's in complex [7]. Axial substitution imposes an upfield shift on the α-CF_2 resonance to -91.05 ppm (unresolved doublet of doublets) and a downfield shift on the β-CF_2 resonance to -125.48 ppm.

^{19}F-^{13}C heteronuclear multiple quantum coherence spectroscopy with the C-F coupling optimized at 250 Hz reveals the location of the metallacycle carbons for complex [8]; the β-carbons resonate at approximately 114 and 115 ppm, while the α-carbons come into resonance further downfield at approximately 143 and 146 ppm. The generated yield of complex [7] was too low for the chemical shift of its metallacycle carbon atoms to be determined.

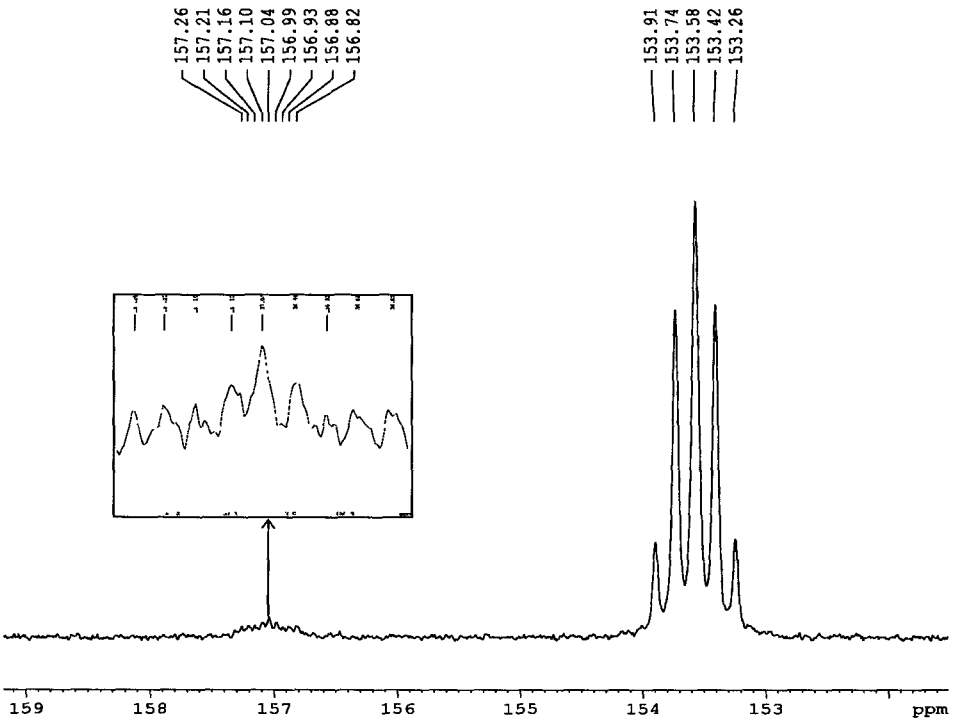

Figure 4: $^{31}P\{^{1}H\}$ NMR spectrum for complexes [7] and [8].

3.3.2 Olefin and metallacycle iron phosphine carbonyl complexes of TFE

Similar reactivity as the iron phosphite carbonyl complexes is demonstrated by the more electron-rich and sterically demanding (cone angle = 145°)[10] triphenylphosphine analogues. The mono- and bis-phosphine iron carbonyl complexes $Fe(PPh_3)(CO)_4$ and $Fe(PPh_3)_2(CO)_3$ can be synthesized from $Fe_2(CO)_9$ and PPh_3 at room temperature in diethyl ether.[12] The bis-substituted complex precipitates out of solution during the course of the reaction. The solvent was removed under reduced pressure from the solution phase of the reaction mixture to yield a mixture of complexes [9] and [10] in an approximately 1:0.1 ratio based upon $^{31}P\{^{1}H\}$ NMR analysis (chemical shifts were assigned based on those reported in the literature).[12] When a C_6D_6 solution of complexes [9] and [10], in a 1:0.1 ratio, is irradiated with UV light with TFE for 19 hours, both metallacycle and olefin complexes of TFE are generated akin to the reaction involving the phosphite complexes.

The mono-phosphine substituted metallacycle complex [11] is produced with the same configuration as the phosphite analogue, complex [6], based upon the same pattern in the ^{19}F NMR spectrum for both. The α-CF_2's give rise to singlets at -74.51 and -82.12 ppm and the β-CF_2's at -139.75 and -139.98 ppm. Two bis-phosphine TFE olefin complexes were also produced in this reaction (Scheme 4). The major isomer likely has the two triphenylphosphines in the *trans* configuration.

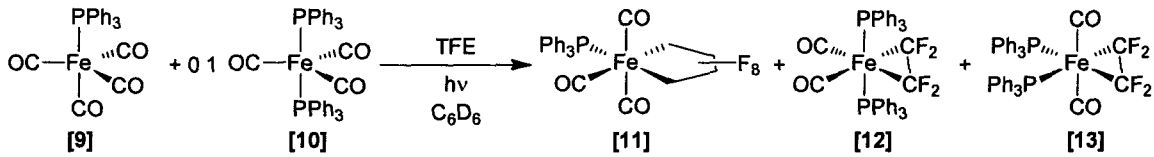

Scheme 4: Synthesis of mono-phosphine substituted metallacycle and bis-phosphine substituted olefin complexes of TFE.

When the reactivity of ruthenium bis-phosphine carbonyl and ruthenium bis-phosphite carbonyl complexes with fluoro-olefins was investigated, it was found that the stereochemistry of the phosphorus-based ligands in the olefin complexes was dictated by the ligand itself, not by the identity of the metal or the fluoro-olefin. Phosphite-containing fluoro-olefin complexes had the phosphites in the equatorial plane, for both iron and ruthenium, and the phosphine analogues contained the phosphines positioned axially for ruthenium. There have been no such phosphine complexes reported for iron. If iron behaves the same way as ruthenium, the assignment of complex [12] as the major isomer is substantiated.

There is a broad singlet in the ^{19}F NMR spectrum due to the four equivalent fluorines of complex [12] at -113.38 ppm. The broadness of this peak may be a result of hindered rotation of the phenyl substituents on the phosphines or about the Fe-P bonds. In addition, there is a sharp singlet at -116.90 ppm from a second olefin complex, which must also be symmetrically substituted (complex [13]). There are three new peaks in the $^{31}P\{^1H\}$ NMR consistent with the production of the three complexes. However, without resolvable phosphorus-

fluorine coupling, the peaks cannot be definitely assigned. Based on relative integration of the peaks in the ^{19}F NMR, similar amounts of complexes [11] and [13] are produced, but complex [12] is the major product. Therefore, the signal in the $^{31}P\{1H\}$ NMR at 49.09 ppm is likely from complex [12]. Because complex [13] has twice as many phosphorus atoms as complex [11], the larger of the remaining two new $^{31}P\{^1H\}$ peaks, at 56.63 ppm can be assigned to it. Furthermore, the chemical shift is closer to the peak for the other olefin complex, than is the peak for complex [11] at 24.39 ppm. The relative yield of the three products is: 19% complex [11], 59% complex [12], and 22% complex [13]. The $^{31}P\{^1H\}$ NMR spectrum for this reaction contains a fourth new peak, for PPh_3. Therefore, PPh_3 is lost by one of the complexes, or by both [9] and [10] in the reaction.

When the bis-phosphine complex [10], is reacted with TFE via irradiating with UV light for 19 hours, slightly different behavior is observed. The $^{31}P\{^1H\}$ NMR shows the production of the same singlet at 22.24 ppm attributed to the mono-substituted metallacycle, complex [11]. The ^{19}F NMR however, indicates that, in this case, irradiating for 19 hours stimulates the formation of additional products proposed to be iron-carbonyl-TFE clusters; the ^{19}F NMR spectrum contains many peaks over the analyzed spectral width. The $Fe(PPh_3)_2(CO)_3$ likely contained traces of $Fe_2(CO)_9$, which is what led to clusters after treatment with TFE.

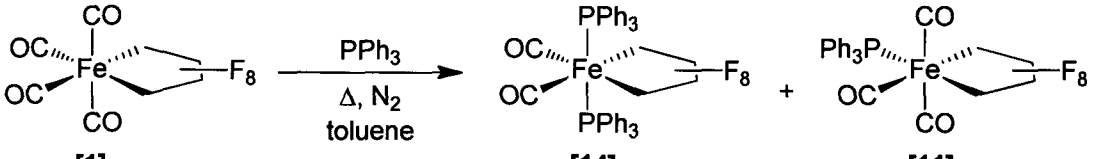

[1] [14] [11]

Scheme 5: Alternative synthesis of triphenylphosphine-substituted iron fluorometallacycle complexes.

A more selective approach to synthesize metallacyclopentanes with phosphine-substituents, is to start from the parent metallacycle, complex [1].[11] Refluxing $Fe(CF_2)_4(CO)_4$ in toluene with one equivalent of PPh_3 produces trace amounts of

complexes [14] and [11] (Scheme 5). A triplet of triplets at 43.71 ppm in the $^{31}P\{^{1}H\}$ NMR suggests the production of the bis-phosphine complex with the phosphines configured axially. The ^{19}F NMR only contains two new peaks, singlets at -79.80 and -137.88 ppm. A second new peak in the $^{31}P\{^{1}H\}$ NMR at 24.82 ppm implies the formation of complex [11] as assigned from the reaction of complexes [9] and [10] with TFE. However, it is not responsible for any peaks in the ^{19}F NMR; therefore, this peak may in fact be due to a fluorine-free phosphine compound.

3.4 Synthesis and Characterization of $Fe(CF_2)_4(CO)_2(\kappa^2\text{-dppe})$

Reacting $Fe_2(CO)_9$ with 1,2-bis(diphenylphosphino)ethane (dppe) in diethyl ether at room temperature, similar to the preparation for complexes [9] and [10],[12] gives two isomers ($^{31}P\{^{1}H\}$ NMR). Attempts to react this product with TFE in C_6D_6 at room temperature, secondly by heating to 83 °C in an oil bath for 19 hours, and finally by irradiating with UV light for 15 hours were unsuccessful. Irradiation does drive the reaction to yield a single isomer of $Fe(CO)_3(\kappa^2\text{-dppe})$.

Previous publications on the reaction of dppe with $Fe(CF_2)_4(CO)_4$ in refluxing methylcyclohexane under N_2 report the formation of a single complex $Fe(CF_2)_4(CO)_2(\kappa^2\text{-dppe})$ [17] as determined by elemental analysis and ^{19}F NMR spectroscopy (in CH_2Cl_2: - 74.2 ppm, triplet, J = 12 Hz; -138 ppm, singlet).[13] A more recent report showed that under similar reaction conditions (heating at 80 °C in a sealed tube in light petroleum) complex [17] as well as dinuclear $[Fe[(CF_2)_4(CO)_3]_2(\mu\text{-}\kappa^{1,}\,\kappa^{1}\text{-dppe})$, complex [18] were generated.[11]

Heating complex [1] with 1 equivalent of dppe at 127 °C in toluene for 3 hours under N_2 also afforded [17]. Pale yellow crystals suitable for diffraction were crystallized from toluene in the glove box freezer; the crystallographically determined molecular structure is shown in Figure 5.

Similar geometrical features are observed in the solid-state structure of [17] as seen for $Fe(CF_2)_4(CO)_4$ (several perspectives of the metallacycle are shown in

Figure 6). $Fe(CF_2)_4(CO)_2(\kappa^2\text{-dppe})$ also crystallizes in monoclinic space group C2/c with slightly distorted octahedral geometry. The axial carbonyl ligands form an angle of 175.0(4)° with iron. The dppe ligand forms the equatorial plane with the fluorometallacycle. Because both chelating equatorial ligands are tethered, the angles they make with iron are less than 90°: (C(1)-Fe-C(4) 85.3(3)°, and P(1)-Fe-P(2) 86.49(7)). The P(1)-Fe-P(2) angle is slightly larger because of the longer CH_2-CH_2 bond (1.520(10) Å) in the backbone of this ligand, versus the shorter C(2)-C(3) bond which is 1.442(13) Å. The total angle in the equatorial plane is 359.89°.

The Fe-P(1) and Fe-P(2) bond lengths are not equivalent; Fe-P(1) is 2.267(2) Å and Fe-P(2) is 2.304(2) Å. As well, there are differences in the bond lengths between iron and the metallacycle carbons: Fe-C(4) is 2.008(8) Å and Fe-C(1) is 1.991(9) Å. The *trans*-effect says that bond distance should be longer to atoms *trans* to stonger donors. However, the Fe-C_F bonds are shorter in complex [17] than in complex [1]. Dppe is a better σ-donor than CO, placing more electron density on iron, which can then be used for back-bonding to the metallacycle C_F groups. This stronger interaction results in a shortening of the Fe-C_F bonds.

The configuration of the ring controls the relative Fe-C bond lengths for the metallacycle. It appears as though the highly electronegative fluorine atoms orient themselves in such a way to try to get as far away from each other as possible. In the equatorial plane, the shorter Fe-C bond (to C(1)) forces the *cis* phosphine (P(2)) further away from iron. Because of the longer Fe-C(4) bond and the orientation of the fluorine atoms on this carbon, P(1) can gain closer contact to the metal, explaining the shorter Fe-P(1) bond. Extending from this, the phenyl groups on the phosphines orient themselves away from the direction the fluorine atoms point on the side of the metallacycle nearest to them.

Presumably imposed by the steric demands of the bulky phenyl groups on the phosphine, there are significant differences in the Fe-C and C-O bond lengths. The Fe-C(6) and C(6)-O(2) bonds are 1.818(11) and 1.111(11) Å, while the Fe-C(5) and C(5)-O(1) bonds are 1.890(12) and 1.041(11) Å.

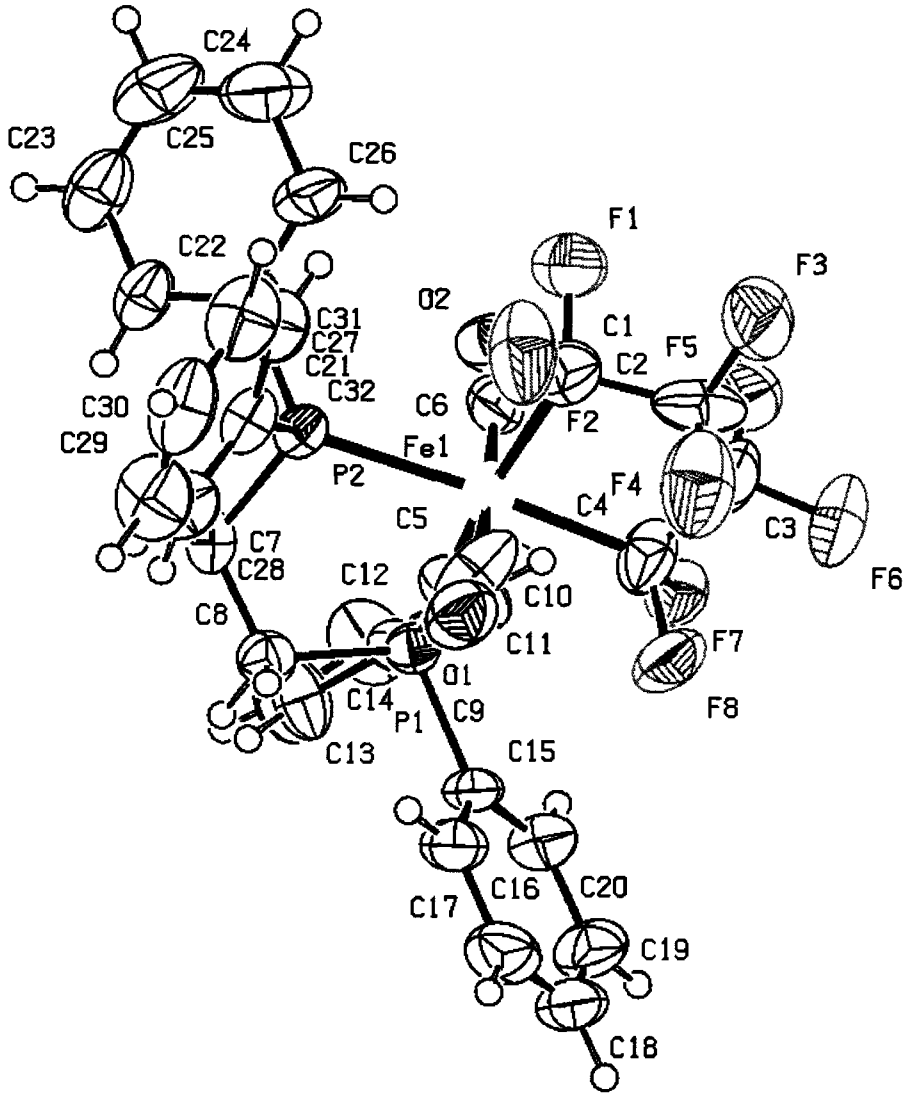

Figure 5: ORTEP diagram of $Fe(CF_2)_4(dppe)(CO)_2$ [17] showing the atom labeling scheme. Important bond lengths and angles: Fe(1)-C(6) 1.818(11) Å, Fe(1)-C(5) 1.890(12) Å, Fe(1)-C(1) 1.991(9) Å, Fe(1)-C(4) 2.008(8) Å, Fe(1)-P(1) 2.267(2) Å, Fe(1)-P(2) 2.304(2) Å, F(1)-C(1) 1.362(10) Å, F(2)-C(1) 1.419(10) Å, F(3)-C(2) 1.307(9) Å, F(4)-C(2) 1.415(11) Å, F(5)-C(3) 1.475(12) Å, F(6)-C(3) 1.345(9) Å, F(7)-C(4) 1.340(9) Å, F(8)-C(4) 1.519(11) Å, O(1)-C(5) 1.041(11) Å, O(2)-C(6) 1.111(11) Å, C(1)-C(2) 1.616(13) Å, C(2)-C(3) 1.442(13) Å, C(3)-C(4) 1.465(13) Å, C(6)-Fe(1)-C(5) 175.0(4)°, C(1)-Fe(1)-C(4) 85.3(3)°, C(4)-Fe(1)-P(1) 89.8(3)°, P(1)-Fe(1)-P(2) 86.49(7)°, C(1)-Fe(1)-P(2) 98.3(3)°, F(1)-C(1)-F(2) 101.8(7)°, F(3)-C(2)-F(4) 106.2(6)°, F(5)-C(3)-F(6) 104.8(7)°, F(7)-C(4)-F(8) 103.4(6)°, Fe(1)-C(1)-C(2) 110.6(5)°, C(1)-C(2)-C(2) 106.3(6)°, C(2)-C(3)-C(4) 115.8(8)°, C(3)-C(4)-Fe(1) 110.4(6)°.

As observed in $Fe(CF_2)_4(CO)_4$, the metallacycle carbon atoms assume a pseudo-tetrahedral geometry. There are significant differences in the carbon-fluorine bond distances on individual carbon atoms in this complex. Those fluorines effectively in the plane of the ring (F(1), F(3), F(6), and F(7)) form shorter bonds, whereas, those fluorines oriented above or below the plane of the ring form longer C-F bonds (F(2), F(4), F(5), and F(8)). Finally, on the side of the ring with the shorter Fe-C bond, the C-C bond is also longer (C(1)-C(2) 1.616(13) Å).

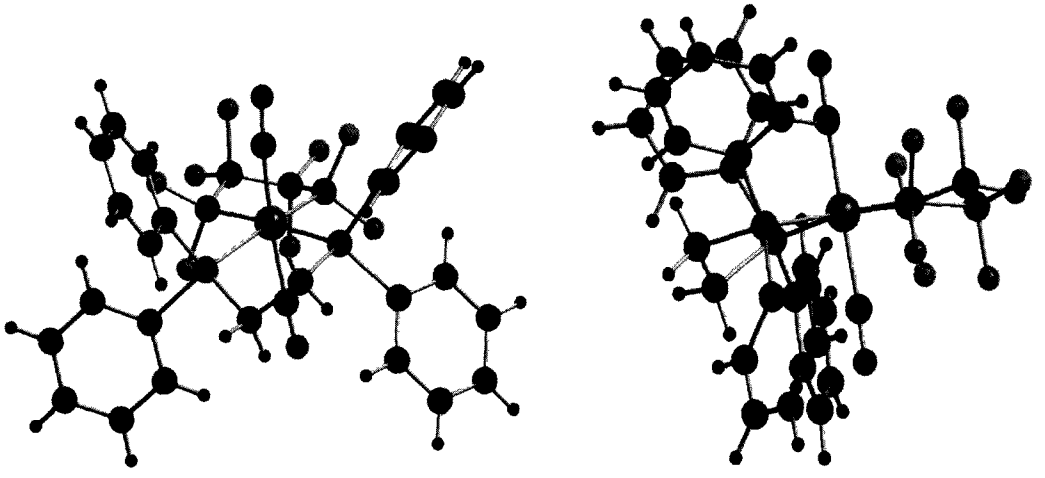

Figure 6: Two perspectives of complex [17] displaying the envelope configuration of the perfluorometallacyclopentane ring.

The $^{31}P\{^1H\}$ NMR spectrum for this complex contains a quintet at 61.36 pm with $^3J_{PF}$ = 13.5 Hz. A second, much more minor product is also generated in this reaction. The $^{31}P\{^1H\}$ NMR spectrum contains a quintet at 57.53 ppm and seven peaks in the ^{19}F NMR spectrum, consistent with the dppe-bridged dinuclear complex [18] reported previously (Scheme 6).[11] As for the $P(O^iPr)_3$ complex discussed earlier (complex [8]), substitution must be equatorial (no large F-F coupling). Only seven of the eight ^{19}F NMR signals were resolved for this complex. The large geminal F-F coupling indicates that the two fluorines on a given carbon are inequivalent, which must be dictated by the orientation of the

phenyl groups on the phosphine. This indicates that there must be a fixed conformation about the C-C bridge of the dppe ligand.

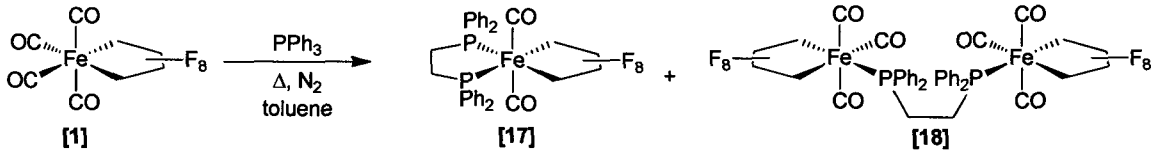

Scheme 6: Synthesis of dppe-substituted iron fluorometallacycle complexes.

The chemical shifts for the signals in the ^{19}F NMR spectrum for complex [17] are shifted slightly upfield from those previously reported for this complex. The α-CF_2's give rise to a triplet at -75.63 ppm ($^3J_{PF}$ = ca. 12 Hz) and the singlet at -138.27 is due to the β-CF_2's. The NMR analyses for complex [17] in this study were performed in CD_3CN. Solvent effects in ^{19}F NMR do not have quite as much of an influence over chemical shifts as in ^1H NMR. Depending on the solvent, there can be variation in fluorine chemical shifts of up to ± 1 ppm.[14]

The splitting pattern displayed by this complex is consistent with that of complex [8], confirming the assignment of the configuration of the two phosphites in that complex as being mutually *cis* in the equatorial plane.

The ^{13}C NMR signal for the carbonyl groups, as well as those signals associated with dppe in complex [17] were observed in the standard $^{13}C\{^1H\}$ NMR experiment. Because the carbon atoms of the metallacycle will be coupled to the fluorine atoms directly bonded to them, the fluorine atoms on the adjacent carbon, and the α-carbons to the phosphorus atoms coordinated to the metal, they will be quite low in intensity. Therefore, it is not surprising that they cannot be observed via standard $^{13}C\{^1H\}$ NMR analysis. ^{19}F-^{13}C HMQC spectroscopy identifies the β-carbon resonances at approximately 114 and 116 ppm, and the α-carbon resonances at 144 and 147 ppm.

The IR spectrum for complex [17] is displayed in Figure 7. The bands in the region 3000-3100 cm^{-1} originate from the C-H stretch of the sp^2 hybridized carbon atoms in the phenyl rings on the phosphines. The corresponding C-C aromatic stretches appear as medium to strong absorptions in the region 1650-1375 cm^{-1}. The stretching bands for the carbonyl groups are present at approximately 2040-1940 cm^{-1}. The presence of phosphine ligands on the metal decreases the C-O stretching frequencies. The lowest carbonyl stretching frequency for complex [1] is 2075 cm^{-1}, while the lowest for [17] is 1942 cm^{-1}. The C-F bonds contribute to the assortment of bands over the region 1155-900 cm^{-1}.

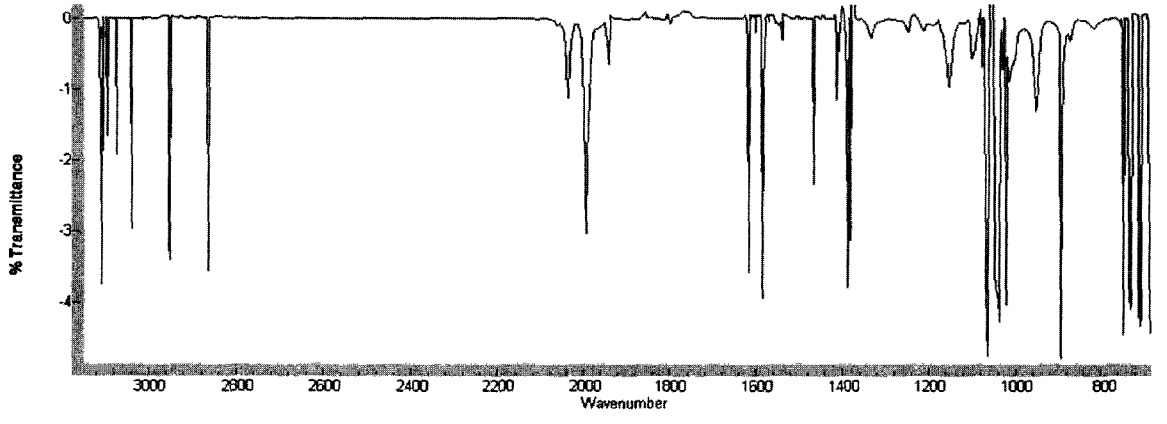

Figure 7: IR spectrum of complex [17] in toluene.

3.5 Synthesis of Novel Iron Isocyanide Complexes

Isocyanide ligands have similar π-acid character as carbonyls and phosphites. 2,6-dimethylphenyl isocyanide (CNAr) has sufficient steric bulk to allow for the facile displacement of one ligand, thus permitting TFE access to the iron centre. This complex provides an alternative to the sought after "four-coordinate" zerovalent iron starting material for fluorometallacycle formation.

Homoleptic $Fe(CNAr)_5$ was synthesized according to a variation on a literature procedure.[15,16] The iron(II) complex, $[FeCl(CNAr)_5]^+[FeCl_4]^-$, was prepared from

anhydrous $FeCl_2$ and 2,6-dimethylphenylisocyanide; reducing it with Mg generated the desired iron(0) complex in low yield (5.2%). Comparison of the ^1H and ^{13}C chemical shifts to the literature confirmed the identity of complex [19].[16]

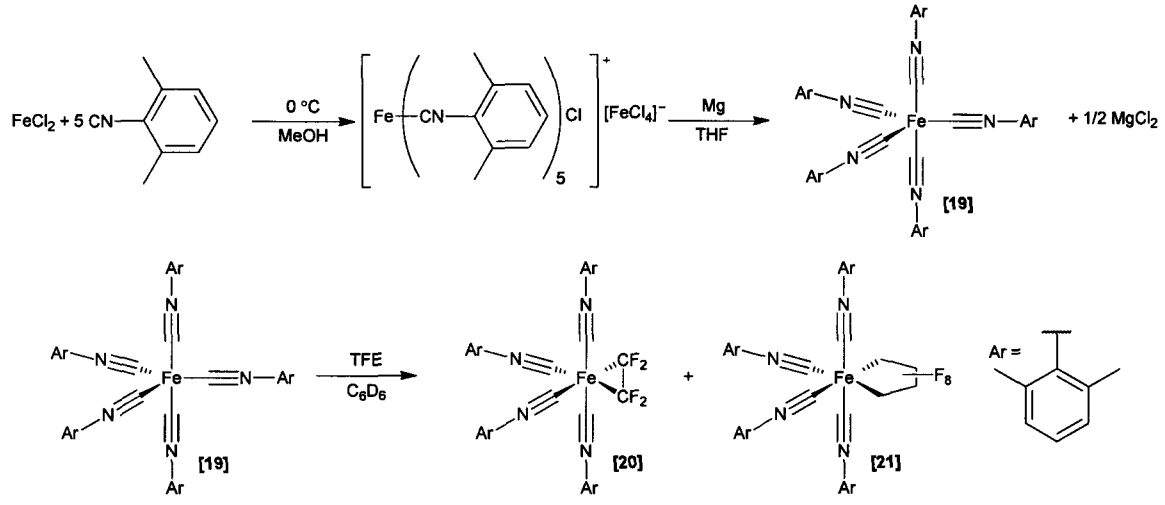

Scheme 7: Synthesis of olefin and metallacycle iron isocyanide complexes of TFE.

Reacting complex [19] with TFE at room temperature produces both the mono-olefin complex [20] and perfluorocyclopentane complex [21] (Scheme 7). The ^1H and ^{13}C spectra reveal that there are two unique isocyanide ligands in both complexes. In the ^1H NMR spectrum, there are peaks corresponding to three inequivalent types of aromatic protons and two unique methyl groups, one for the axial and one for the equatorial ligands, in each complex. The assignment of chemical shifts for the ^{13}C NMR was accomplished with the combination of a proton decoupled and dept-135 experiment. The ^{13}C for the methyl groups of both compounds can be distinguished; however, there are only assignable aromatic carbons for the major product. The ^{13}C NMR signals for the metallofluorocyclopropane ring carbon atoms were distinguished with ^{19}F-^{13}C HMQC spectroscopy optimized for 400 Hz carbon-fluorine coupling. They resonate at approximately 135 ppm. An attempt was made to find the chemical shift of the carbon atoms of the metallacycle in complex [19] by performing a ^{19}F-^{13}C HMQC experiment with 250 Hz carbon-fluorine coupling. Previously located

metallacycle carbons had C-F coupling constants on the order of 250 Hz, making this an appropriate guess; however, no correlations were resolved at this frequency.

Ligand substitution of TFE for isocyanide, accompanied by oxidation of the metal centre, significantly affects the chemical shift of the isocyanide carbon atoms of the remaining isocyanide ligands. In starting complex [19], the isocyanide carbon exhibits a peak at 197.08 ppm. The ^{13}C spectrum for the product has peaks from the isocyanide carbons shifted upfield to 178.20 and 183.29 ppm. The more electropositive iron with fluoro-olefin and metallacycle ligated to it provides greater shielding for the isocyanide carbons.

Similar to the already discussed TFE olefin and metallacycle complexes, the ^{19}F chemical shift for the fluorine atoms in olefin complex [20] is -115.66 ppm, and -83.90 and -136.35 ppm for the α- and β-fluorines of the metallacycle, respectively. All three peaks were singlets as expected because the complexes are symmetrical and there are no significantly abundant spin-active nuclei in close proximity to couple to the fluorines.

The olefin complex is the major product in this reaction. Iron must lose a second isocyanide ligand if the intermediate for five-membered ring formation has two molecules of TFE coordinated to iron. Even if a second molecule of 2,6-dimethylphenylisocyanide does readily dissociate, it will still be in solution and provide competition with TFE for the coordination site. The isocyanide is a better σ-donor than TFE and will more easily bind to the already electron deficient iron atom coordinated to three heavily electron-withdrawing isocyanides and a molecule of TFE.

This reaction has not been attempted at elevated temperature or using photolysis. It is promising that reactivity is observed at room temperature, however, heat or UV irradiation may be necessary to stimulate the loss of a second isocyanide to selectively generate only the metallacycle.

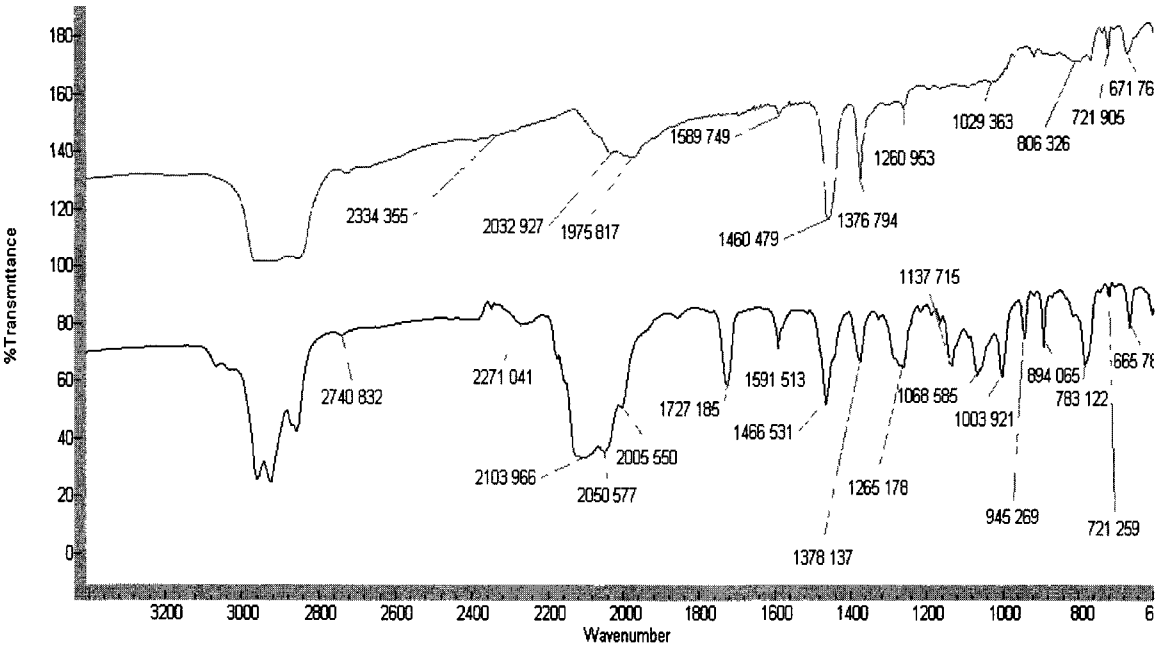

Figure 8: IR spectra of complex [19] (top) and complexes [20] and [21] (bottom) in Nujol.

IR spectra for complexes [19], and [20] and [21] are compared in Figure 8. The observed bands for complex [19] are consistent with those reported in the literature for $Fe(CNAr)_5$ (C≡N stretching bands at 2040 and 1965 cm^{-1}).[16] The ligands in this complex are configured in an approximately trigonal bipyramidal geometry whereby the two axial ligands are the only two directly *trans* to each other and compete the strongest for the metal's electron density and thus absorb at a higher wave number. The isocyanide ligands more involved in π-backbonding would be expected to exhibit C≡N stretching vibrations at a lower wavenumber. This trend is consistently observed for the IR spectra of [19], [20] and [21]. The C≡N stretching bands in complex [19] are at 2034 and 1976 cm-1; they are shifted to higher frequency (2104, 2051 and 2006 cm-1) on complexation of TFE. There are no reports of iron isocyanide complexes of fluoro-olefins for comparison to complexes [20] and [21]; the most similar complex is *cis*-dichlorotetrakis(2,6-diphenylphenyl isocyanide) iron. This iron(II) compound has the expected geometry for the fluoro-olefin and –metallacycle complexes presented here: pseudo-octahedral with two isocyanides filling the

apical sites, two *cis* isocyanides and two chlorides in the equatorial plane.[17] The chlorides behave similarly electronically to the electron-withdrawing alkyl fluorides. The IR spectrum for *cis*-dichlorotetrakis(xylyl isocyanide) iron contains two C≡N stretching bands at 2146 and 2120 cm^{-1}.[17] It is evident by the frequency at which isocyanides absorb that the alkyl fluorides are almost as efficient at withdrawing electron density from iron as chloride, decreasing the amount of π-backbonding between iron and the isocyanides. Bands for the C-F bonds are in the region 1400-1000 cm^{-1}.

3.6 Preparation of Anionic Iron Metallacycle Complexes Containing a Cyclopentadienyl Ligand

Under the assumption that a lack of sufficient electron density on iron may explain its inability to completely form the five-membered versus the three-membered metallacycle, the preparation of anionic iron metallacycles was attempted. The similarly π-acidic ligands, phosphite and isocyanide, generate both the olefin and metallacycle complexes when reacted with TFE. Even the less π-acidic phosphine complexes produce both. The iron complex $Fe(CO)_4(\kappa^2$-dppe) is completely unreactive towards TFE.

The monomeric complex potassium cyclopentadienyliron dicarbonyl was prepared from the dimer $[FeCp(CO)_2]_2$ by reduction with potassium in THF. Previous reports of the reduction of the dimer employed a 30% excess of a 1% Na/Hg amalgam.[18] In the reduction with potassium, two products were synthesized: potassium cyclopentadienide and complex [22], $K[FeCp(CO)_2]$. KCp is the major product (1.00:0.89 KCp:[22] from integrals of peaks in ^1H NMR spectrum).

Reaction of complex [22] with TFE results in an immediate color change from a clear, red/orange solution to a darker red. This reaction was carried out at room temperature and without irradiation, giving $[FeCp(CO)_2]_2$ as the major product

(80%) as well as two metallacycles (trace [23] and 11% [24]) (Scheme 8), as confirmed by ^{1}H and ^{13}C NMR spectroscopy. Two singlets in the ^{1}H NMR spectrum at 4.92 and 5.01 ppm are the remaining 9%; the Cp containing product(s) responsible for these peaks has not been identified.

The major metallacycle [24] has four triplets for two types of α-CF_2 and two types of β-CF_2 groups on the metallacycle. The α-CF_2's resonate at -61.34 and -61.36 ppm with vicinal fluorine coupling constants of 4.7 Hz. The triplets for the β-CF_2's are at -126.76 and -126.96 ppm with $^{3}J_{FF}$ = 4.6 Hz. It is obvious from the size of this coupling constant that the fluorine atoms on a given carbon are isochronous; geminal coupling constants are much greater than 5 Hz. The greater amount of electron density on iron from the anionic Cp ligand deshields the fluorine atoms on the metallacycle more than in the other complexes, shifting its ^{19}F NMR signals further downfield.

The oxidative-addition of two molecules of TFE to complex [22] to form the metallacycle would generate a 20 electron complex. Therefore, one of the carbonyl ligands must be lost during the reaction, to give the 18 electron complex [24] (Scheme 8). This is consistent with the presence of one new CO peak in the $^{13}C\{^{1}H\}$ NMR spectrum at 215.18 ppm (the other peaks in this region are for $[FeCp(CO)_2]_2$ and an unidendified $[FeCp(CO)_2]$ derivative). The proposed configuration for [24] has both the metallacycle and the single CO in the same plane, parallel to each other, with the Cp ring occupying the apex, as in the proposed structure for $CoCp(CF_2)_4(CO)$.[19] The plane of the Cp ring is perpendicular to the plane formed by the CO and carbon atoms of the metallacycle. A configuration of this sort is proposed because the fluorine atoms on a single carbon are equivalent. Any other orientation would break the symmetry of the ring.

In a second much more minor fluorine-containing product, the symmetry of the ring is broken with different geometry above and below the plane of the metallacycle. The fluorine atoms on the same carbon are not equivalent. Peaks for four unique fluorines are distinguishable from the ^{19}F NMR spectrum. The

peaks at -56.56 ppm and -84.01 ppm are the α-fluorines of complex [23]; they share a germinal coupling constant of ca. 59 Hz. The two signals for the β-fluorines are doublets at approximately -134.54 and -134.56 ppm. Their geminal coupling constant is 86 Hz. In this complex, the Cp ring invokes a "piano stool" geometry whereby, the CO and metallacycle form the legs of the piano stool.

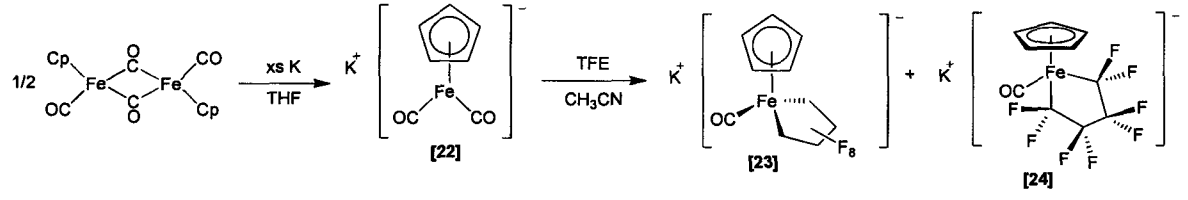

Scheme 8: Synthesis of cyclopentadienyliron carbonyl complexes of TFE.

Four additional very minor doublets are observed in the ^{19}F NMR spectrum for this reaction. Based on previous results, they are proposed to be due to two olefin complexes as the peaks are found in this region of the spectrum (-105 to -125 ppm). It is also possible that they originate from a reaction of TFE with KCp, if all traces were not removed from [22] prior to the reaction with TFE.

The IR spectrum for the products of this reaction is shown in Figure 9. There are four new CO stretching bands in the spectrum, consistent with the reformation of the starting dimer $[FeCp(CO)_2]_2$, the production of metallacycle complex [24], and an unidentified derivative of $[FeCp(CO)_2]$.

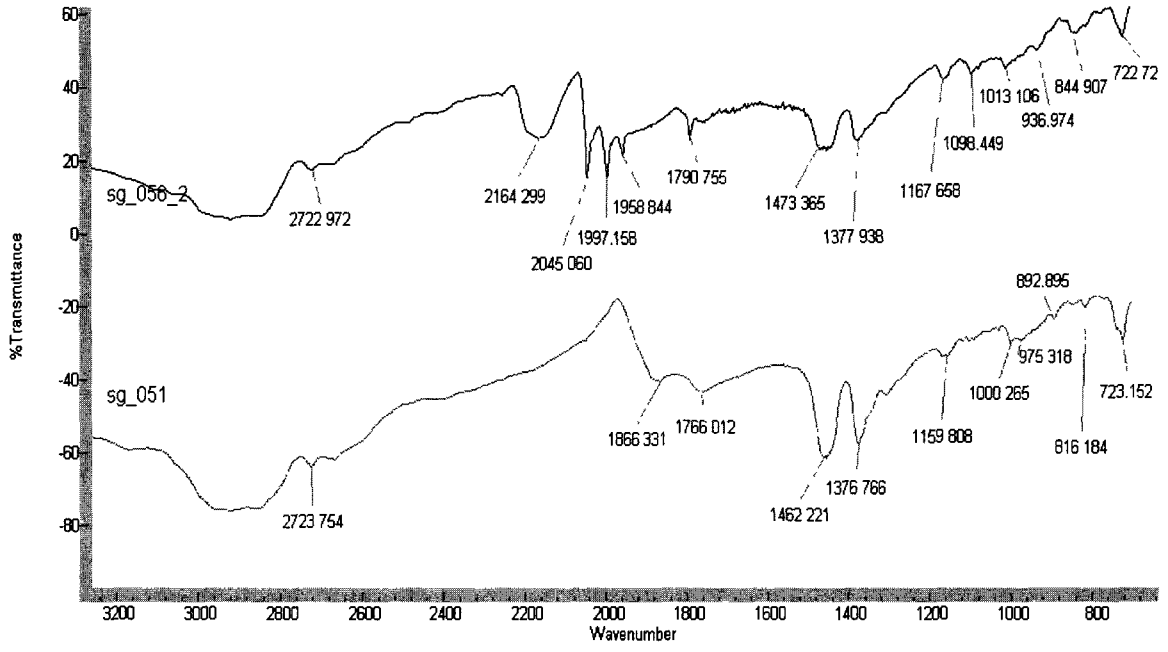

Figure 9: IR spectra for complex [22] (bottom) and complexes [23] and [24] (top) in a Nujol mull.

3.7 Conclusions

It appears as though steric considerations exert greater control than electronic ones over the relative bond lengths and strengths of the iron-C_F bonds in the metallacycle complexes that have been crystallographically characterized. If sterics are responsible here, they may also dictate formation of three- versus five-membered metallacycles. The driving force is less likely due to an electronic origin as both olefin and metallacycle complexes are synthesized from iron phosphite carbonyl, isocyanide, and phosphine carbonyl complexes, whose ligands all have different electronic properties. The cases where five-membered rings were preferentialy formed were in the complexes with the less sterically hindered metal sites, using $Fe_2(CO)_9$ and $K[FeCp(CO)_2]$ as precursors. These complexes take opposite ends of the electronics spectrum when considering only those iron complexes investigated here. Therefore, the amount of access on the metal granted to the incoming fluoro-olefin by the ancillary ligands must drive or inhibit five-membered ring formation; hence the selective formation of olefin

complexes by the bis-substituted phosphine and phosphite complexes, and metallacycle formation by the mono-substituted analogues.

Table 1: The ^{13}C NMR chemical shifts for the metallacycle carbon atoms in complexes [1], [8], and [17], and olefin complex [20].

Complex	^{13}C NMR Chemical Shift (ppm)	
	α-CF_2	β-CF_2
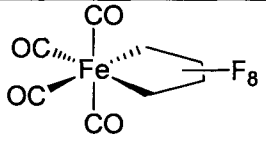 **[1]**	140.59	114.39
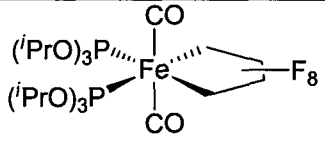 **[8]**	143 146	114 115
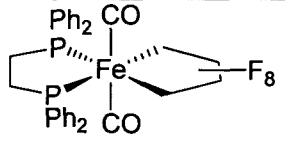 **[17]**	144 147	114 116
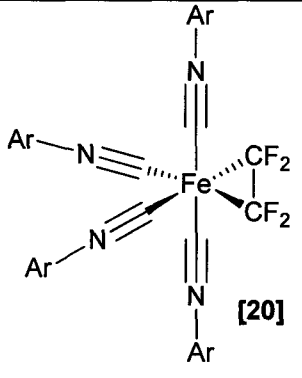 **[20]**	135	

Several trends have been observed from the NMR spectroscopic analysis of the iron fluorometallacycle complexes in this study. Consistent with previous reports

on transition metal fluorometallacycle complexes, the fluorine atoms on the carbons directly bonded to the iron are more deshielded and are shifted to lower field than the β- fluorine atoms. For the same reason, the α-carbons' ^{13}C resonances are further downfield than the resonance for the β-carbon atoms. The ^{13}C NMR chemical shift for the metallacycle carbon atoms that have been determined are compared in Table 1. The chemical shift for the β-carbons is not greatly affected by a change in ancillary ligands. However, the α-carbons are shifted further downfield (more deshielded), as the equatorial carbonyl ligands are replaced by more σ-donating, less π-acidic ligands. The chemical shift for the carbon atoms of the olefin complex [20] is further upfield than the α-carbons, but not as far as the β-carbons, of the metallacycle complexes.

It was formerly assessed that the ^{19}F NMR chemical shift of the resonance due to the β-CF_2 groups does not vary greatly from compound to compound. Conversely, the chemical shift for the resonance for the α-CF_2 groups is considerably different for different complexes.[6] It can be concluded from this study considering a more extensive group of ligands, that the ^{19}F NMR chemical shift of both the α- and β-CF_2 groups is influenced by the ancillary ligands and by their geometry. The ^{19}F NMR chemical shifts for the metallacycle complexes generated in this investigation are listed in Table 2. The chemical shift for the β-CF_2's are relatively constant for complexes [1], [6], [8], [11], [14], [17], and [21]. The α-CF_2 groups are more shielded as the carbonyl groups are replaced by other ligands. The complexes in which one of the equatorial CO ligands is replaced by a phosphite or phosphine, the signal for the α-CF_2 group *trans* to it is shifted further upfield. The greatest effect on the chemical shift of both α- and β-CF_2 groups is seen for complex [24]. With the metallacycle *trans* to the anionic Cp ligand, the α- and β-CF_2's are shifted downfield. The most surprising effect on chemical shift was observed for complex [7], which has the two axial CO's substituted by $P(O^iPr)_3$. The signal for the α-CF_2 groups is shifted significantly upfield, while the signal for the β-CF_2's is drastically shifted downfield. This same effect is not seen for the analogous phosphine complex [14].

Table 2: ^{19}F NMR chemical shifts for complexes [1], [6], [7], [8], [11], [14], [17], [21], and [24].

Complex	^{19}F NMR Chemical Shift (ppm)		Complex	^{19}F NMR Chemical Shift (ppm)	
	α-CF_2	β-CF_2		α-CF_2	β-CF_2
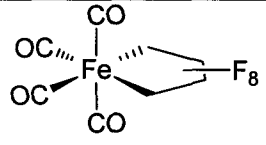 **[1]**	-72.29	-137.18	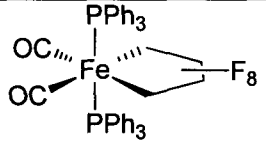 **[14]**	-79.80	-137.88
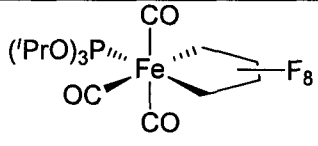 **[6]**	-75.60 -79.26	-137.21 -137.98	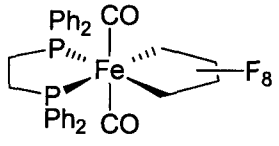 **[17]**	-75.63	-138.27
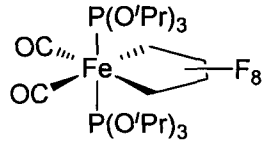 **[7]**	-91.05	-125.48	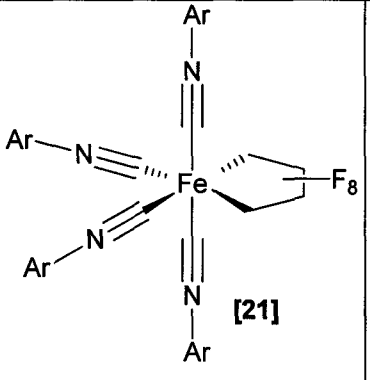 **[21]**	-83.90	-136.55
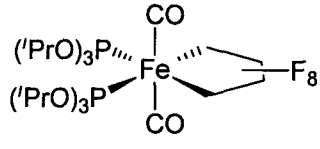 **[8]**	-81.16	-138.42	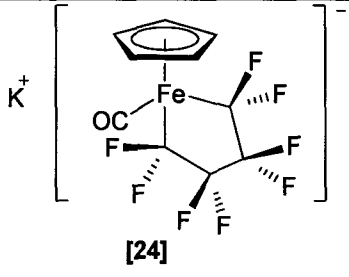 **[24]**	-61.34 -61.36	-126.76 -126.96

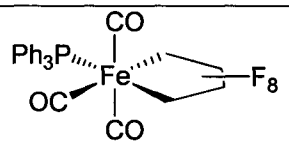 [11]	-74.51 -82.12	-139.75 -139.98			

Table 3: ^{19}F NMR chemical shifts for complexes [4], [5], [12], [13], and [20].

Complex	^{19}F NMR Chemical Shift (ppm)	Complex	^{19}F NMR Chemical Shift (ppm)
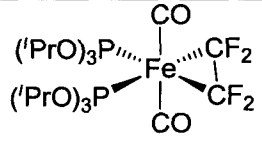 [4]	-111.56	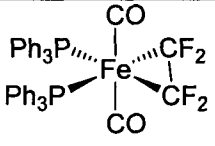 [13]	-116.90
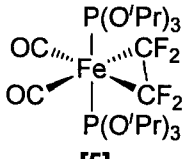 [5]	-112.27	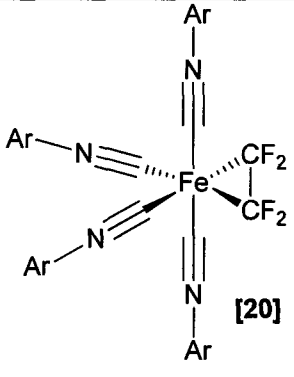 [20]	-115.66
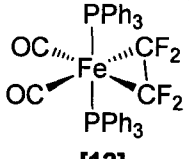 [12]	-113.38		

Variation of the ligands in the olefin complexes does not have much of an effect on the ^{19}F NMR chemical shift. All five olefin complexes generated were symmetrical, making all four fluorine atoms in the metallacyclopropane ring chemically equivalent. Their chemical shifts are intermediate between the chemical shifts of the α- and β-CF_2 groups in the metallacyclopentane complexes.

3.8 References

[1] Manuel, T.A.; Stafford, S.L.; Stone, F.G.A. *J. Am. Chem. Soc.* **1961**, *83*, 249.

[2] Fields, R.; Germain, M.M.; Haszeldine, R.N.; Wiggans, P.W. *Chem. Comm.* **1967**, 243.

[3] Hoehn, H.H.; Pratt, L.; Watterson, K.F.; Wilkinson, G. *J. Chem. Soc.* **1961**, 2738.

[4] Fields, R.; Germain, M.M.; Haszeldine, R.N.; Wiggans, P.W. *J. Chem. Soc. (A)* **1970**, 1969.

[5] Pitcher, E.; Buckingham, A.D.; Stone, F.G.A. *J. Chem. Phys.* **1962**, *36*, 124.

[6] Stone, F.G.A. *Pure Appl. Chem.***1972**, *30*, 551.

[7] Lindner, V.E.; Schauβ, E.; Hiller, W.; Fawzi, R. *Angew. Chem.* **1984**, *96*, 727.

[8] Braga, D.; Grepioni, F.; Orpen, A.G. *Organometallics*, **1993**, *12*, 1481.

[9] Burt, R.; Cooke, M.; Green, M. *J. Chem. Soc. (A)* **1970**, 2975.

[10] (a) Tolman, C.A. *Chem. Rev.* **1977**, *77*, 313. (b) Tolman, C.A. *J. Am. Chem. Soc.* **1970**, *92*, 2956.

[11] Fields, R.; Germain, M.M.; Haszeldine, R.N.; Wiggans, P.W. *J. Chem. Soc. (A)* **1970**, 1964.

[12] Farrer, N.J.; McDonald, R.; McIndoe, J.S. *Dalton Trans.* **2006**, 4570.

[13] Manuel, T.A. *Inorg. Chem.* **1963**, *2*, 854.

[14] Dolbier, W.R. Jr. *Guide to Fluorine NMR for Organic Chemists*; Wiley: New Jersey, **2009**.

[15] Drew, M.G.B.; Dodd, G.H.; Williamson, J.M.; Willey, G.R. *J. Organomet. Chem.* **1986**, *314*, 163.

[16] Bassett, J.M.; Berry, D.E.; Barker, G.K.; Green, M.; Howard, J.A.K.; Stone, F.G.A. *J .Chem. Soc., Dalton Trans.* **1979**, 1003.

[17] Perry, M.C.; Law, T.C.; Wheeler, K.A. *J. Chem. Crystallogr.* **2010**, *40*, 482.

[18] King, R.B.; Bisnette, M.B. *J. Organomet. Chem.* **1964**, *2*, 38.

[19] Coyle, T.D.; Kings, R.B.; Pitcher, E.; Stafford, S.L.; Treichel, P.; Stone, F.G.A. *J. Nucl. Inorg. Chem.* **1961**, *20*, 172.

Chapter 4: Exploring the Reactivity of Iron Fluorometallacycles with a Variety of Lewis Acids

4.1 Introduction

An iron fluorocarbene is the suspected intermediate in the hydrogenolysis of $Fe(CF_2)_4(CO)_4$ (Chapter 1, Scheme 10). If this carbene complex can be accessed and isolated, characterizing it and probing its reactivity may provide insight into the hydrogenolysis mechanism. Developing methods to exploit the ability of transition metals to effect synthetic transformations of fluorocarbons is also a goal of this part of the research project. The high strength of the carbon-fluorine bond makes it quite unreactive. Mediation of fluoride abstraction by a transition metal is a potential route to the functionalization of fluorocarbons on the way to the production of new fluorochemicals. By accessing the fluorocarbene analogue of one of the metallacycle complexes discussed in Chapter 3, a wide selection of functional groups could be introduced to this carbon. Selective hydrogenolysis to remove the FCD from iron would permit isolation of classes of new fluorochemicals.

Fluorocarbene complexes of mid- to late-transition metals do not fit into the discrete classification of the two types of carbene complexes as Schrock alkylidenes or Fischer carbenes.[1] Schrock alkylidenes are generally represented by high-valent early transition metals containing H- or alkyl-substituents on the carbene carbon. Fischer carbenes contain late-transition metals with good π-donating heteroatoms substituents (such as N or O) on the carbene carbon. Iron fluorocarbene complexes have the electron-rich metal centre of the Fischer-type, but with electron-withdrawing substituents on the carbene carbon. The reactivity at the carbene carbon thus cannot easily be predicted, and will likely vary depending on the oxidation state of the metal and the ancillary ligands.[1]

4.2 Attempts to Synthesize Fluorocarbene Complexes of Iron Metallacycles with Tris(pentafluorophenyl)boron

Boron forms the strongest covalent bond with fluorine (181 kcal/mol),[2] making it an excellent candidate for Lewis acid-induced synthesis of an iron fluorocarbene complex. The boron-fluorine bond is so strong that the fluoride abstraction should be irreversible, allowing for isolation of the iron fluorocarbene complex.

The only report related to fluoride abstraction from an iron fluorometallacycle complex discusses the lack of reactivity of $Fe(CF_2)_4(CO)_4$ towards BF_3.[3] Also, there was no evidence for halogen exchange in the complex when reacted with BCl_3.[3] These Lewis acids are extremely moisture sensitive and volatile, rendering them difficult to handle. The strong Lewis acid properties, as well as its lack of propensity to undergo fluoride migration to the boron from its fluorophenyl substituents,[4] make tris(pentafluorophenyl)boron an excellent candidate to explore the ability to isolate a stable iron fluorometallacyclic carbene.

Before use, the borane ($B(C_6F_5)_3$) was sublimed under reduced pressure at 86 °C. As purchased from Strem, the borane contained both the expected compound, $B(C_6F_5)_3$, and its water adduct, $H_2O{\bullet}B(C_6F_5)_3$. These two boron compounds give rise to the following peaks in the ^{19}F NMR spectrum, where the peaks for the water adduct are labelled with "$_{H2O}$": -130.87 ppm; -136.15 ppm $_{H2O}$; -143.50 ppm; -156.67 ppm $_{H2O}$; -161.88 ppm; -164.59 ppm $_{H2O}$. The peaks furthest downfield are for the *ortho* fluorines, then *para*, with the *meta* fluorine signals furthest upfield. All three peaks for $B(C_6F_5)_3$ are broad singlets, whereas peaks for $H_2O{\bullet}B(C_6F_5)_3$ have the multiplicity of doublet, triplet, and unresolved doublet of doublets for the *ortho, para,* and *meta* fluorines, respectively.

The reactivity of complexes [1], [7]/[8], [19]/[20], and [23]/[24] with tris(pentafluorophenyl)boron was explored and analyzed by NMR. The results for all reactions were different, but somewhat related. Chemical shifts cited for the peaks in the ^{19}F NMR spectra for these reactions are calculated from the midpoint of the complex second order multiplets, and are not thus not always accurate. Coupling constants are

estimated from the spectra. Full spectral simulation would be necessary, but was not performed, to determine the coupling constants and chemical shifts accurately.

4.2.1 Reaction of $B(C_6F_5)_3$ with $Fe(CF_2)_4(CO)_4$

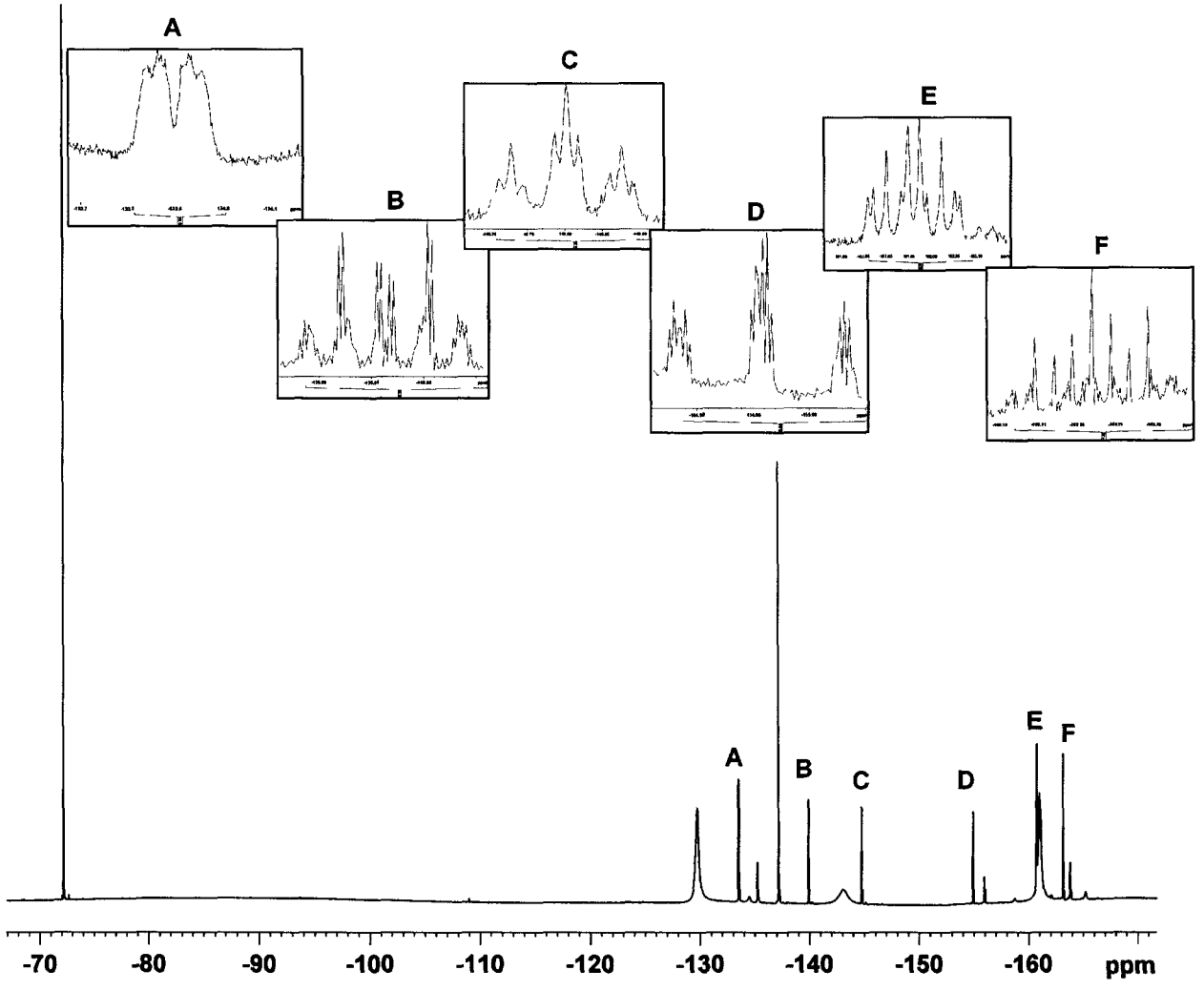

Figure 1: ^{19}F NMR spectrum (C_6D_6) for the reaction of $Fe(CF_2)_4(CO)_4$, complex [1], with $B(C_6F_5)_3$ (reaction 2.3.1).

After treatment of complex [1], $Fe(CF_2)_4(CO)_4$, with a slight excess of $B(C_6F_5)_3$ in C_6D_6 by stirring under N_2 at room temperature for 20 hours, only a small amount of the iron complex was transformed, generating six new peaks in the ^{19}F NMR spectrum. A one

fold excess of $B(C_6F_5)_3$ was added to the reaction mixture; stirring for 10 days resulted in only a slight increase in conversion. To see if the reaction could be driven further thermally, the reaction mixture was heated at 50 °C for four days. As can be seen in the ^{19}F NMR spectrum of the resulting mixture (reaction 2.3.1,Figure 1), the starting material still represents more than half of the total fluorine. The six new peaks are labelled A-F. Based on the coupling constants estimated from the spectrum, peaks A (2F), C (1F), and E (2F) are related to each other, as are B(2F), D(1F), and F(2F). The ^{19}F COSY spectrum, (Figure 2), indicates correlations between the peaks from the boron compounds and also relates A to E, C to E, and E to A and C, and similarly, B to F, D to F, and F to B and D. Therefore, two new compounds were produced, each with three unique fluorine environments.

Note also that all observed fluorine resonances are at higher field than that of the original α-CF_2 resonance in [1], suggesting they are not due to the metallacycle. Indeed the 2:1:2 ratios are more consistent with new C_6F_5 resonances.

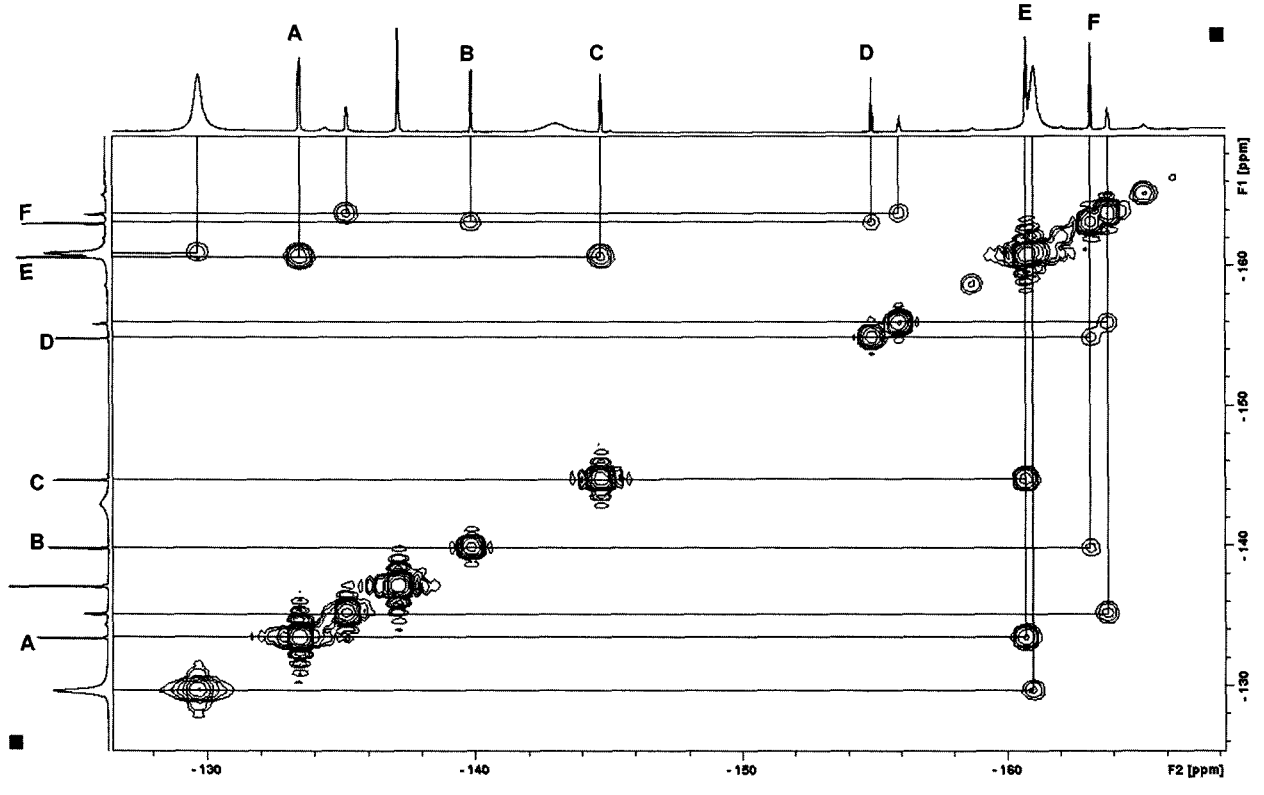

Figure 2: ^{19}F COSY spectrum for the reaction of $Fe(CF_2)_4(CO)_4$, complex [1], with $B(C_6F_5)_3$ (reaction 2.3.1).

4.2.2 Attempted fluoride abstraction from $Fe(CF_2)_2(CNAr)_4$ and $Fe(CF_2)_4(CNAr)_4$ with $B(C_6F_5)_3$ [CNAr = 2,6-$(CH_3)_2C_6H_4$]

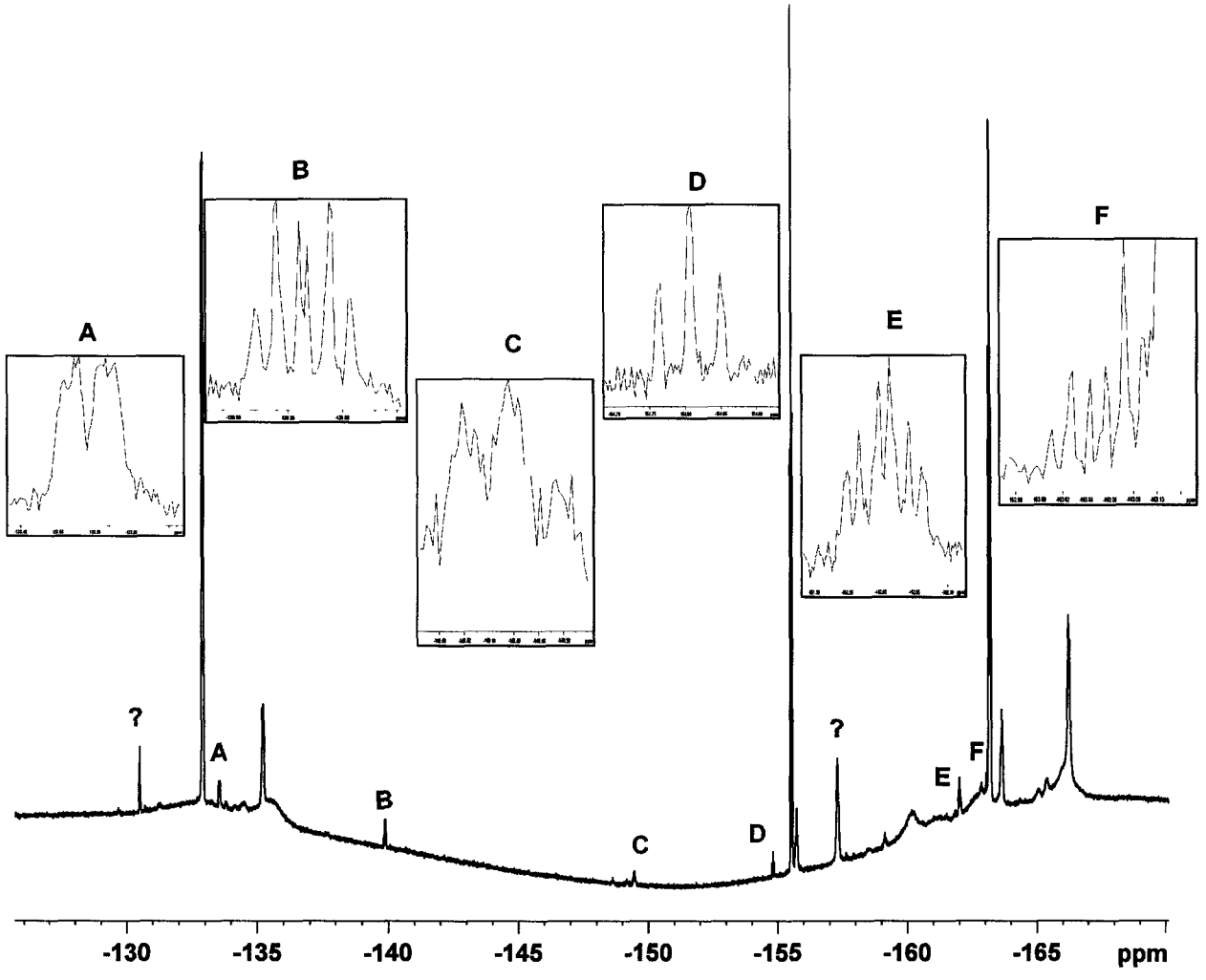

Figure 3: ^{19}F NMR spectrum for the reaction of $Fe(CF_2)_2(CNAr)_4$ [20] and $Fe(CF_2)_4(CNAr)_4$ [21] with $B(C_6F_5)_3$ (CNAr = 2,6-$(CH_3)_2C_6H_4$) (reaction 2.3.2).

Similar A-F peaks show up in the ^{19}F NMR spectrum from the room temperature reaction of complexes [20] and [21] with $B(C_6F_5)_3$ in C_6D_6. The peaks occur at slightly different chemical shifts and the coupling patterns are not quite as clearly resolved, however, they do closely resemble the corresponding peaks from the reaction with complex [1] as listed in Table 1.

Table 1: Comparison of the approximate chemical shifts and estimated coupling constants for the reactions of complexes [1] and [20]/[21] with $B(C_6F_5)_3$.

	Reaction 2.3.1	**Reaction 2.3.2**
A	-133.46 ppm dd J = 20.5, 7 Hz	-133.54 ppm dd J = 24, 7 Hz
B	-139.86 ppm ddddd J = 24, 10, 10, 2.3, 1	-139.86 ppm ddd J = 24, 10, 10
C	-144.72 ppm ddddd, J = 20.5, 20.5, 4, 4, 0.5 Hz	-149.55 ppm tr J = 19 Hz
D	-154.89 ppm ddddd J = 24, 20.5, 2.8, 1, 1 Hz	-154.81 ppm tr J = 21 Hz
E	-160.71 ppm dddd J = 20.5, 11, 11, 3.5 Hz	-161.01 ppm ddd J = 24, 21, 8 Hz
F	-163.14 ppm dddd J = 24, 20.5, 8, 7 Hz	-163.64 ppm tr J = 20 Hz

Complexes [20] and [21] have completely reacted with the borane; all of the peaks in the ^{19}F NMR spectrum corresponding to these complexes have disappeared, yet no resonances indicative of α-CF_2 groups are observed. New major C_6F_5 environments are evidenced by three sharp peaks at -133 (ortho), -155.5 (para) and -163 ppm (meta) as well as broad peaks at -135.2, -160.7, -163.8, and -165.1 that may be due to the $[BF(C_6F_5)_3]^-$ anion. The peaks labelled with "?" likely result from the reaction of the olefin

complex [20] with $B(C_6F_5)_3$. The ^{11}B NMR spectrum for this reaction (Figure **7**) shows broad peaks at 2.5 and -9 and a sharper peak at -20 ppm. The ^1H NMR spectra for reactions 2.3.1 and 2.3.2 both contain a unique triplet of triplet of doublets resonance (J_{HF} = 10.2, 7, 2.6 Hz) at 5.8 ppm (Figure 4).

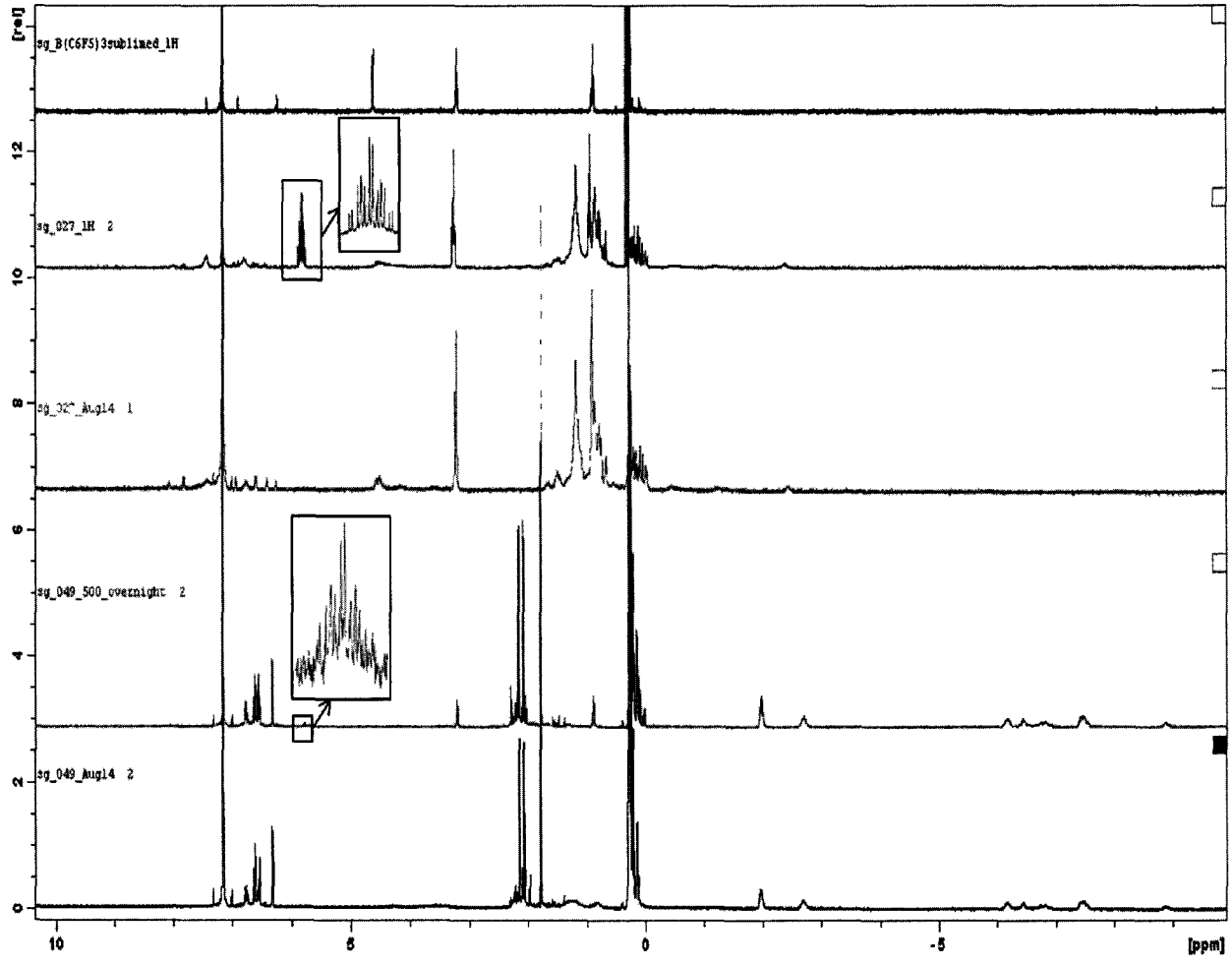

Figure 4: ^1H NMR spectra (C_6D_6) of (from top to bottom): sublimed $B(C_6F_5)_3$; $Fe(CF_2)_4(CO)_4$+ $B(C_6F_5)_3$; $Fe(CF_2)_4(CO)_4$+ $B(C_6F_5)_3$ with volatiles removed; $Fe(CF_2)_2(2,6\text{-}(CH_3)_2C_6H_4NC)_4$ and $Fe(CF_2)_4(2,6\text{-}(CH_3)_2C_6H_4NC)_4$ + $B(C_6F_5)_3$; $Fe(CF_2)_2(2,6\text{-}(CH_3)_2C_6H_4NC)_4$ and $Fe(CF_2)_4(2,6\text{-}(CH_3)_2C_6H_4NC)_4$ + $B(C_6F_5)_3$ with volatiles removed.

If the fluorocarbon has been removed from the metal by reaction with $B(C_6F_5)_3$, it should be volatile and easily removed under reduced pressure. To determine if this is the case, all of the solvent and volatile materials were removed via vacuum from the reaction mixture. The residue was redissolved in a small amount of C_6D_6 and

reanalyzed by ^{1}H, ^{19}F, and ^{11}B NMR spectroscopy. The ^{1}H NMR spectrum of the sublimed $B(C_6F_5)_3$ is compared with those for reactions 2.3.1 and 2.3.2, before and after removing the volatile material, in Figure 4. There was no evidence from this analysis that pointed to the production of a new fluorocarbon originating from the metallacycle.

Note that the multiplet at 5.8 ppm is removed via vacuum, and while the ^{11}B NMR spectra remained the same after removing the volatiles, the peaks shaded in grey (B,D,F) in Table 1 are no longer present in the ^{19}F NMR spectra. Comparison with literature values identifies this species as C_6F_5H, consistent with degradation of the Lewis acid as the major reaction pathway in experiment 2.3.1. In experiment 2.3.2, on the other hand, disappearance of starting metallacycle is accompanied by appearance of multiple broad, high-field ^{1}H NMR resonances that could indicate formation of paramagnetic iron product(s).

4.2.3 Attempted carbene formation from *trans*-bis(triisopropylphosphite) perfluorotetramethyleneiron dicarbonyl with $B(C_6F_5)_3$

The product of the reaction of the mixture of phosphite metallacycle complexes [7] and [8] with $B(C_6F_5)_3$ is more distinct than the reactions with $B(C_6F_5)_3$ discussed thus far. The borane selectively reacts only with the minor isomer, complex [7], which has the two phosphites *trans* to each other, in the axial positions. The peak in the $^{31}P\{^{1}H\}$ corresponding to complex [7] is no longer present following the reaction; however, there is no new peak in the spectrum. This result is surprising because the α-carbon of the metallacycle is more sterically hindered, making it difficult for the borane with its bulky pentafluorophenyl substituents to gain access to the fluorines on the α-carbons. Several peaks in the ^{19}F NMR spectrum for this reaction R-U resemble the new C_6F_5 peaks produced in the previous reactions, but we now observe a number of new resonances in the α-CF_2 region (Figure 5). The reaction, however, is clearly not selective for formation of a single product and further analysis was not pursued.

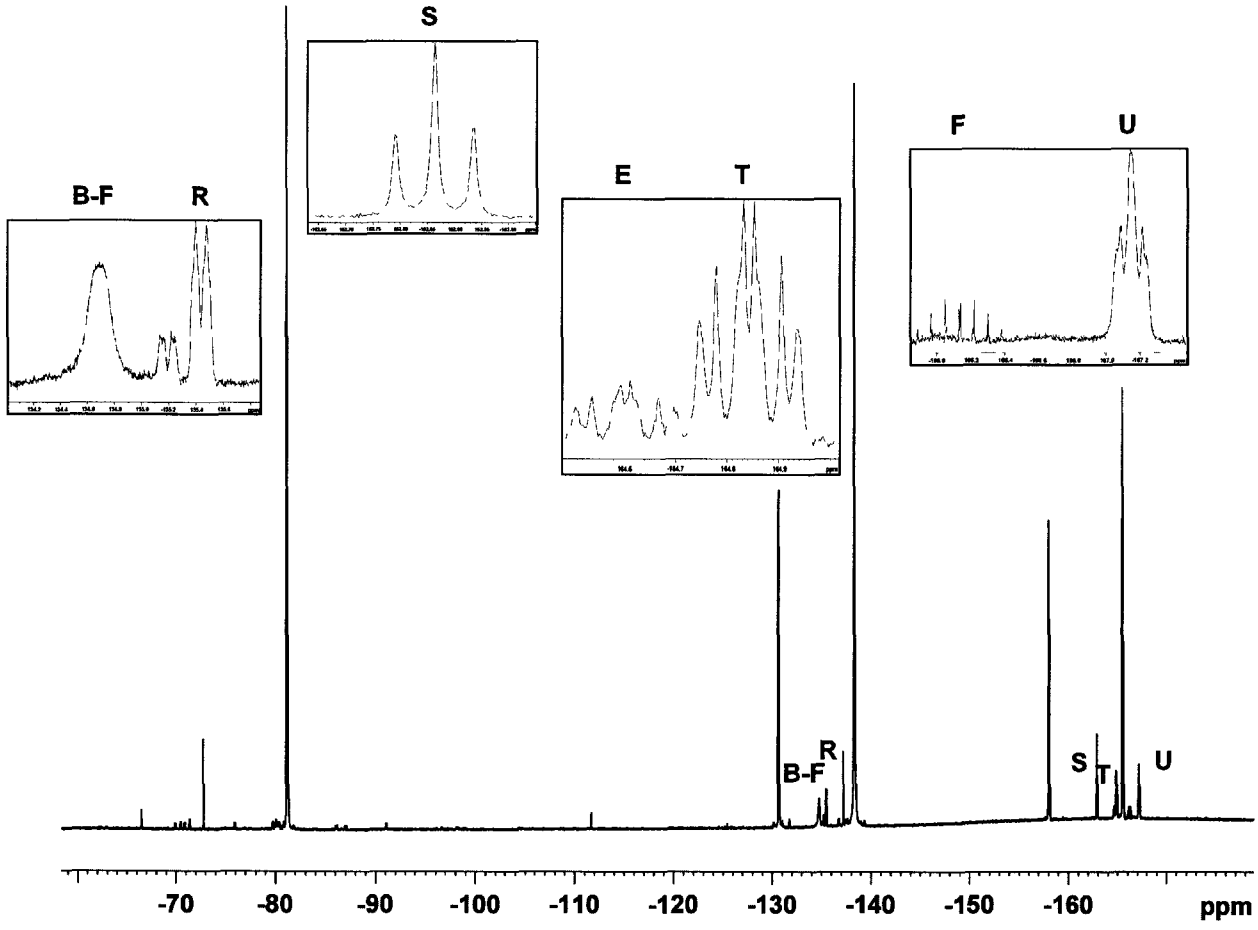

Figure 5: ^{19}F NMR spectrum for the reaction of phosphite complexes [7] and [8] with $B(C_6F_5)_3$ (reaction 2.3.3).

4.2.4 Attempted carbene formation from $K[FeCp(CF_2)_4(CO)]$ with $B(C_6F_5)_3$

The fourth and final attempt to use $B(C_6F_5)_3$ to abstract a fluorine anion from an iron metallacycle complex in this investigation is the reaction with the iron-cyclopentadiene metallacycle. Because the ^{19}F NMR signals cannot be reliably correlated based upon their estimated coupling constants (many of the new peaks from this reaction are broad singlets), only those peaks related in the ^{19}F COSY have been labelled and analyzed (Figure 6).

Of the signals correlated in the ^{19}F COSY (Table 2), those labelled as H, L, and O can be grouped into a single molecule, A', C', and E' a second, a third new compound

contains fluorines B',D', and F', while I, J, K and N represent the fluorines in a fourth compound. The first three compounds are again likely C_6F_5 derivatives; these broad singlets H, L, and O resemble the peaks for $B(C_6F_5)_3$. As seen in the ^{19}F NMR for experiment 2.3.2, the peaks labelled I, J, K and N may be due to the $[BF(C_6F_5)_3]^-$ anion Note also that new α-CF_2 resonances were again not observed.

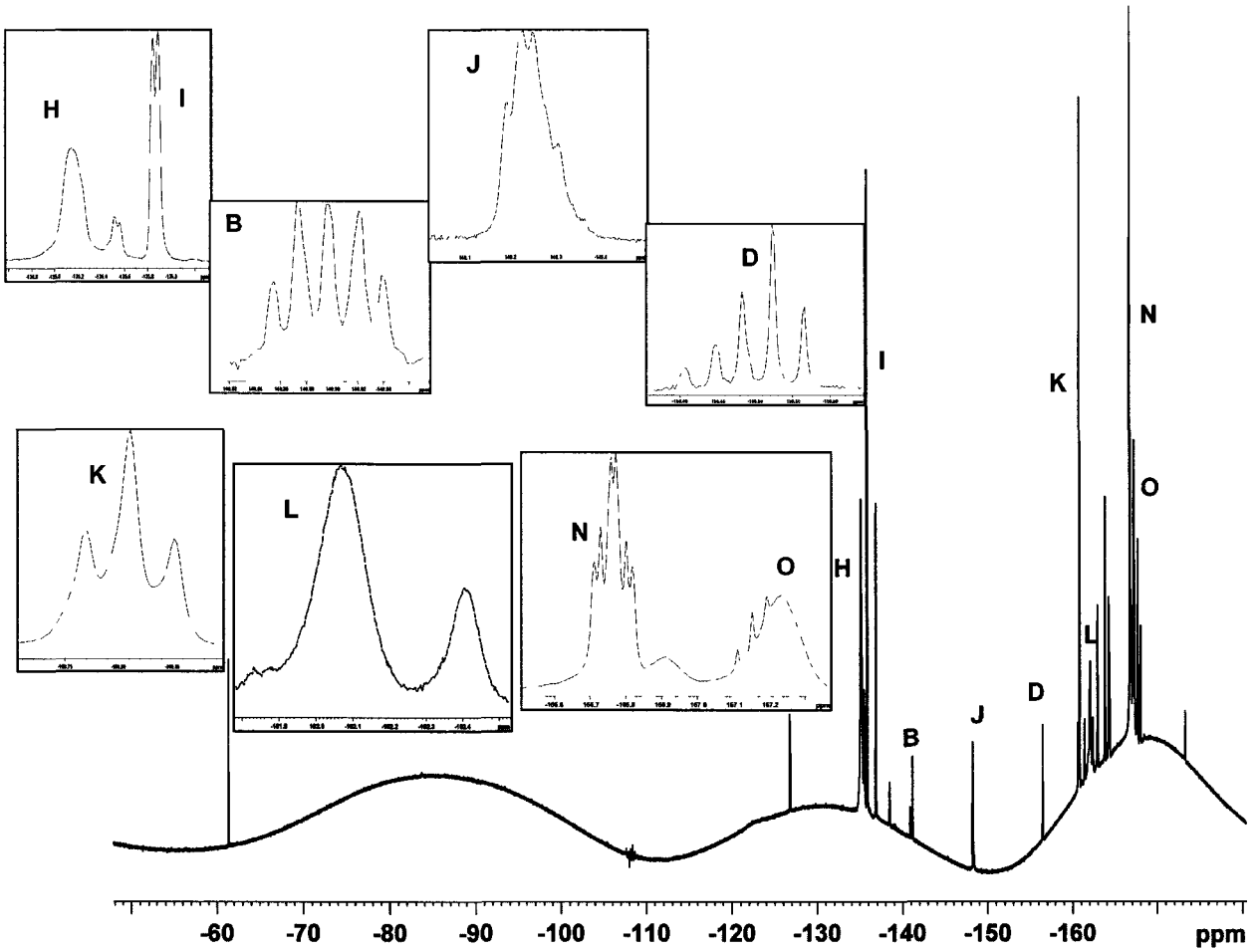

Figure 6: ^{19}F NMR spectrum for the reaction of complexes [23] and [24] with $B(C_6F_5)_3$ (reaction 2.3.4).

Table 2: Analysis of the ^{19}F NMR spectrum for reaction 2.3.4.

[a] It was not possible to determine the relative integrals for peaks B', D', and F' because D' overlaps with another peak and the base-line is not flat around peak F'.

Peak	Chemical Shift (ppm)	Multiplicity	Estimated F-F Coupling Constants (Hz)	Correlations from ^{19}F COSY	Relative Integration
H	-135.15	Singlet	-	O	2
L	-162.07	Singlet	-	O	1
O	-167.23	Singlet	-	H and L	2
A'	-136.88	Doublet	22	E'	2
C'	-163.82	Triplet	20	E'	1
E'	-167.68	Triplet of doublets	21, 8	A' and C'	2
B'	-138.49	Singlet	-	-	-[a]
D'	-167.15	Triplet	20	-	-
F'	-173.32	Triplet	22	B' and D'	-
I	-135.86	Doublet	21	N	2
J	-148.25	Apparent quintet	12	K	1
K	-160.81	Triplet	19	J and N	2
N	-166.77	Triplet of doublets	20, 8	I and K	2

The ^{11}B spectra of the products from all four $B(C_6F_5)_3$ reactions are displayed in Figure 7. The only reaction that appears to contain unreacted $B(C_6F_5)_3$ is 2.3.1 with $Fe(CF_2)_4(CO)_4$ whereby excess was added. Similar ^{19}F NMR spectra were obtained for reactions 2.3.1 and 2.3.2, however, their ^{11}B NMR spectra do not completely agree. There is a new sp^2 hybridized product at 38.57 ppm and an sp^3 hybridized product at -17.58 ppm. A different sp^3 hybridized product was generated in reaction 2.3.2. The assignment of a signal in the ^{19}F NMR spectrum of reaction 2.3.3 as $[B(C_6F_5)_3F]^-$ is consistent with the doublet at -16.29 ppm with a boron-fluorine coupling constant of

approximately 135 Hz in its ^{11}B spectrum. The cleanest ^{11}B NMR spectrum was obtained for reaction 2.3.4. The doublet at -11.74 ppm is also likely $[B(C_6F_5)_3F]^-$. The other peaks would correspond to the uncharacterized derivatives of $B(C_6F_5)_3$ proposed from analysis of the ^{19}F NMR spectrum.

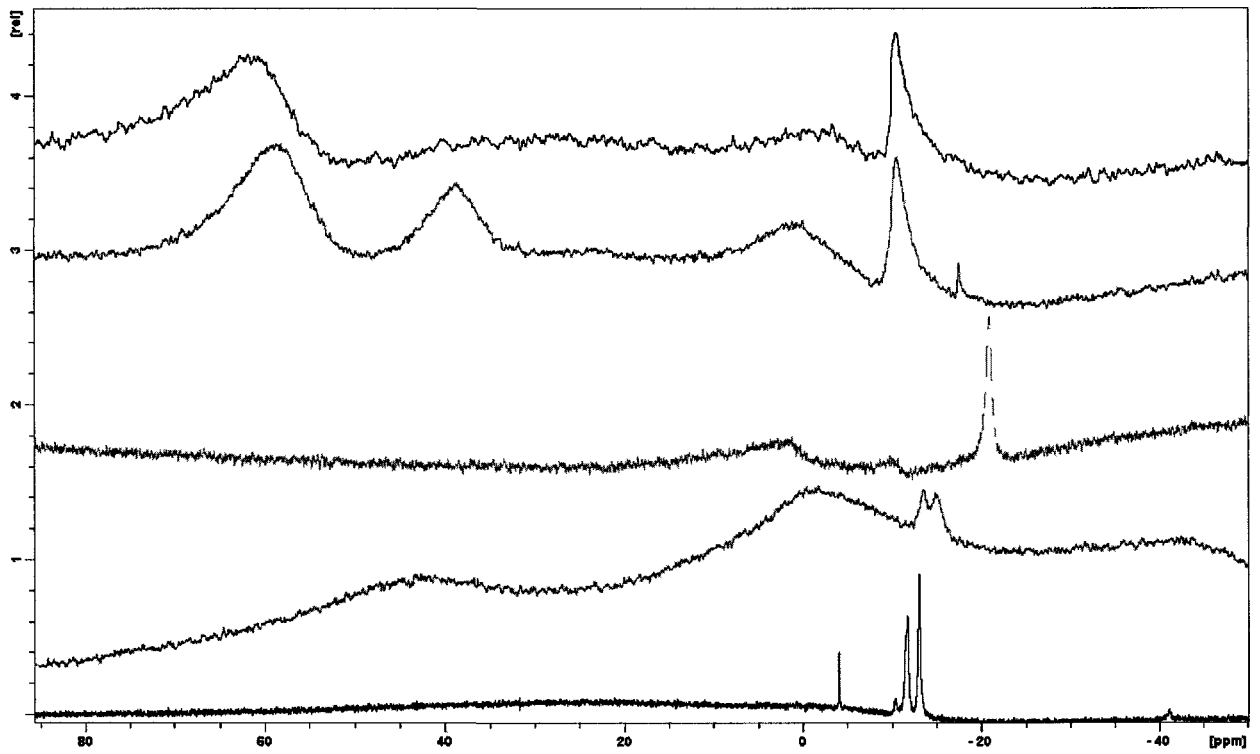

Figure 7: ^{11}B spectra of (from top to bottom): sublimed $B(C_6F_5)_3$ (navy); and the products of reaction 2.3.1 (purple); reaction 2.3.2 (green); reaction 2.3.3 (red); and 2.3.4 (blue).

Despite many efforts to discern the, sometimes incredibly ambiguous, results of the reactions of iron metallacycle complexes with $B(C_6F_5)_3$ they remain quite unclear. The next step to determine what iron complexes, if any, are being produced would be to sublime the mixtures to attempt to isolate pure iron complexes.

Even though it has been reported that $Fe(CF_2)_4(CO)_4$ is unreactive towards BF_3,[3] the reaction was attempted in C_6D_6. The ^{19}F NMR spectrum indicates that no reaction took place after two days. TMSOTf was also unsuccessful at abstracting a fluoride from this complex.

4.3 Carbene Formation from Potassium Cyclopentadienyl perfluorotetramethyleneiron Carbonyl

Further attempts to prepare the carbene anologue of complex [24] were performed using the Lewis acids BF_3•Et_2O and TMSOTf. This anionic complex has been found to only be soluble in acetonitrile. While it may be soluble in other polar solvents that would be unreactive towards Lewis acids, it is important to be able to monitor the reaction by NMR, including ^1H NMR.

Reacting complexes [23] and [24] with BF_3•Et_2O by adding the borane drop-wise to the iron complex, followed by the addition of the minimum amount of CD_3CN (approximately 0.5 mL) to shim the magnet in NMR analysis, resulted in the evolution of a white gas. The solvent was added last in hopes that some of the BF_3•Et_2O would have a chance to react with K[FeCp$(CF_2)_4$(CO)] before reacting with acetonitrile. New peaks in the ^{19}F NMR at -146.50, -148.12, -149.09, -152.18, and -152.40 ppm are the result of reaction of BF_3 with acetonitrile.

The ability to obtain useful ^1H NMR spectra was sacrificed by attempting the same reaction in chlorobenzene. The carbene complex [FeCp(CO)$(PPh_3)(CF_2)$][BF_4] was obtained previously in CH_2Cl_2; no chloride was added to the carbene from the solvent.[6] Using chlorobenzene as the solvent, with a much more robust C-Cl bond, should not interfere with the carbene, if produced. K[FeCp$(CF_2)_4$(CO)] was only partially soluble in chlorobenzene, however, if the reaction was successful, more would be expected to dissolve as the reaction progressed. The reaction mixture was stirred overnight; the ^{19}F NMR spectrum of the reaction (carried out at room temperature) contained only a peak at -152.52 ppm for BF_3•Et_2O and two much smaller peaks at -117.90 and -153.39 ppm. Evidenced by the lack of signals for complexes [23] or [24], they either decomposed or merely were not soluble enough in chlorobenzene.

Silicon forms a fairly strong covalent bond with fluorine (132 kcal/mol), though not quite as strong as the boron-fluorine bond. TMSOTf also reacts with acetonitrile, but to a lesser extent than BF_3•Et_2O. Reacting [23] and [24] with TMSOTf in CD_3CN resulted in

the successful synthesis of the sought-after carbene complex. Conversion is achieved after two days; after 10 days the reaction goes to completion.

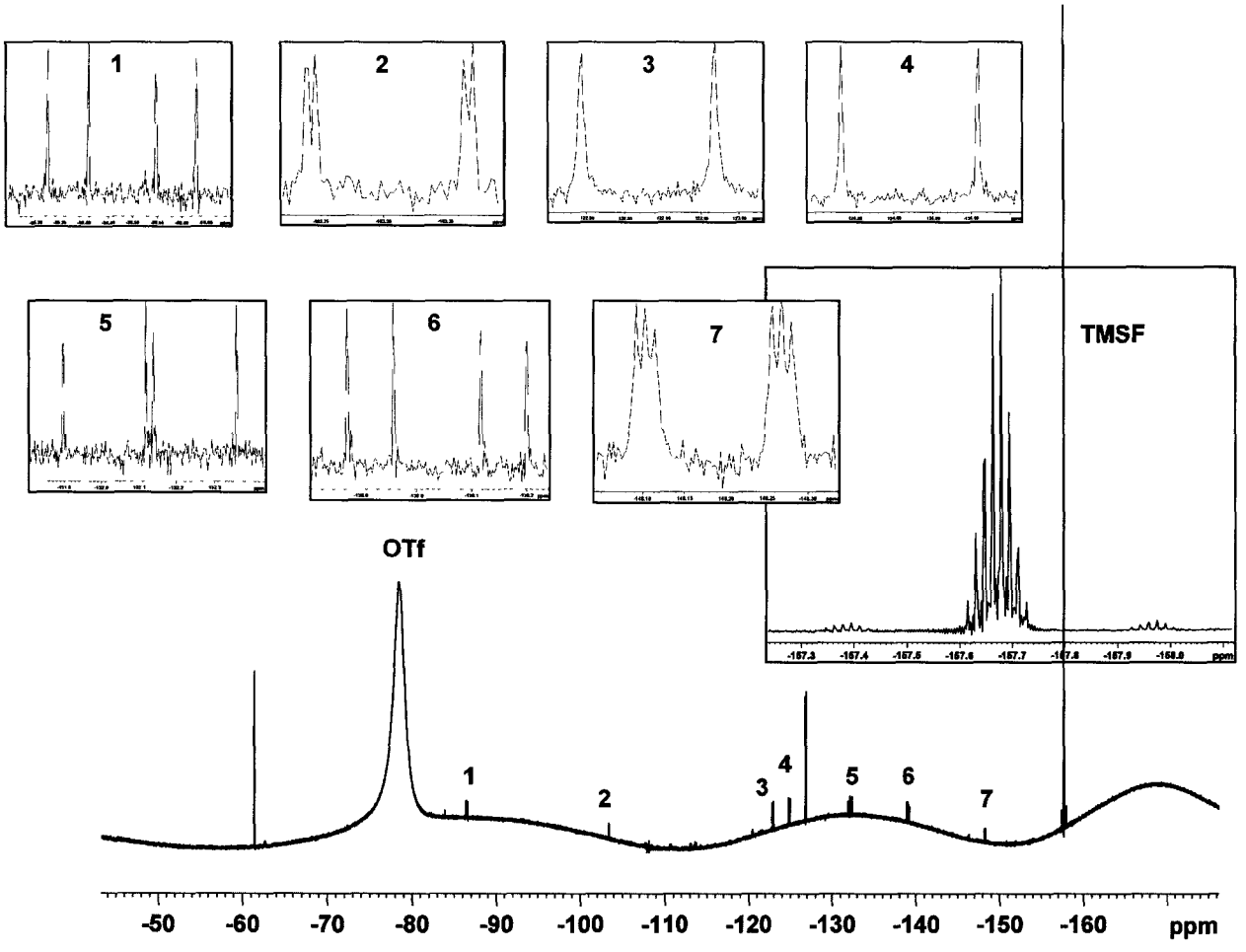

Figure 8: ^{19}F NMR spectrum for the reaction of complexes [23] and [24] with TMSOTf (reaction 2.3.9).

It is clear that a carbene complex has indeed been synthesized in the reaction of $K[FeCp(CF_2)_4(CO)]$ with TMSOTf in CD_3CN based upon the ^{19}F NMR spectrum (Figure 8). The ^1H NMR spectrum indicates that some of the TMSOTf has reacted with acetonitrile, however, enough was added to the reaction mixture to abstract a fluoride from the metallacycle. The silicon of TMS forms a strong enough bond to the fluorine that it is not replaced on the ring. The Si satellites are present in the ^{19}F spectrum; the Si-F coupling constant is approximately 275 Hz.

Table 3: Chemical shifts and coupling constants for the fluorine atoms on the metallacycle of the iron fluorocarbene complex [25].

	Chemical Shift (ppm)	Multiplicity	F-F Coupling Constants (Hz)		Correlations from coupling constants	Correlations from 19F COSY
			Geminal Coupling	Vicinal Coupling		
1	-86.48	dd	39	104	5 and 6	5
2	-103.31	dd	59	3		
3	-122.88	d	83		4	
4	-124.87	d	83		3	
5	-132.13	dd		113, 104	1 and 6	1 and 6
6	-139.04	dd	39	114	1 and 5	5
7	-148.19	ddd	78	6, 4.8		

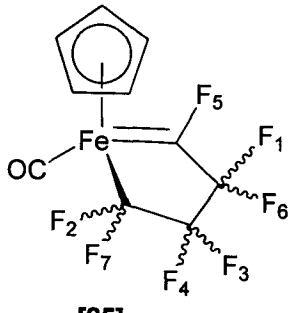

[25]

Figure 9: Proposed structure for the iron-fluorocarbene complex [25] from the reaction of complexes [23] and [24] with TMSOTf.

The structure of the fluorocarbene complex [25] (shown in Figure 9) can be confirmed from the 1-dimensional ^{19}F NMR spectrum. There are seven new unique fluorine peaks

aside from those for the triflate anion and trimethylsilyl fluoride. The chemical shift and multiplicity for each of the signals are detailed in Table 3. The first clue to the assignment of fluorine 5 as that residing on the carbene carbon is its two large coupling constants; all of the other peaks have only one large coupling constant. Therefore, its F-F coupling constants must be vicinal; they cannot be geminal because there is no carbon with three fluorine atoms whereby a fluorine would have to couple to each of the other fluorines differently. $^{3}J_{FF}$ = 113 and 104 Hz indicate that fluorine 5 is coupled to 1 and 6, who share a coupling of 39 Hz. Fluorines 6 and 1 occupy the β-carbon adjacent to the carbene carbon. Remaining are fluorines 2, 3, 4, and 7. Fluorines 3 and 4 share a coupling constant of 83 Hz and do not appear to be coupled to any other fluorine atoms, placing them on the same carbon. Fluorine atoms 2 and 7 do not have a coupling constant in common, however, they appear to be related based upon their similar line widths; they are broader than all of the other peaks. This broadening must be due to their proximity to the metal centre and the carbene, which has also affected their coupling constants.

The ^{19}F COSY spectrum (Figure 10) only indicates correlations between the fluorine signal identified as that for the fluorine on the carbene carbon (fluorine 5) with the signals for fluorines 1 and 6. There are no significant correlations between any of the fluorines on the same carbon atoms when the ^{19}F COSY experiment was run for 256 experiments of 172 scans.

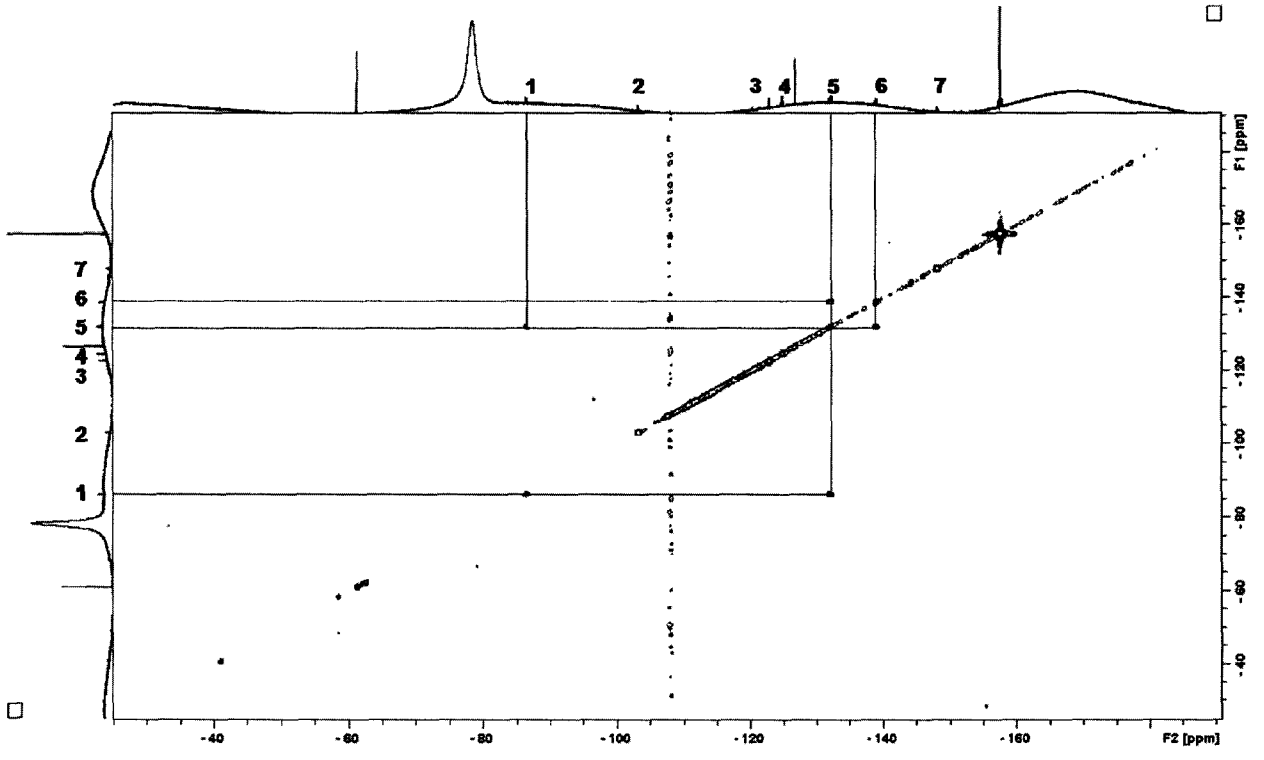

Figure 10: ^{19}F COSY NMR spectrum for the reaction of complexes [23] and [24] with TMSOTf (reaction 2.3.9).

The hybridization of the carbon atom has a significant effect on the magnitude of the fluorine-fluorine coupling constant. The largest coupling observed in this complex is between the fluorine on the sp^2 hybridized carbon of the carbene and the fluorines on the adjacent β-carbon. The closeness to the sp^2 hybridized carbon affects the geminal coupling constant of the fluorines on this β-carbon; 39 Hz, is quite a bit smaller than that of the fluorines on the other β-carbon, $^2J_{FF}$ = 83 Hz.

There is a trend in the chemical shifts of the fluorines in this complex. The more negative chemical shift of fluorines 7, 4, and 6 versus 2, 3, and 1 is likely based on the side of the metallacycle on which they are oriented, whereby one plane of the ring would face the Cp ring and the fluorines on the other side would be angled more towards the CO ligands.

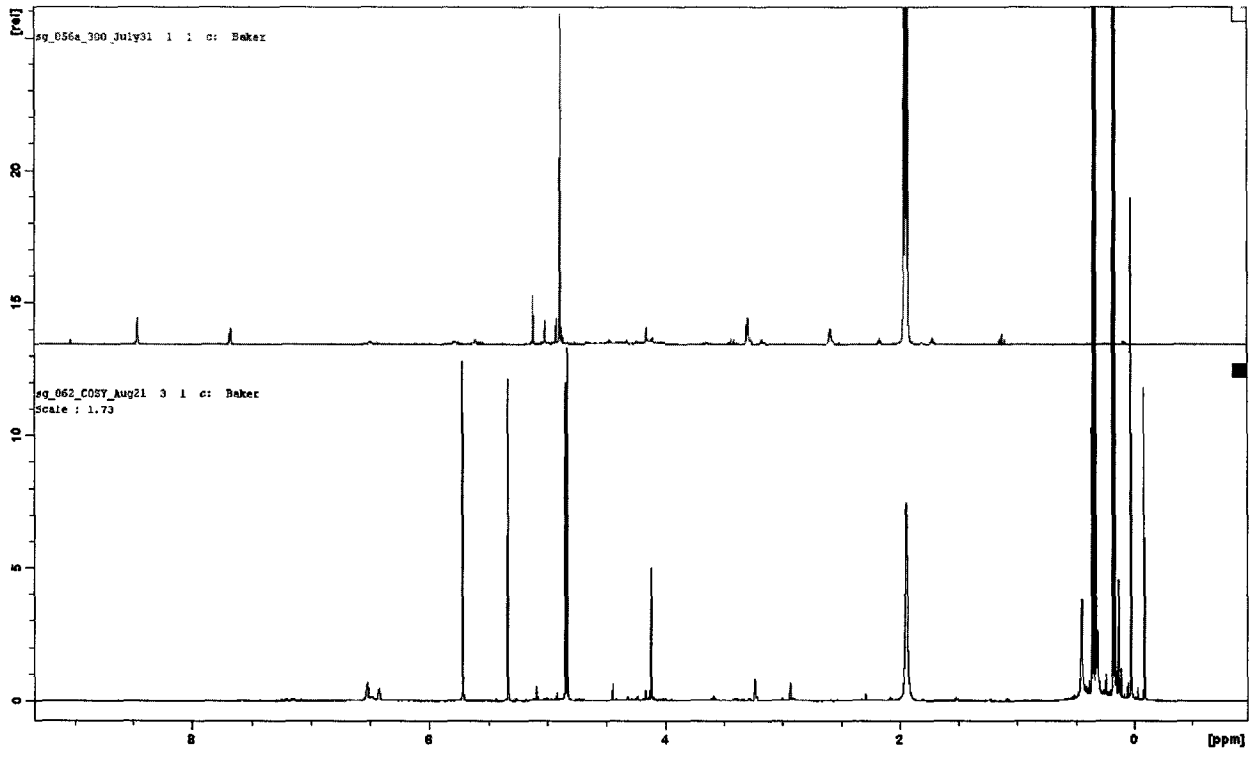

Figure 11: ^{1}H NMR spectra for complexes [23] and [24] (top) and complex [25] (bottom).

The ^{1}H NMR spectrum for this reaction (Figure 11) shows that, despite the clean ^{19}F NMR spectrum, other side reactions have occurred. The peaks in the region ca. 0 to 0.5 ppm are due to trimethylsilyl groups. Evidently over time TMSOTf has reacted with CD_3CN. The doublet at 0.19 ppm corresponds to TMSF and the peak for unreacted TMSOTf is at 0.35 ppm. The two singlets at 4.85 and 4.86 ppm arise from derivatives of $[FeCp(CO)_2]_2$, or are merely due to $[FeCp(CO)_2]_2$ itself, but is resolved as two peaks because of the change in the medium. Because there was only one new fluorine-containing product in this reaction, according to the ^{19}F NMR spectrum, one of the two peaks at 5.35 and 5.73 ppm is another Fe-Cp byproduct. Optimizations of the conditions for this reaction are necessary for full characterization and further studies relating to this carbene complex.

In order to definitively say that the carbene has been produced, the carbene carbon needs to be located by ^{13}C NMR spectroscopy. Generally, the signals from the carbon atoms of the metallacycles, in any of the complexes studied in this investigation, do not

show up in the spectrum from the basic $^{13}C\{^{1}H\}$ experiment. The coupling between these carbons and fluorine atoms of the ring decreases the intensity of their signals enough that they are not discernable from the baseline. Taking advantage of the high abundance of the ^{19}F isotope of fluorine to "see" the carbene carbon is the best approach to locating its ^{13}C signal. Two ^{19}F-^{13}C HMQC experiments were performed to attempt just this, one optimized with a ^{19}F-^{13}C coupling constant of 250 Hz and another with 350 Hz. For the experiment with a coupling constant of 350 Hz, the pulse widths for ^{19}F were calibrated for the sample (90° pulse 13.5 μs, and 180° pulse 27 μs), recycle delay extended from 1 to 2 seconds, and the sweep widths were narrowed down to 30 ppm centered at -136 ppm for ^{19}F and 150 ppm centered at 300 ppm for ^{13}C. Running this experiment with 256 slices for 96 scans (14 hours) was not enough to locate the ^{13}C signal for the carbene.

It is possible that the experiment was not run for long enough, that 350 Hz was not a good enough estimate for the coupling constant, or the recycle delay was not set long enough, meaning the bulk magnetization of the sample was not allowed enough time reorient itself along the z-axis, thus saturating the sample. The estimate that the carbene carbon's signal should come in the range of 250 to 350 ppm may not have been correct. For the carbene complex $Fe(CF_2)(CO)_4$, the ^{13}C signal for the carbene carbon was calculated to be at approximately 271 ppm.[5] Because of the anionic Cp ligand on the iron in this complex, the signal for the carbene carbon may have been shifted further upfield by comparison to that calculated for $Fe(CF_2)(CO)_4$, putting it out of range of the sweep width of this experiment. No data is available for the experimental ^{13}C chemical shift of an iron-fluorocarbene. Finally, the ^{13}C-^{19}F coupling constant of 350 Hz may not have been a good estimate. The C-F coupling constant for the metallacycle complexes analyzed in this investigation is on the order of 250 Hz. The change in hybridization of this carbon atom to sp^2 will have an effect on the magnitude of the coupling. To accurately determine the coupling constant, the ^{19}F experiment could be run with its sweep width focused on the ^{19}F of the carbene with a very high S/N ratio to see if the ^{13}C satellites could be identified. The S/N was too low to identify the ^{13}C satellites in the ^{19}F NMR spectra previously obtained.

4.4 Fluoride Abstraction from $Fe(CF_2)_4(\kappa^2\text{-dppe})(CO)_2$ with TMSOTf

As expected, the better σ-donating Cp ligand (versus CO, $P(O^iPr)_3$, and xylyl isocyanide) is necessary to facilitate fluoride abstraction and stabilize the carbene. It is possible that dppe and PPh_3 would be similarly stabilizing. $Fe(CF_2)_4(\kappa^2\text{-dppe})(CO)_2$ in CD_3CN immediately reacts with TMSOTf resulting in a color change of the solution from clear, yellow to a darker, yellow/orange. After stirring at room temperature for 24 hours, a small peak is resolved in the ^{19}F NMR spectrum corresponding to TMSF. An excess of TMSOTf was added to the reaction mixture. The reagents were allowed to react for a further 24 hours, resulting in a slight increase in the amount of TMSF produced. The reaction mixture was heated in a sand bath at 50 °C for 19 hours deepening the colour of the solution to an orange/brown. Again, there was a small increase in TMSF, but no new peaks for the desired metallacycle complex. Evidently, a small amount of fluoride has been abstracted from the complex, but there is not a significant enough amount of a new iron complex being produced to show up in the ^{19}F NMR spectrum.

4.5 Conclusions

A lot of knowledge has been gained through these investigations regarding the ease of fluoride abstraction from an iron fluorometallacycle complex and the required stabilization of the resulting carbene. Because carbenes behave as π-acids, it is not surprising that increasing the electron density on a metal facilitates fluoride abstraction and carbene stabilization. As noted previously, this behaviour is illustrated in fluoro-carbene formation from the complexes $[FeCp(CF_3)(CO)L]$, where L = PPh_3 or CO, with BF_3. [6,7]

The iron-fluorocarbene complex [25] may be a suitable catalyst precursor for oligomerization or metathesis of fluoro-olefins. Reacting [25] with other olefins could potentially lead to the production of novel fluorochemicals with interesting properties for useful applications. For other ligand frameworks, if the fluorocarbene can be generated,

but is not isolable, methods can be developed to quench the carbene in solution with either the migration of an ancillary ligand from the metal or with a substrate in solution.

4.6 References

[1] Brothers, P.J.; Roper, W.R. *Chem. Rev.* **1988**, *88*, 1293.

[2] Uneyama, K. *Organofluorine Chemistry*; Blackwell: Oxford, **2006**.

[3] Burch, R.R.; Calabrese, J.C.; Ittel, S.D. *Organometallics* **1988**, *7*, 1642.

[4] Piers, W.E.; Chivers, T. *Chem. Soc. Rev.* **1997**, *26*, 345.

[5] Chen, Y.; Zhao, L.; Xu, C.M.; Liu, Z.C.; Frenking, G. *J. Mol. Struct. THEOCHEM* **2009**, *905*, 40.

[6] Crespi, A.M.; Shriver, D.F. *Organometallics* **1985**, *4*, 1830.

[7] Richmond, T.G.; Crespi, A.M.; Shriver, D.F. *Organometallics* **1984**, *3*, 314.

Chapter 5: Progress Towards the Synthesis of Iron Complexes of 1,1-difluoroethylene

5.1 Synthesis of Iron Complexes of 1,1-difluoroethylene

Achieving the desired configuration and arrangement of fluorines on a hydrocarbon is a significant challenge.[1] There is a structure-property relationship based on the position of halogens on a (hydro)carbon framework. As continuously pointed out throughout this thesis, the iron-mediated reaction of fluoro-olefins with each other and various substrates may generate new hydrofluorocarbons.

Developing procedures to control the reactivity of other fluoro-olefins, such as 1,1-difluoroethylene (vinylidene fluoride, VDF) and trifluoroethylene (HTFE), with themselves, each other and with TFE are useful enroute to the production of novel fluorochemicals. In this section the reactivity of VDF with $Fe_2(CO)_9$, $Fe[P(O^iPr)_3](CO)_4$ and $Fe[P(O^iPr)_3]_2(CO)_3$, $Fe(PPh_3)(CO)_4$, $Fe(2,6\text{-}(CH_3)_2C_6H_4NC)_5$, and $K[FeCp(CO)_2]$ was explored under a variety of conditions.

The same conditions used for the synthesis of $Fe(CF_2)_4(CO)_4$ from TFE and $Fe_2(CO)_9$ were employed in the reaction of $Fe_2(CO)_9$ with VDF. A solution of $Fe_2(CO)_9$ in hexane was irradiated with UV light and stirred with VDF for 24 hours. The ^{19}F NMR spectrum contained no peaks, indicating that no reaction took place. The reaction was attempted at room temperature in the glove box using a balloon of VDF to react with $Fe_2(CO)_9$ in each of the following solvents: THF, toluene and hexane. The only solvent in which a reaction took place was toluene. The ^{19}F NMR spectrum for this reaction is shown in Figure 1. All of the coupling observed in this spectrum is heteronuclear; in the $^{19}F\{^1H\}$ spectrum all of the peaks collapse to singlets (Figure 2).

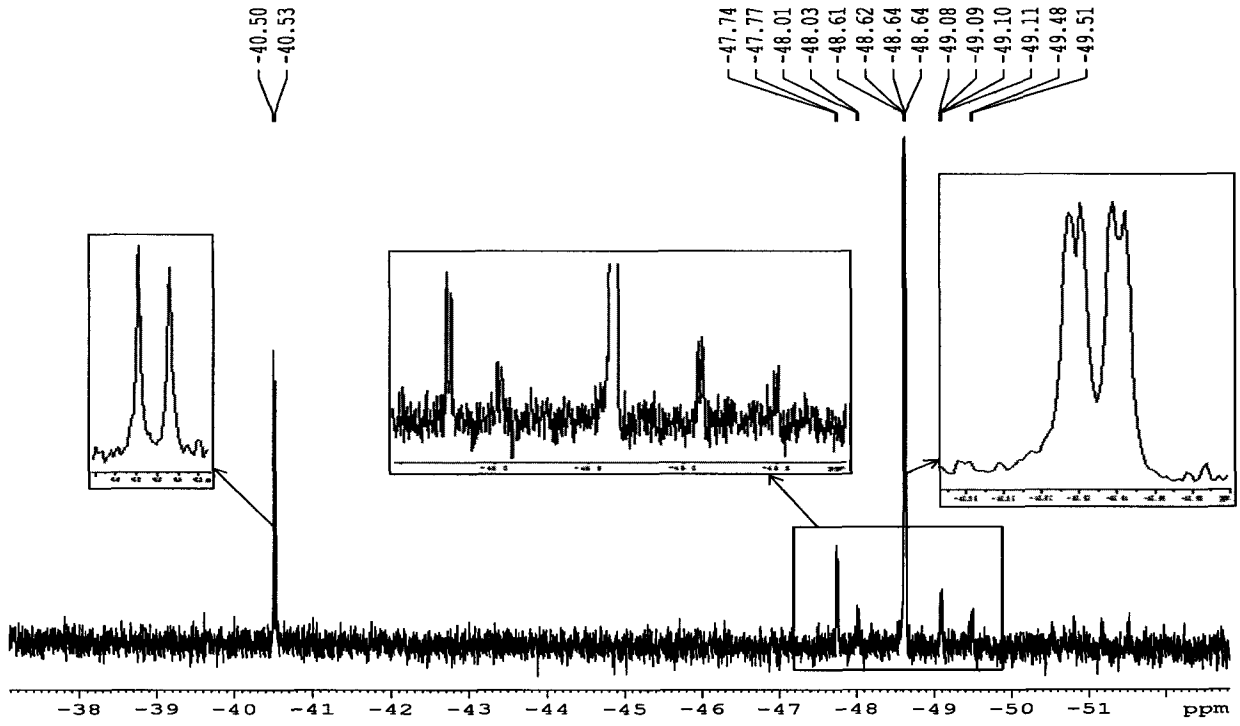

Figure 1: ^{19}F NMR spectrum for the reaction of $Fe_2(CO)_9$ with VDF.

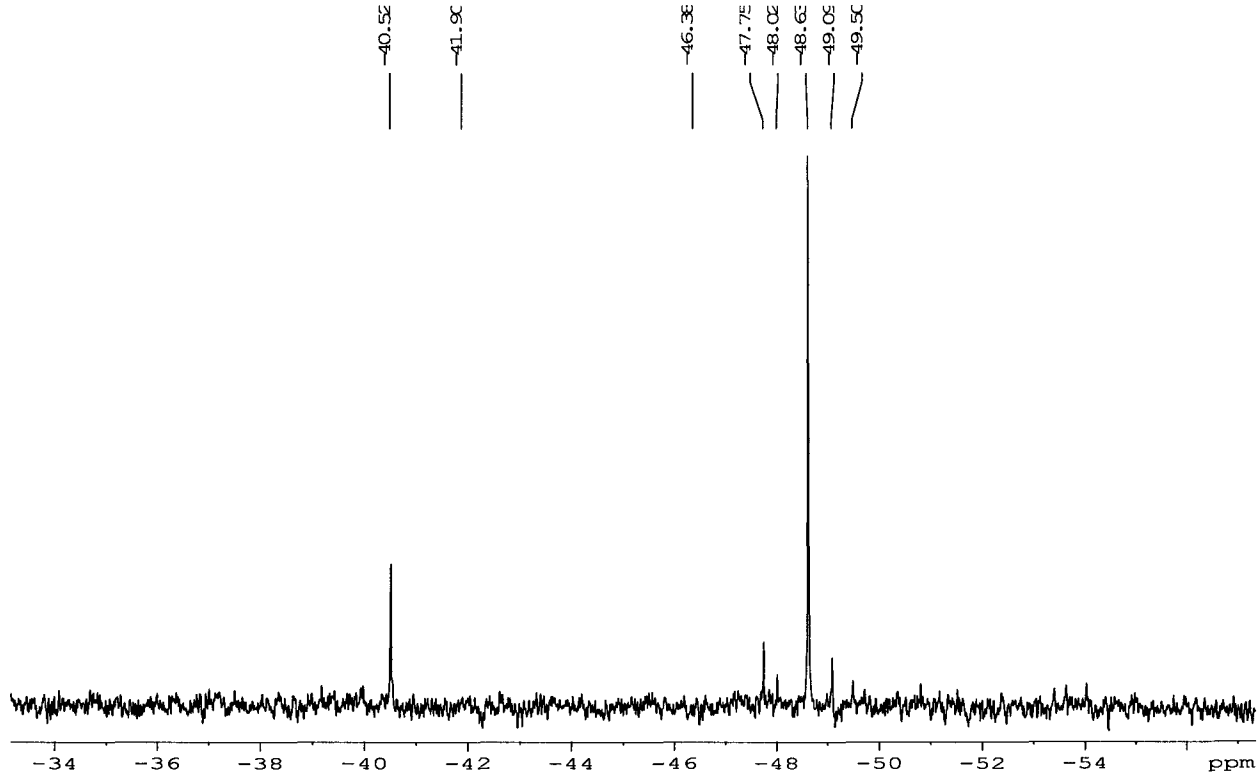

Figure 2: $^{19}F\{^1H\}$ NMR spectrum for the reaction of $Fe_2(CO)_9$ with VDF.

The patterns in the ^{19}F and $^{19}F\{^1H\}$ NMR spectra of the two major products are not consistent with formation of a metallacyclopentane ring. In fact, all peaks resolved in the ^{19}F and $^{19}F\{^1H\}$ NMR spectra appear due to olefin or vinylic iron complexes as confirmed by the many olefinic resonances observed in the ^1H NMR spectrum (Figure 3). From the information available, structures cannot be reliably proposed; multiple VDF molecules have likely been complexed in multinuclear iron carbonyl compounds. Higher temperatures and pressures may be necessary to overcome the competition between VDF complexation and CO loss to give clusters.

.

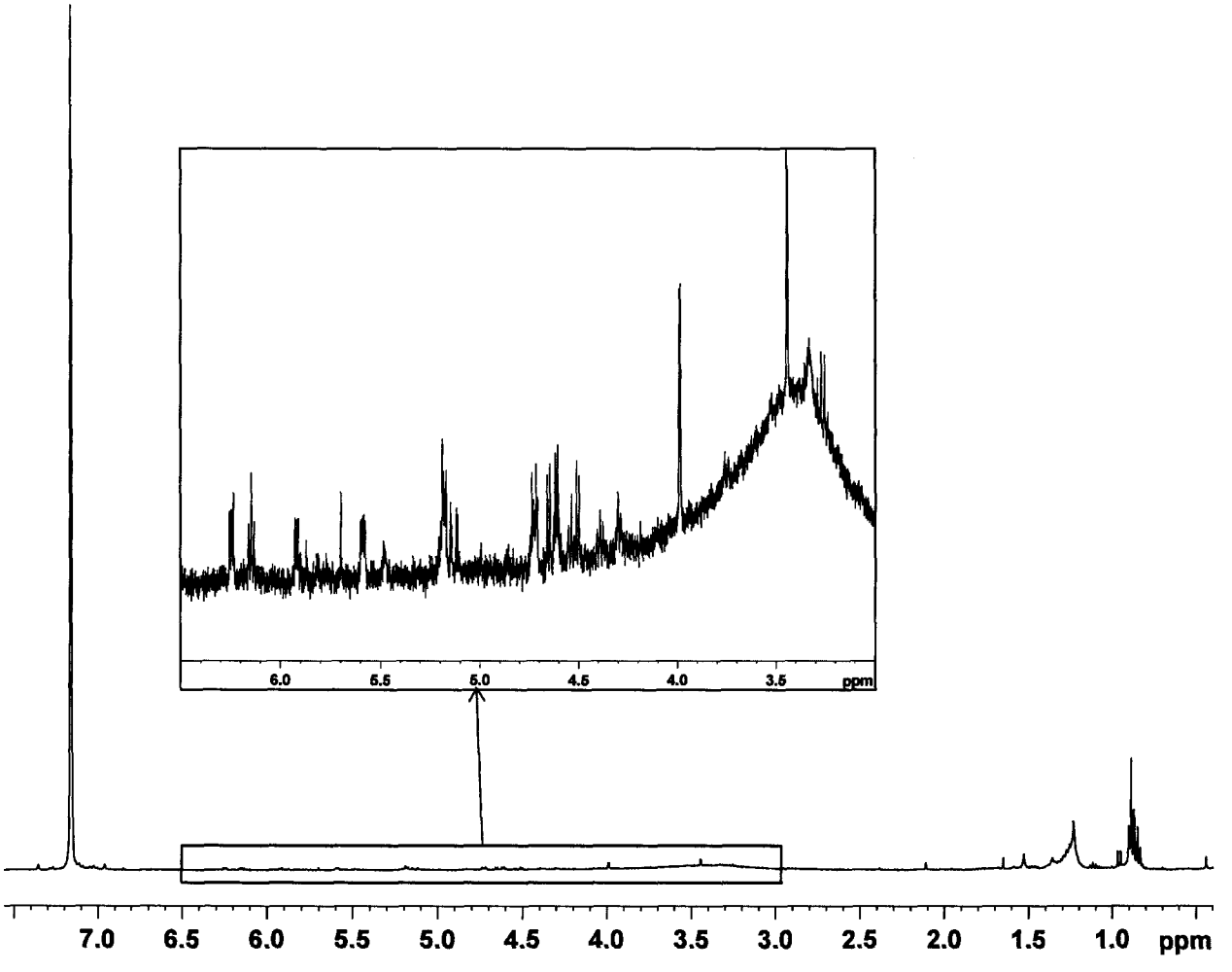

Figure 3: ^1H NMR spectrum for the reaction of $Fe_2(CO)_9$ with VDF.

Attempts were made to prepare iron carbonyl phosphite complexes of VDF via the *in situ* preparation of $Fe[P(O^iPr)_3](CO)_4$ and $Fe[P(O^iPr)_3]_2(CO)_3$ from $Fe_2(CO)_9$ and $P(O^iPr)_3$. The reaction was performed at atmospheric pressure with a balloon of VDF, and at elevated pressure of VDF. Success was only in the form of the production of more of the bis-phosphite complex $Fe[P(O^iPr)_3]_2(CO)_3$.

A 1:0.1 mixture of $Fe(PPh_3)(CO)_4$ and $Fe(PPh_3)_2(CO)_3$ was irradiated with UV light with VDF for a total of 36 hours. Analysis by $^{31}P\{^1H\}$ NMR spectroscopy shows that the irradiation stimulated the conversion of some of the mono-phosphine complex to the bis-phosphine complex, such that their relative integrals transformed to 1:1.57. There was also a new broad peak at 56.86 ppm and a corresponding broad peak in the ^{19}F NMR spectrum at -79.3 ppm. Based upon the knowledge gained from the reactivity of TFE, the probable product from this reaction is a bis-phosphine-substituted olefin complex, with the two PPh_3 in the axial positions, as is the preferred configuration for phosphines.[2]

A more interesting result was obtained from the photochemical reaction of just the bis-phosphine complex with VDF. The reaction mixture was irradiated for 18 hours. During the reaction, some of the PPh_3 was displaced from the iron as evidenced by the $^{31}P\{^1H\}$ NMR spectrum. Two new multiplets, a doublet of doublets of doublets at -116.32 ppm, with J = 86, 55, 22 Hz, and a triplet at -142.85 ppm, with J = ca. 50 Hz, were resolved in the ^{19}F NMR, while there were no significant new peaks in the $^{31}P\{^1H\}$ NMR.

A large number of scans had to be run in the ^{19}F NMR experiment in order to resolve the two new peaks; it was not reasonable to run a similarly long experiment for such an abundant nucleus to obtain the proton-decoupled spectrum. Running a ^{19}F COSY NMR experiment would also be futile; although, it is not likely that the two signals are related because of their differences in intensity and line shape. The relative integration of the two mutliplets is 1.00:0.22 for the peaks at -116.32 and -142.85 ppm, respectively.

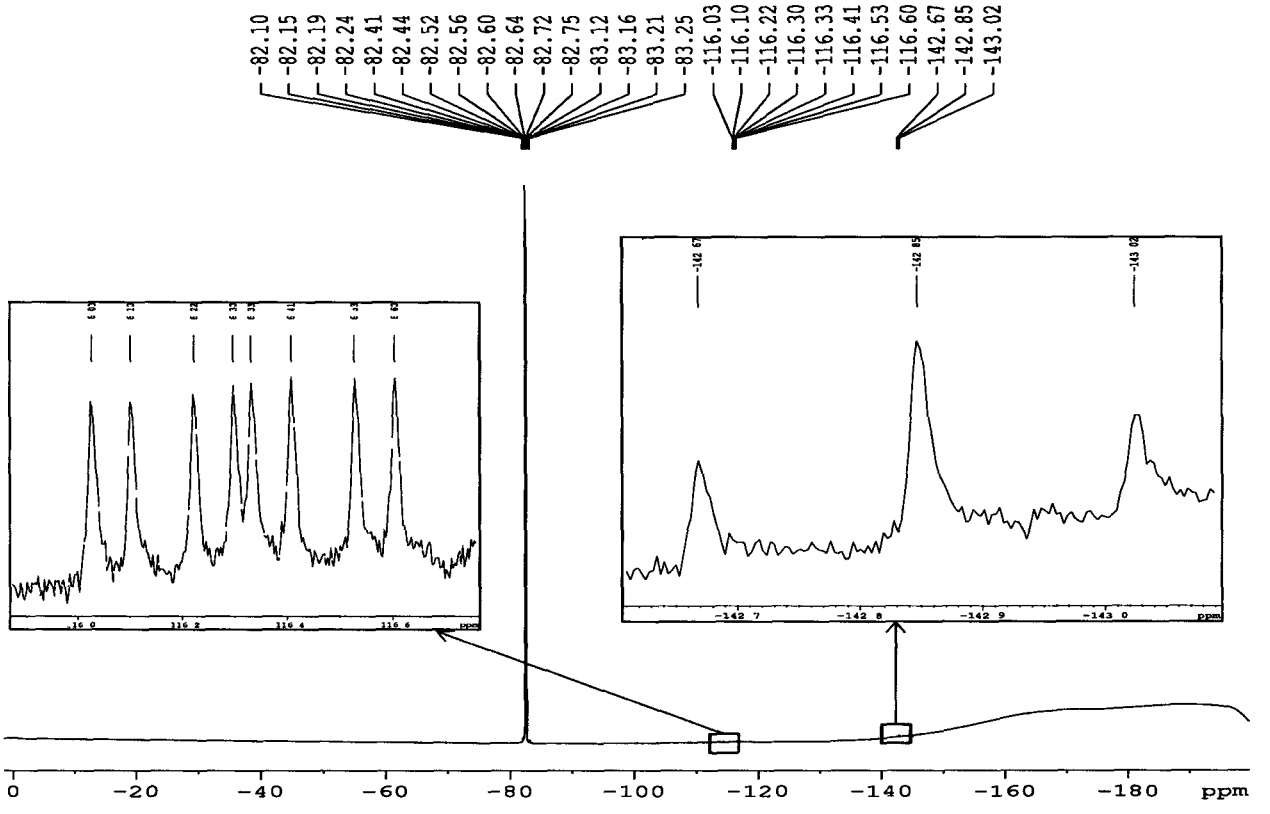

Figure 4: ^{19}F NMR spectrum for reaction 2.4.6 indicating the production of iron phosphine carbonyl complexes of VDF.

Some of the coupling seen in the ^{19}F NMR spectrum could be due to ^{31}P or ^{1}H. Without a significant new peak in the $^{31}P\{^{1}H\}$ NMR spectrum, the coupling cannot be identified as fluorine-phosphorus. Also, the loss of some PPh_3 means the new complexes could contain either: no PPh_3, one PPh_3, or two PPh_3's. The reaction was attempted on a larger scale, with the hope of synthesizing enough of the VDF complex to more extensively characterize it, but was unsuccessful.

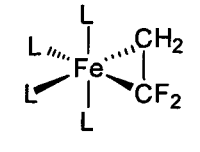

L = PPh_3 or CO

[26]

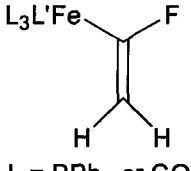

L = PPh_3 or CO

L' = PPh_3 or F

[27]

Figure 5: Proposed sub-structures for the products of reaction 2.4.6; iron phosphine carbonyl complexes of VDF.

Proposed fragments of the structures for the complexes produced in this reaction are shown in Figure **5**. The peak in the ^{19}F NMR spectrum at -142.85 is consistent with a symmetrical VDF-olefin complex [26] whereby both fluorines would be equivalent and couple equally to the protons. The broader line shape is similar to the broad singlets observed for olefin complexes produced with TFE. The complex is expected to contain four CO ligands, or two CO's and two PPh_3 in either mutually *trans* or *cis* configuration to make it symmetrical. If it does indeed contain PPh_3, it is not surprising that no P-F coupling is resolved; P-F coupling was never observed in any of the phosphite/phosphine TFE olefin complexes either.

A vinylic VDF complex [27] is proposed to be responsible for the ^{19}F NMR signal at -116.32 ppm, in which Fe is coordinated to the carbon bearing a fluorine atom. The other fluorine of this VDF molecule may also have added to the iron center, or it may have been eliminated as a side product. The coupling pattern is consistent with similar vinylic-fluoroolefin complexes reported in the literature.[3] Although they cannot be definitively assigned without the proton decoupled spectrum, the coupling constants of ca. 55 and 22 Hz are likely *trans* and *cis* H-F couplings, respectively. The larger coupling of 86 Hz is proposed to be coupling of the fluorine to either another fluorine on the metal center or to the phosphorus a PPh_3. Coupling to fluorine is more plausible based upon the magnitude; coupling to a phosphine would be expected to be on the order of 5-10 Hz. The signal for this metal fluoride was not identified because it would not have been within the spectral range; metal fluorides resonate at around 200 ppm.

Finally, the iron complexes [19] and [22] were individually reacted with VDF both thermally and photochemically without generating any fluorinated products. VDF does not provide enough competition for substitution to win out over the outer sphere electron transfer process which converts $K[FeCp(CO)_2]$ back to the dimer $[FeCp(CO)_2]_2$. Similarly, the lack of reactivity of the isonitrile complex [19] towards VDF indicates that the VDF is not a good enough ligand to compete with 2,6-dimethylphenylisocyanide.

It has become increasingly evident that VDF is quite unreactive and, despite the lack of reactivity with $K[FeCp(CO)_2]$, will likely require very electron rich metal centres to achieve complexation. At this point, there are no examples in the literature of any

transition metal complexes of VDF. More efforts to develop the preparations with positive results in this study to achieve greater conversion are necessary. Elevated temperature, as well as pressure of VDF, allowing it to provide more competition for the ligands that it must displace may be the answer.

5.2 References

[1] Baker, R.T.; Beatty, R.P.; Farnham, W.B.; Wallace, R.L. Jr. *US patents* 5, 760, 282, **1998**.

[2] Burt, R.; Cooke, M.; Green, M. *J. Chem. Soc. (A)* **1970**, 2975.

[3] Braun, T.; Blöcker, B.; Schorlemer, V.; Neumann, B.; Stammler, A.; Stammler, H.G. *J. Chem. Soc., Dalton Trans.* **2002**, 2213.

Chapter 6: Conclusions and Future Directions

The goal of the research project discussed in this thesis was to increase our knowledge of organofluorometallic chemistry specific to the transition metal iron. A greater understanding of the basics of this field has been achieved through studies of the bonding and chemistry of iron fluoro-olefin complexes with a variety of ancillary ligands.

A method for the use of (in this case fluorinated) gases as reagents under air free conditions, without the necessity of condensing the gas, and with minimal amounts of gas wasted, has been developed. The apparatus for this procedure will be put to good use in future studies related to this project by the Baker group.

The known compound, $Fe(CF_2)_4(CO)_4$, has been successfully synthesized following a new procedure. This complex has been thoroughly characterized by ^{19}F and ^{13}C NMR spectroscopy, IR spectroscopy, and X-ray crystallography. Ligand substitution reactions have been performed with this complex. The photochemical reaction of $Fe(CF_2)_4(CO)_4$ with $P(O^iPr)_3$ yields two bis-substituted isomers, complexes [7] and [8]. With PPh_3, the mono-substituted complex [11] and a bis-substituted complex, proposed to have the phosphines occupying the axial positions, were produced. The analogous reaction with dppe, generates two products. The major product has the phosphine chelating to iron in the equatorial plane, complex [17]. The solid state structure of this complex has been determined. The minor product, complex [18], contains a dppe bridging two $Fe(CF_2)_4(CO)_3$ units in which the phosphine is coordinated equatorially to both iron centres.

Several other iron phosphite and phosphine carbonyl complexes of TFE were synthesized. From a combination of the phosphite complexes [2] and [3], two isomeric bis-substituted olefin complexes [4] and [5], and a mono-substituted metallacycle complex [6] were generated. The same selective formation of a mono-substituted metallacycle and two bis-substituted olefin complexes was observed by reacting $Fe(PPh_3)(CO)_4$ and $Fe(PPh_3)_2(CO)_3$ with TFE. The introduction of phosphorus-

containing ligands provided a new handle for NMR analysis to study the reactivity of the fluorometallacycle complexes.

The reactivity of pentakis(2,6-dimethylphenylisocyanide)iron with TFE was also explored. Again, both an olefin and a metallacycle complex were produced, but this time the reaction was found to be successful thermally, where the phosphite and phosphine reactions required photolysis. Five-membered metallacycles were the major products formed with TFE from $K[FeCp(CO)_2]$; only trace amounts of a proposed olefin complex were generated. These results lead to the proposal that it is not electronic, but steric factors that govern the formation of a three- versus five-membered metallacyclic complex.

Theory may provide some insight into the ideal combination of ancillary ligands to provide the best balance of steric and electronic properties to promote five-membered ring formation. Based on what is now known, the ideal complex would have both isocyanides and carbonyl ligands. CO ligands are beneficial if you want to displace a ligand and have it removed from the metal forever (i.e. not able to re-coordinate or provide competition for incoming ligands). The isocyanides on the other hand, can come off the metal to make available a coordination site to bind a second molecule of TFE to form the metallacycle, and then the isocyanide can resume its position on the metal. The downside in this scenario, however, is that because the isocyanide remains in solution, it can provide competition for the TFE and will likely win out because it is a better ligand. The perfect complex needs to be able to lose a ligand to make room for the coordination of a second molecule of TFE. A second benefit with isocyanide ligands is the ability to tune its sterics.

When designing the best complex to promote metallacycle formation, but also promote fluoride abstraction and fluoro-carbene stabilization, the Cp or Cp* ligand needs to be considered. Cp is a good ligand for this situation because it is electron donating, placing more electron density on the metal, increasing its ability to strongly coordinate electron-withdrawing fluoro-olefins. As well, Cp ligands can vary their coordination hapticity.

An investigation of the reactivity of iron fluoro-metallacycle complexes with Lewis acids was performed. The reactivity of $B(C_6F_5)_3$ with complexes [1], [20] and [21], [7] and [8], and [23] and [24], was different in each case. While Lewis acid degradation was the predominate reaction in all cases, electron transfer was likely involved in experiment 2.3.2 wherein all ^{19}F NMR resonances for the $Fe(CF_2)_4(CNAr)_4$ and $Fe(CF_2)_2(CNAr)_4$ starting materials disappeared. Triisopropylphosphite substitution afforded several new uncharacterized metallacycle products, whereas sterically more hindered metallacycles such as those with Cp ligands were unreactive with the bulky borane Lewis acid.

In contrast, the successful generation of a more clearly defined fluorocarbene complex from $K[FeCp(CF_2)_4(CO)]$ is quite promising. This complex shows the most promise for future developments and inquiries into the reactivity of iron fluoroolefin-based complexes. Two benefits that this complex has over the others studied was the thermal (versus photochemical) production of the fluorometallacycle and the ability to stabilize the fluoro-carbene. A route to the clearer production of this complex may be to carry out the reaction of $K[FeCp(CO)_2]$ with TFE at a reduced temperature to favour more substitution over the competing outer sphere electron transfer leading to $[FeCp(CO)_2]_2$.

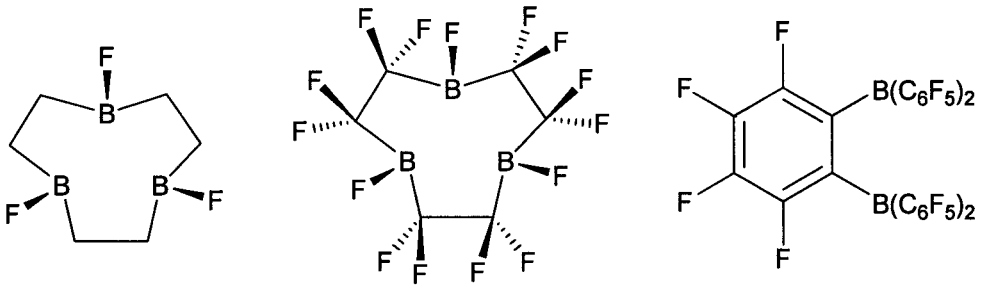

1 2 3

Figure 1: Organic boron compounds with multidentate Lewis acid sites.

Organic boron compounds with multidentate Lewis acids sites are another option to explore for fluoride abstraction. The model compounds 1 and 2 shown in Figure 1 have been calculated to have fluoride binding energies of 307.9 and 595.7 kJ/mol respectively.[1] For the cyclic examples, coordination of a fluoride ion to form a pyramidalized chelate releases ring strain of the planar boron centres. Perfluorination of the triboramacrocycle increases the binding energy. For comparison, the calculated

binding energy of methyl anion is 298.3 kJ/mol for 1, 555.3 kJ/mol for 2 and 472.4 kJ/mol for $B(C_6F_5)_3$.[2] An example with multidentate Lewis acid sites that is currently synthetically accessible is compound 3.[3]

Following optimization of conditions for the synthesis of fluoro-carbene complexes, the complexes should be screened for metathesis and oligomerization activity with fluoro-olefins and other unsaturated organic compounds. Potential substrates include ethylene and other unsaturated hydrocarbons, and nitriles. Addition of HX (where X = halide, CN^-, etc.) or HE (where E = BR_2, SiR_3) to the carbene may provide valuable new compounds following hydrogenolysis to cleave the M-C bonds.

There are no examples in the literature of VDF-containing transition metal complexes. Complexation of VDF has been achieved from the iron precursors $Fe_2(CO)_9$ and $Fe(PPh_3)_2(CO)_3$. Further development of this chemistry may be possible by focusing on more electron-rich complexes. As well, more attempts using a pressure reactor in reactions with this fluoro-olefin should be made.

The reactions of HTFE with the iron complexes studied here should be carried out in the future to enrich the knowledge gained in this study regarding the chemistry of fluoro-olefins. Exploring this reactivity will also be helpful for the development of methods for the controlled synthesis of novel fluorochemicals.

The abundance of preliminary results that have been unearthed related to the reactivity of TFE and VDF with a variety of iron complexes, as well as the ideal conditions for the formation of a stable iron fluorocarbene complex set the stage well for this project. Extensions of these results will hopefully lead to the production of catalyst precursors suitable for metathesis and/or oligomerization of fluoro-olefins to yield short-chain fluorocarbons or new fluoropolymers.

---

[1] Aldridge, S.; Fallis, I.A.; Howard, S.T. *Chem. Comm.* **2001**, 231.

[2] Uneyama, K. *Organofluorine Chemistry*; Blackwell: Oxford, **2006**.

[3] (a) Melaimi, M.; Gabbai, F.P. *Adv. Organomet. Chem.* **2005**, *53*, 61. (b) Andrews, M.A.; Kirtley, S.W.; Kaesz, H.D. (R. Bau, Ed.) *Transition Metal Hydrides*, American Chemical Society, Washington, 1978, p.215.

Appendix

Appendix A: NMR Spectra

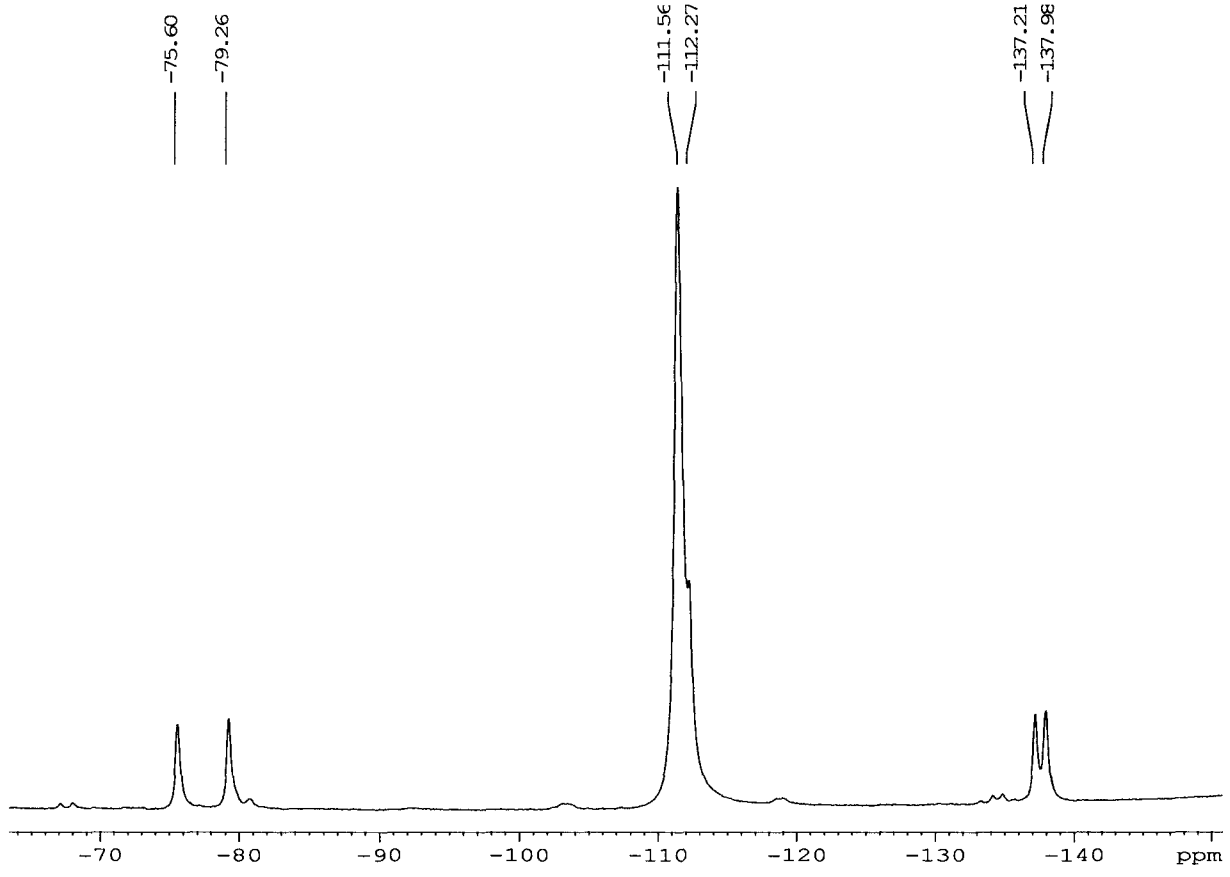

Figure A1: ^{19}F NMR spectrum for reaction 2.2.4, synthesis of complexes [4], [5], and [6] (282 MHz, C_6D_6, 298 K).

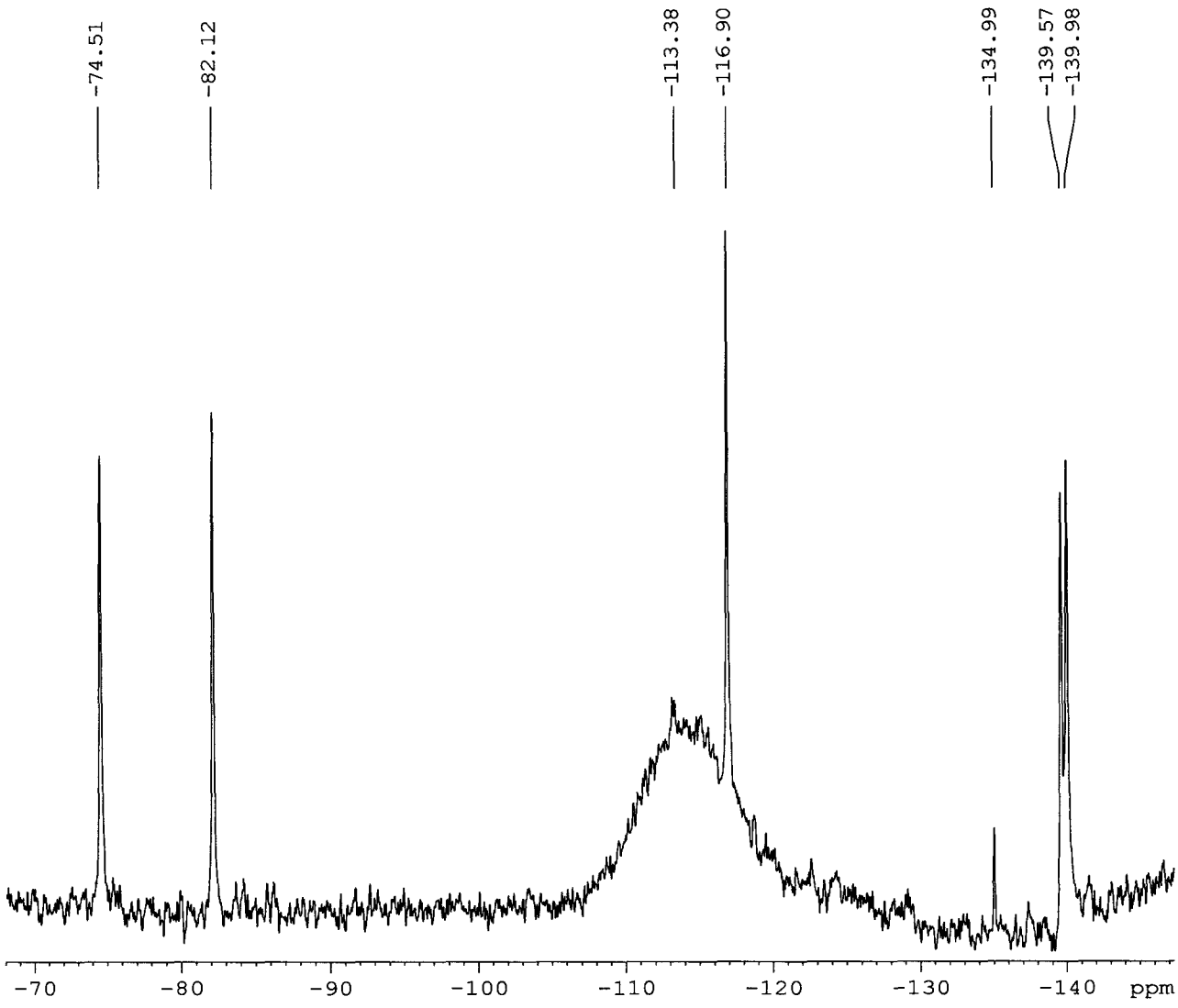

Figure A2: ^{19}F NMR spectrum for reaction 2.2.7, synthesis of complexes [11], [12], and [13] (282 MHz, C_6D_6, 298 K).

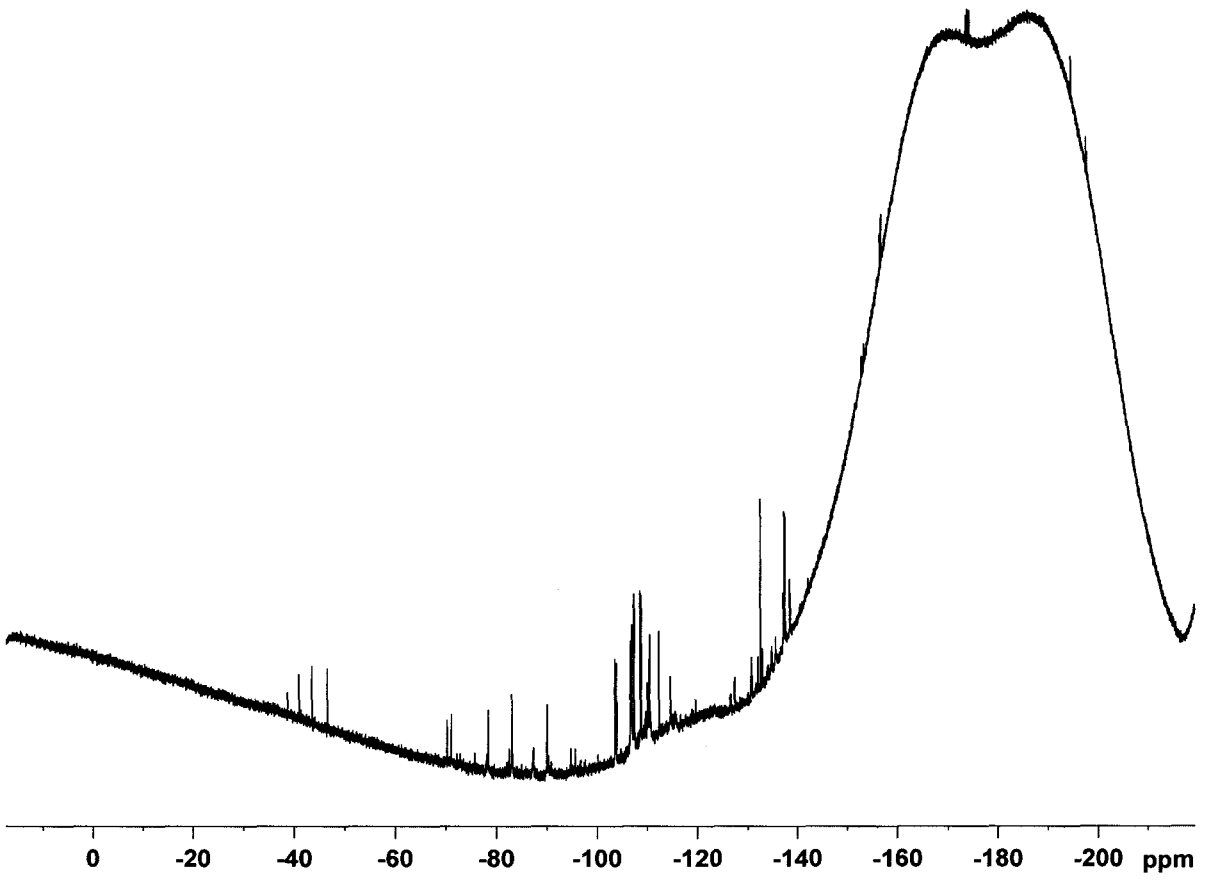

Figure A3: ^{19}F NMR spectrum for reaction 2.2.8, proposed iron-carbonyl-TFE clusters (282 MHz, C_6D_6, 298 K).

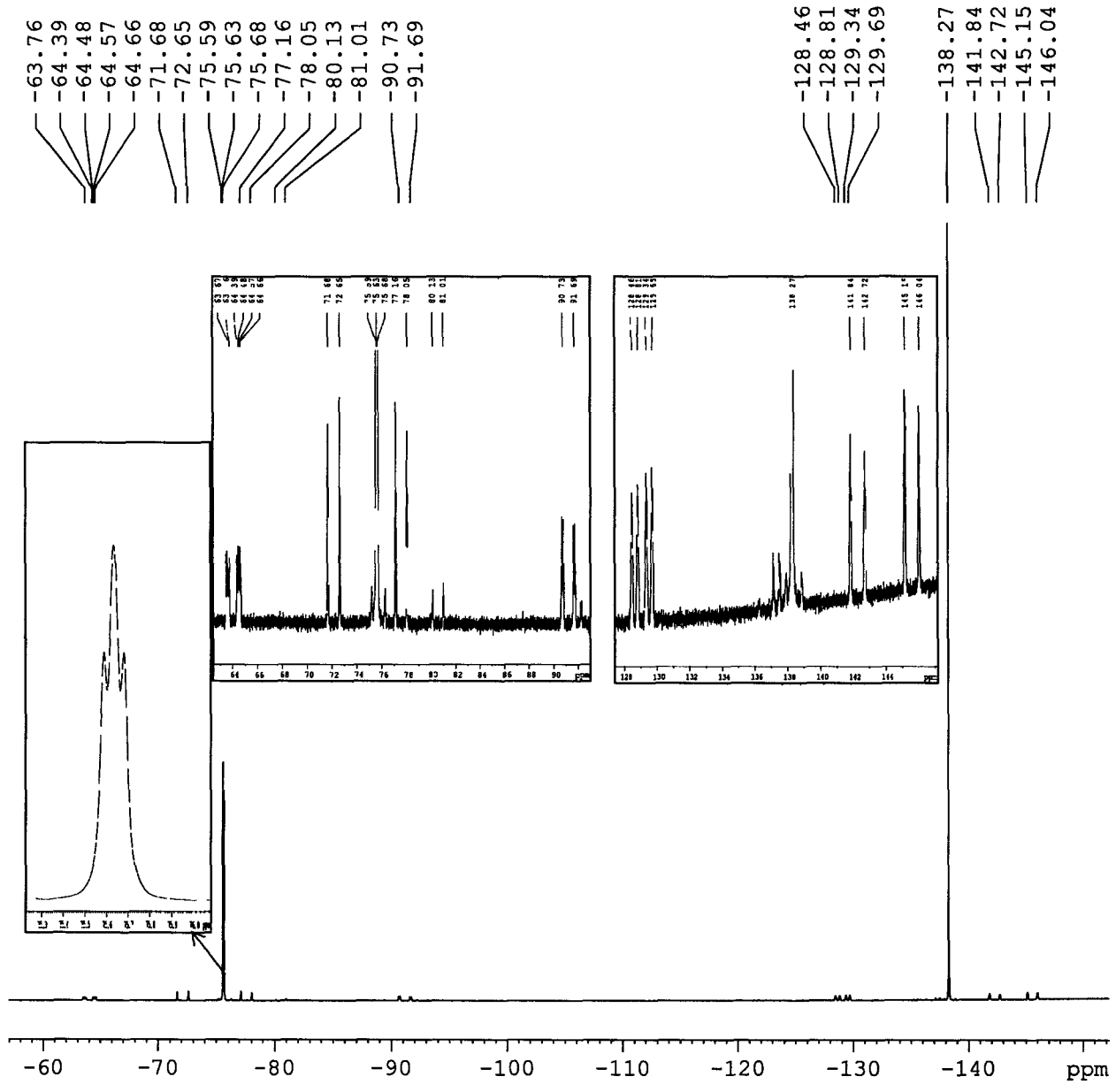

Figure A4: ^{19}F NMR spectrum for reaction 2.2.12, synthesis of complexes [17] and [18] (282 MHz, CD_3CN, 298 K).

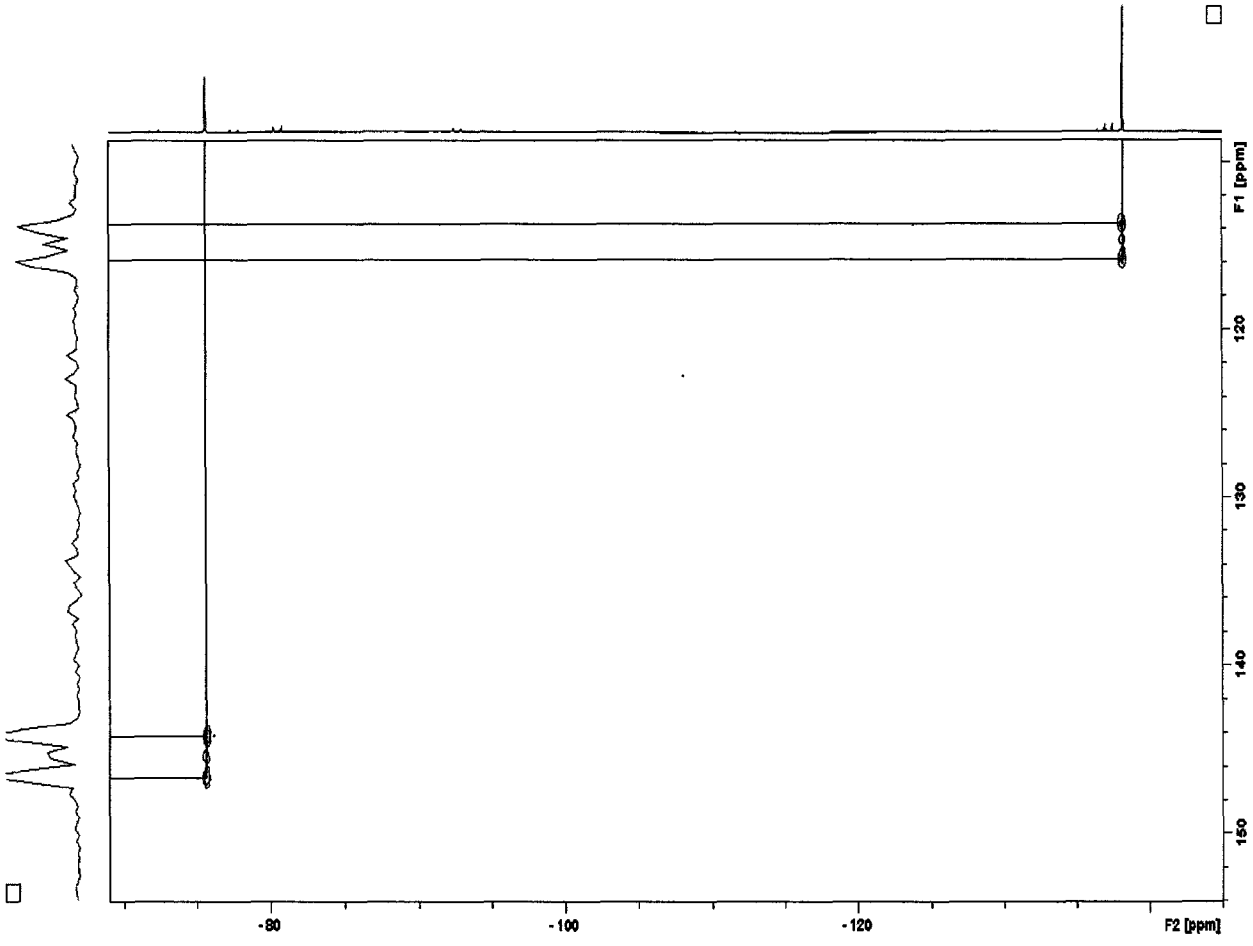

Figure A5: ^{19}F-^{13}C HMQC NMR spectrum for reaction 2.2.12 synthesis of complexes [17] and [18] (471 MHz, 250 Hz coupling, CD_3CN, 298 K).

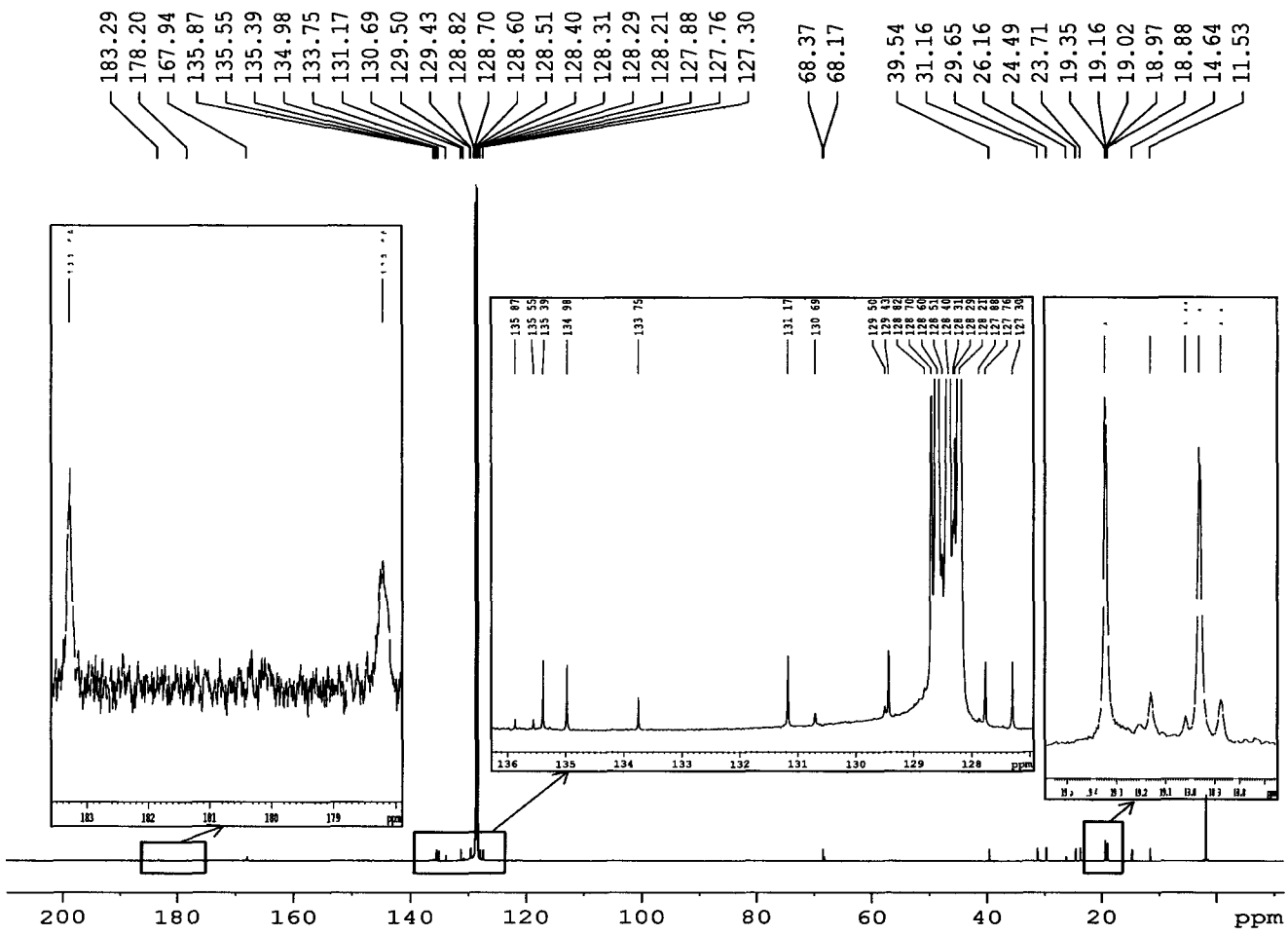

Figure A6: $^{13}C\{^{1}H\}$ NMR spectrum for reaction 2.2.14, synthesis of complexes [20] and [21] (126 MHz, C_6D_6, 298 K).

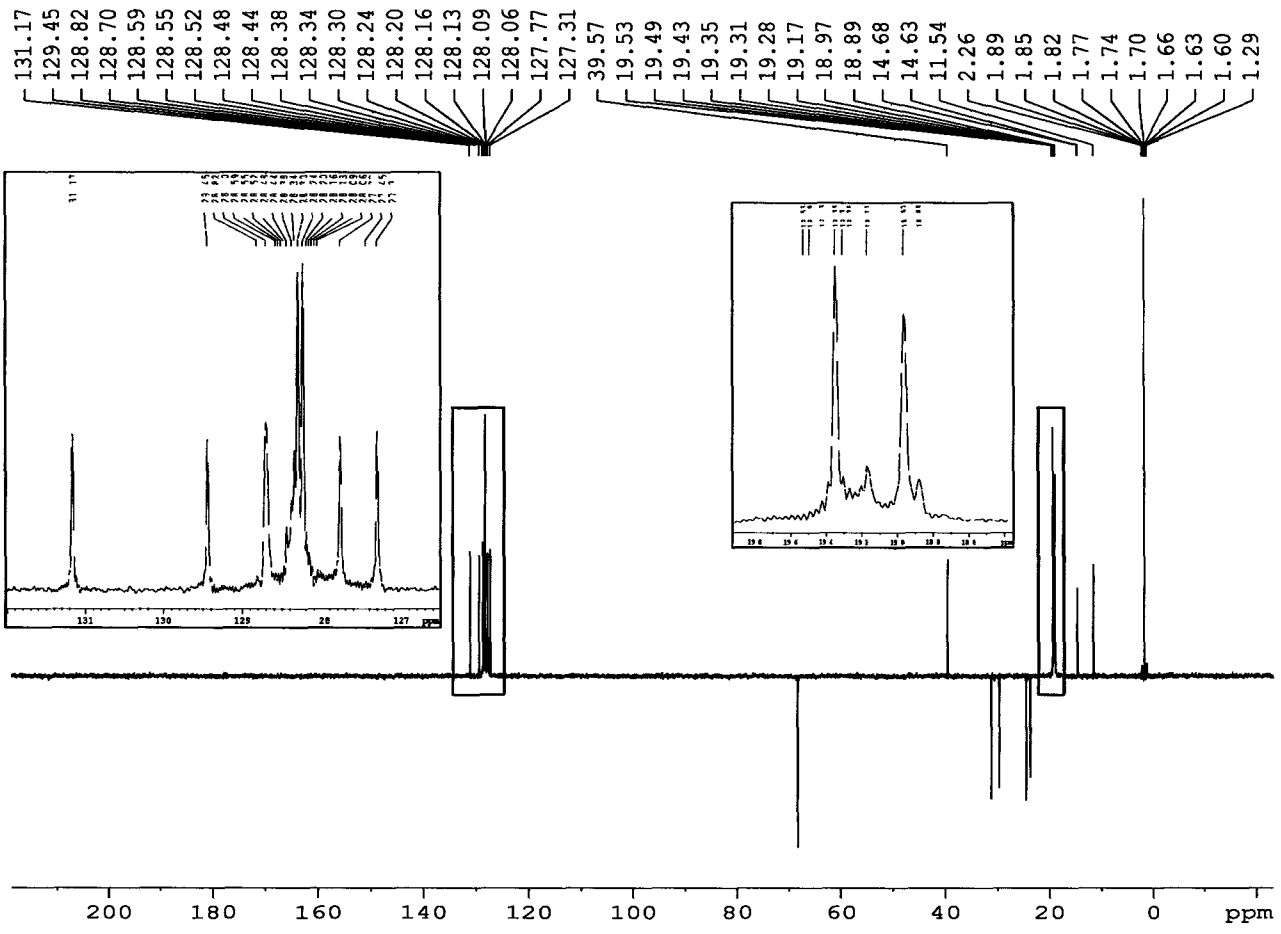

Figure A7: dept-135 NMR spectrum for reaction 2.2.14, synthesis of complexes [20] ($Fe(2,6\text{-}(CH_3)_2C_6H_4NC)_4(CF_2)_2$) and [21] ($Fe(2,6\text{-}(CH_3)_2C_6H_4NC)_4(CF_2)_4$) (126 MHz, C_6D_6, 298 K).

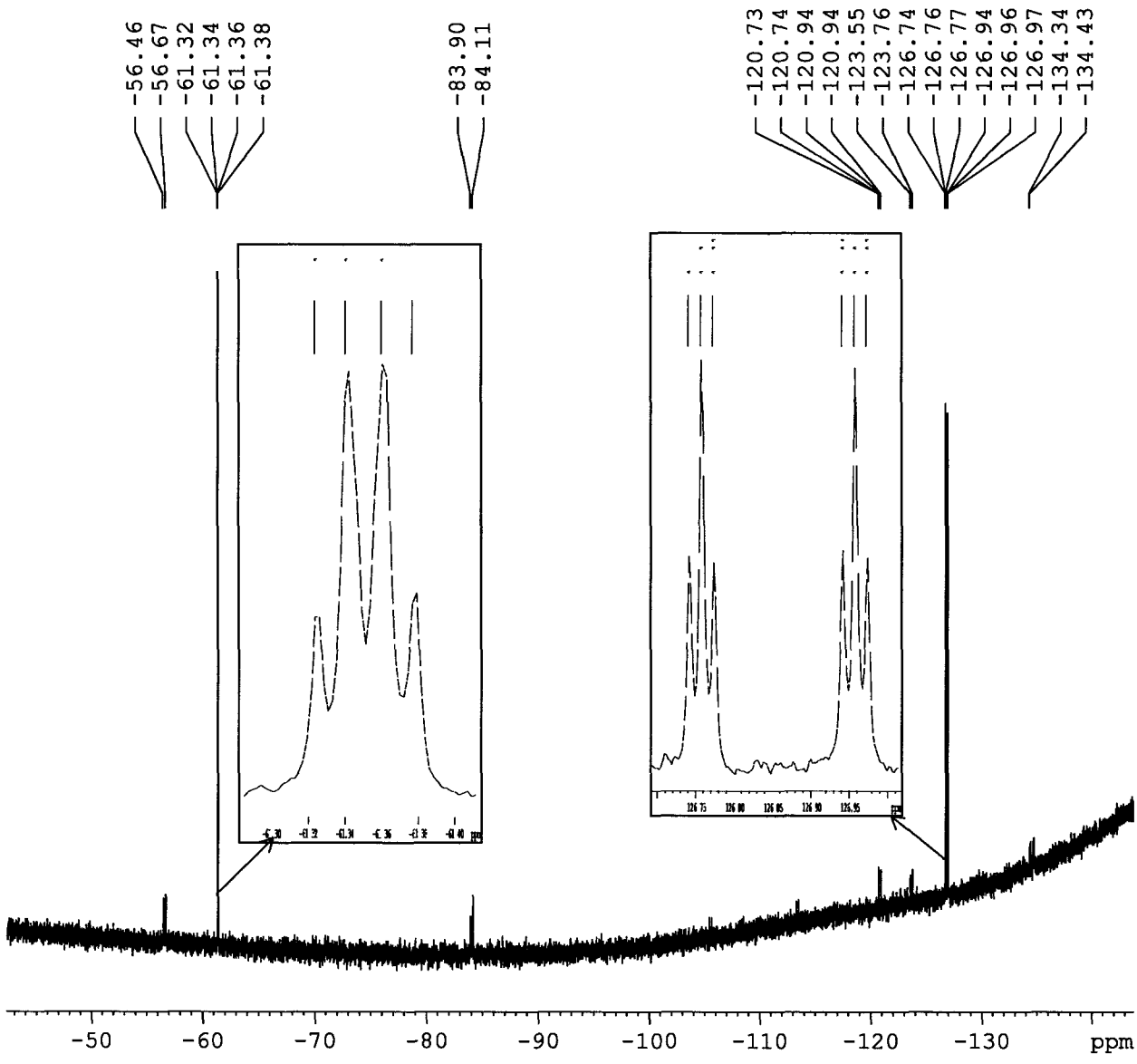

Figure A8: ^{19}F NMR spectrum for reaction 2.2.16, synthesis of complexes [23] and [24] (282 MHz, CD_3CN, 298 K).

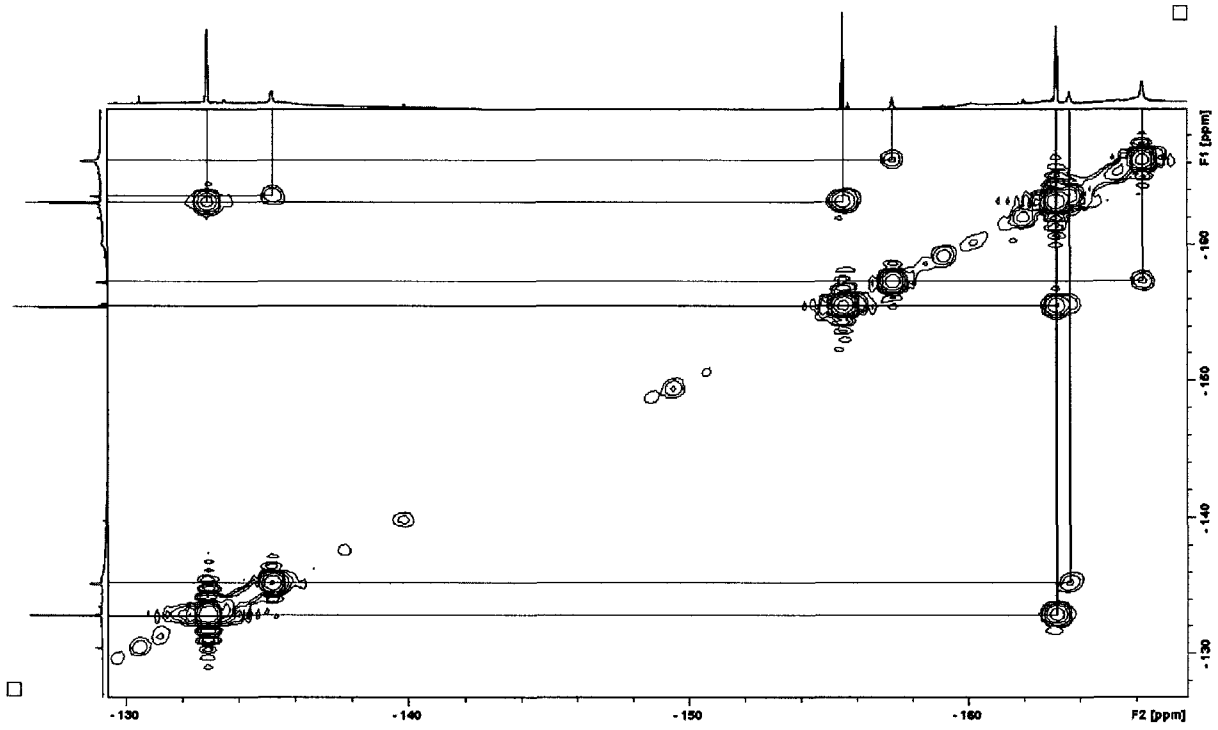

Figure A9: ^{19}F COSY NMR spectrum for reaction 2.3.2 (471 MHz, C_6D_6, 298 K).

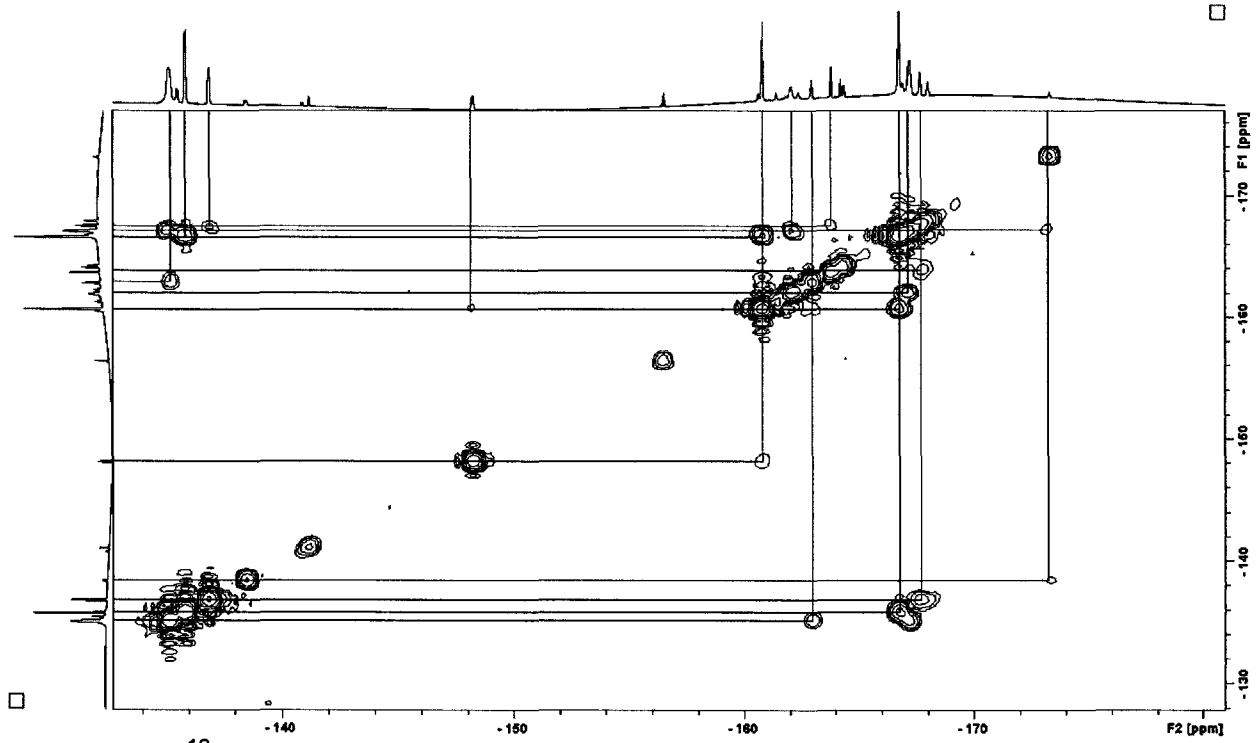

Figure A10: ^{19}F COSY NMR spectrum for reaction 2.3.4 (471 MHz, CD_3CN, 298 K).

Appendix B: XRD Data

Table B1: Crystal data details for $Fe(CF_2)_4(CO)_4$ [1].

Bond precision:	C-C = 0.0047 A	Wavelength=0.71073	
Cell	a = 26.5404(4)	b = 7.5146(1)	c = 25.2489(3)
	Alpha = 90	Beta = 115.979(1)	Gamma = 90
Temperature	200 K		
	Calculated	Reported	
Volume	4526.82(11)	4526.82(11)	
Space group	C 2/c	C2/c	
Hall group	-C 2yc	?	
Moiety formula	C8 F8 Fe O4	?	
Sum formula	C8 F8 Fe O4	C16 F16 Fe2 O8	
Mr	367.93	735.86	
Dx,g cm-3	2.159	2.159	
Z	16	8	
Mu (mm-1)	1.458	1.458	
F000	2848.0	2848.0	
F000'	2856.49		
h,k,lmax	35,10,33	35,10,33	
Nref	5634	5563	
Tmin,Tmax	0.743,0.804	0.730,0.811	
Tmin'	0.715		
Correction method=	MULTI-SCAN		
Data completeness=	0.987	Theta(max)=	28.320
R(reflections)=	0.0402 (4762)	wR2(reflections)=	0.1212 (5563)
S = 1.031		Npar= 379	

Table B2: Bond distances (Å) in $Fe(CF_2)_4(CO)_4$ [1].

Bond	Distance (Å)	Bond	Distance (Å)
Fe1-C1	1.846(3)	Fe2-C10	1.845(3)
Fe1-C4	1.846(3)	Fe2-C12	1.835(3)
Fe1-C3	1.865(3)	Fe2-C9	1.858(3)
Fe1-C2	1.853(3)	Fe2-C11	1.857(3)
Fe1-C5	2.010(3)	Fe2-C16	2.021(3)
Fe1-C8	2.024(3)	Fe2-C13	2.023(3)
C1-O1	1.118(3)	C9-O5	1.128(4)
C2-O2	1.124(4)	C10-O6	1.124(4)
C3-O3	1.120(3)	C11-O7	1.118(4)
C4-O4	1.123(3)	C12-O8	1.117(4)
C5-F2	1.368(3)	C13-F9	1.373(3)
C5-F1	1.384(3)	C13-F10	1.365(3)
C5-C6	1.535(4)	C13-C14	1.517(5)
C6-F3	1.346(4)	C14-F12	1.340(3)
C6-F4	1.356(3)	C14-F11	1.394(4)
C6-C7	1.525(4)	C14-C15	1.482(5)
C7-F6	1.347(4)	C15-F14	1.359(4)
C7-F5	1.354(3)	C15-F13	1.392(5)
C7-C8	1.532(4)	C15-C16	1.531(4)
C8-F7	1.372(3)	C16-F15	1.345(4)
C8-F8	1.372(3)	C16-F16	1.371(3)

Table B3: Bond angles (°) in $Fe(CF_2)_4(CO)_4$ [1].

Bond	Angle (°)	Bond	Angle (°)
C1-Fe1-C4	175.26(12)	C10-Fe2-C12	175.49(13)
C1-Fe1-C3	89.91(11)	C10-Fe2-C9	91.01(13)
C4-Fe1-C3	93.22(11)	C12-Fe2-C9	91.50(13)
C1-Fe1-C2	91.43(12)	C10-Fe2-C11	92.34(13)
C4-Fe1-C2	91.66(12)	C12-Fe2-C11	91.02(13)
C3-Fe1-C2	97.96(11)	C9-Fe2-C11	98.08(13)
C1-Fe1-C5	89.30(11)	C10-Fe2-C16	89.19(13)
C4-Fe1-C5	87.21(11)	C12-Fe2-C16	87.95(13)
C3-Fe1-C5	88.87(10)	C9-Fe2-C16	174.40(12)
C2-Fe1-C5	173.13(11)	C11-Fe2-C16	87.50(12)
C1-Fe1-C8	87.75(11)	C10-Fe2-C13	87.56(12)
C4-Fe1-C8	88.79(12)	C12-Fe2-C13	88.73(11)
C3-Fe1-C8	173.93(11)	C9-Fe2-C13	89.18(12)
C2-Fe1-C8	87.69(11)	C11-Fe2-C13	172.73(13)
C5-Fe1-C8	85.50(11)	C16-Fe2-C13	85.24(11)
O1-C1-Fe1	178.4(3)	O5-C9-Fe2	177.4(3)
O2-C2-Fe1	176.3(3)	O6-C10-Fe2	178.7(3)

O3-C3-Fe1	176.9(2)	O7-C11-Fe2	176.6(3)
O4-C4-Fe1	178.4(3)	O8-C12-Fe2	179.0(3)
F2-C5-F1	103.91(19)	F9-C13-F10	103.2(2)
F2-C5-C6	107.3(2)	F9-C13-C14	106.5(2)
F1-C5-C6	107.1(2)	F10-C13-C14	108.7(2)
F2-C5-Fe1	114.43(17)	F9-C13-Fe2	114.35(18)
F1-C5-Fe1	113.52(17)	F10-C13-Fe2	114.04(18)
C6-C5-Fe1	110.12(17)	C14-C13-Fe2	109.54(19)
F3-C6-F4	107.2(2)	F12-C14-F11	105.1(3)
F3-C6-C7	108.6(2)	F12-C14-C15	113.0(3)
F4-C6-C7	110.5(3)	F11-C14-C15	105.4(3)
F3-C6-C5	108.9(2)	F12-C14-C13	115.2(3)
F4-C6-C5	113.2(2)	F11-C14-C13	108.0(3)
C7-C6-C5	108.3(2)	C15-C14-C13	109.6(3)
F6-C7-F5	107.7(2)	F14-C15-F13	106.5(3)
F6-C7-C6	108.3(2)	F14-C15-C14	113.3(3)
F5-C7-C6	110.7(2)	F13-C15-C14	104.5(3)
F6-C7-C8	109.2(2)	F14-C15-C16	113.5(3)
F5-C7-C8	112.8(2)	F13-C15-C16	109.0(3)
C6-C7-C8	108.1(2)	C14-C15-C16	109.6(3)
F7-C8-F8	104.3(2)	F15-C16-F16	104.2(2)
F7-C8-C7	107.1(2)	F15-C16-C15	109.3(3)
F8-C8-C7	107.8(2)	F16-C16-C15	105.5(3)
F7-C8-Fe1	113.58(18)	F15-C16-Fe2	114.6(2)
F8-C8-Fe1	114.01(18)	F16-C16-Fe2	113.6(2)
C7-C8-Fe1	109.64(17)	C15-C16-Fe2	109.2(2)

Table B4: Crystal data details for $Fe(CF_2)_4(\kappa^2\text{-dppe})(CO)_2$ [17].

Bond precision:	C-C = 0.0126 A	Wavelength=0.71073	
Cell:	a=32.336(4)	b=11.5459(14)	c=19.260(2)
.	Alpha=90	Beta=90.384(7)	Gamma=90
Temperature:	200 K		
	Calculated	Reported	
Volume	7190.5(15)	7190.6(15)	
Space group	C 2/c	C2/c	
Hall group	-C 2yc	?	
Moiety formula	C32 H24 F8 Fe O2 P2, C7 H8	?	
Sum formula	C39 H32 F8 Fe O2 P2	C39 H32 F8 Fe O2 P2	
Mr	802.44	802.44	
Dx, gcm-3	.482	1.482	
Z	8	8	
Mu (mm-1)	0.585	0.585	
F000	3280.0	3280.0	
F000'	3286.31		
H, k, lmax	34,12,20	34,12,20	
Nref	4697	4529	
Tmin, Tmax	0.900,0.916	0.858,0.917	
Tmin'	0.854		
Correction method =	MULTI-SCAN		
Data completeness =	0.964	Theta (max) =	22.460
R(reflections)	0.0857(3873)	wR2 (reflections) =	0.2393(4529)
S = 1.051		Npar = 508	

Table B5: Bond distances (Å) in $Fe(CF_2)_4(\kappa^2\text{-dppe})(CO)_2$ [17].

Bond	Distance (Å)	Bond	Distance (Å)
Fe1-C6	1.818(11)	C15-C20	1.390(11)
Fe1-C5	1.890(12)	C15-C16	1.377(10)
Fe1-C1	1.991(9)	C16-C17	1.397(12)
Fe1-C4	2.008(8)	C17-C18	1.370(13)
Fe1-P1	2.267(2)	C18-C19	1.363(13)
Fe1-P2	2.304(2)	C19-C20	1.391(11)
P1-C8	1.820(7)	C21-C22	1.390(10)
P1-C9	1.830(6)	C21-C26	1.401(11)
P1-C15	1.831(7)	C22-C23	1.387(12)
P2-C21	1.816(7)	C23-C24	1.379(15)
P2-C27	1.837(7)	C24-C25	1.390(15)
P2-C7	1.836(7)	C25-C26	1.382(13)
F1-C1	1.362(10)	C27-C28	1.372(11)
F2-C1	1.419(10)	C27-C32	1.372(12)
F3-C2	1.307(9)	C28-C29	1.385(12)
F4-C2	1.415(11)	C29-C30	1.338(15)
F5-C3	1.475(12)	C30-C31	1.381(15)
F6-C3	1.345(9)	C31-C32	1.392(12)
F7-C4	1.340(9)	C33-C34	1.3900
F8-C4	1.519(11)	C33-C38	1.3900
O1-C5	1.041(11)	C33-C39	1.48(2)
O2-C6	1.111(11)	C34-C35	1.3900
C1-C2	1.616(13)	C35-C36	1.3900
C2-C3	1.442(13)	C36-C37	1.3900
C3-C4	1.465(13)	C37-C38	1.3900
C7-C8	1.520(10)	C40-C41	1.3900
C9-C10	1.364(10)	C40-C45	1.3900
C9-C14	1.395(10)	C40-C46	1.478(18)

C10-C11	1.383(11)	C41-C42	1.3900
C11-C12	1.367(13)	C42-C43	1.3900
C12-C13	1.359(13)	C43-C44	1.3900
C13-C14	1.394(11)	C44-C45	1.3900

Table B6: Bond angles (°) in $Fe(CF_2)_4(\kappa^2\text{-dppe})(CO)_2$ [17].

Bond	Angle (°)	Bond	Angle (°)	Bond	Angle (°)
C6-Fe1-C5	175.0(4)	C3-C2-F4	103.5(7)	C15-C20-C19	119.4(8)
C6-Fe1-C1	91.7(4)	F3-C2-C1	111.5(7)	C22-C21-C26	118.8(7)
C5-Fe1-C1	85.3(4)	C3-C2-C1	106.3(6)	C22-C21-P2	120.9(6)
C6-Fe1-C4	93.1(4)	F4-C2-C1	105.5(8)	C26-C21-P2	120.2(6)
C5-Fe1-C4	90.5(4)	F6-C3-C2	112.4(8)	C23-C22-C21	120.0(8)
C1-Fe1-C4	85.3(3)	F6-C3-C4	115.2(8)	C24-C23-C22	120.2(9)
C6-Fe1-P1	95.8(3)	C2-C3-C4	115.8(8)	C23-C24-C25	120.9(9)
C5-Fe1-P1	87.5(3)	F6-C3-F5	104.8(7)	C24-C25-C26	118.6(10)
C1-Fe1-P1	171.2(3)	C2-C3-F5	104.6(7)	C21-C26-C25	121.3(9)
C4-Fe1-P1	89.8(3)	C4-C3-F5	102.1(7)	C28-C27-C32	118.7(7)
C6-Fe1-P2	88.1(2)	F7-C4-C3	109.4(7)	C28-C27-P2	122.2(6)
C5-Fe1-P2	88.4(3)	F7-C4-F8	103.4(6)	C32-C27-P2	119.1(6)
C1-Fe1-P2	98.3(3)	C3-C4-F8	101.8(7)	C27-C28-C29	120.4(9)
C4-Fe1-P2	176.2(3)	F7-C4-Fe1	118.6(5)	C30-C29-C28	121.5(10)
P1-Fe1-P2	86.49(7)	C3-C4-Fe1	110.4(6)	C29-C30-C31	118.8(8)
C8-P1-C9	104.6(3)	F8-C4-Fe1	111.7(6)	C30-C31-C32	120.5(9)
C8-P1-C15	103.6(3)	O1-C5-Fe1	175.3(9)	C31-C32-C27	120.0(9)
C9-P1-C15	103.5(3)	O2-C6-Fe1	174.9(8)	C34-C33-C38	120.0
C8-P1-Fe1	104.9(2)	C8-C7-P2	110.7(5)	C34-C33-C39	119.5(8)
C9-P1-Fe1	118.2(2)	C7-C8-P1	108.0(5)	C38-C33-C39	120.3(8)
C15-PZ-Fe1	120.2(2)	C10-C9-C14	118.1(6)	C33-C34-C35	120.0
C21-P2-C27	101.4(3)	C10-C9-P1	122.2(5)	C36-C35-C34	120.0

C21-P2-C7	103.7(3)	C14-C9-P1	119.7(5)	C35-C36-C37	120.0
C27-P2-C7	105.3(3)	C9-C10-C11	121.9(7)	C36-C37-C38	120.0
C21-P2-Fe1	122.3(2)	C12-C11-C10	119.5(8)	C37-C38-C33	120.0
C27-P2-Fe1	116.7(2)	C11-C12-C13	120.1(8)	C41-C40-C45	120.0
C7-P2-Fe1	105.7(2)	C14-C13-C12	120.6(8)	C41-C40-C46	120.5(8)
F1-C1-F2	101.8(7)	C13-C14-C9	119.7(8)	C45-C40-C46	119.4(8)
F1-C1-C2	105.0(7)	C20-C15-C16	119.5(7)	C42-C41-C40	120.0
F2-C1-C2	103.8(7)	C20-C15-P1	119.4(5)	C41-C42-C43	120.0
F1-C1-Fe1	116.9(6)	C16-C15-P1	121.1(6)	C42-C43-C44	120.0
F2-C1-Fe1	117.2(6)	C15-C16-C17	119.7(8)	C45-C44-C43	120.0
C2-C1-Fe1	110.6(5)	C16-C17-C18	121.0(8)	C44-C45-C40	120.0
F3-C2-C3	122.4(10)	C19-C18-C17	119.0(8)		
F3-C2-F4	106.2(6)	C18-C19-C20	121.5(8)		

Appendix C: List of Contributions

93rd Canadian Society Chemistry Conference and Exhibition, 2010

"Studies of Iron Perfluorometallacycle Complexes Enroute to the "Green" Catalytic Synthesis of Hydrofluorocarbons" Stephanie L. Granville, Ilia Korobkov, and R. Tom Baker*